Molecular regulation of mitochondrial dynamics by dynamin-related protein 1 (Drp1) and Bid in model systems of neuronal cell death

Dissertation

zur

Erlangung des Doktorgrades

der Naturwissenschaften

(Dr. rer. nat.)

dem

Fachbereich Pharmazie (16)

der Philipps-Universität Marburg

vorgelegt von

Julia Grohm

aus Stuttgart

Marburg/Lahn 2011

Vom Fachbereich Pharmazie der Philipps-Universität Marburg als Dissertation am 22.03.2011 angenommen.

Erstgutachter:	Prof. Dr. Carsten Culmsee
Zweitgutachter:	Prof. Dr. Moritz Bünemann
Drittgutachter:	Prof. Dr. Nikolaus Plesnila

Tag der mündlichen Prüfung am 23.03.2011

Meinen Eltern

Eidesstattliche Versicherung

Ich versichere, dass ich meine Dissertation

“Molecular regulation of mitochondrial dynamics by dynamin-related protein 1 (Drp1) and Bid in model systems of neuronal cell death”

selbständig ohne unerlaubte Hilfe angefertigt und mich dabei keiner anderen als der von mir ausdrücklich bezeichneten Quellen bedient habe.

Die Dissertation wurde in der jetzigen oder einer ähnlichen Form noch bei keiner anderen Hochschule eingereicht und hat noch keinen sonstigen Prüfungszwecken gedient.

Marburg, den 11.02.2011

....

Julia Grohm

Table of contents

1 Introduction 1

1.1 Programmed cell death in neurons 1

1.1.1 Necrosis 1

1.1.2 Apoptosis 1

1.1.3 Oxidative stress as mediator of neuronal apoptosis 6

1.2 The role of Bcl-2 family proteins in neuronal cell death 7

1.3 Activation of Bid and the regulation of apoptosis 9

1.4 Mitochondria in neurons 10

1.4.1 Mitochondrial dysfunction in neuronal apoptosis and neurodegeneration 11

1.4.2 Regulation of mitochondrial fission and fusion 13

1.5 Aims of the thesis 17

2 Material and methods 18

2.1 Chemicals and reagents 18

2.2 Cell culture materials 18

2.3 Inducers and inhibitors of apoptosis 19

2.3.1 Inducers of apoptosis 19

2.3.2 Inhibitors of apoptosis 20

2.3.3 Transfection reagents 21

2.3.4 Primary antibodies 22

2.3.5 Secondary antibodies 22

2.3.6 Kits 22

2.4 Cell culture methods 23

2.4.1 Cell culture and induction of neuronal cell death 23

2.4.2 Transfection protocols 28

2.4.3 Morphological cell viability analysis 29

2.5 Cell viability assays 29

2.5.1 MTT-assay 29

2.5.2 ATP-assay 29

2.5.3 DAPI /Hoechst 33342 staining 30

2.5.4 Real-time measurements with xCELLigence System 31

2.6 Flow cytometric measurements 31

2.6.1 Annexin-V-FITC staining 31

2.6.2 Analysis of mitochondrial membrane potential with JC-1 32

2.6.3 Evaluation of oxidative stress/lipid peroxidation with Bodipy 32
2.7 Immunocytochemistry 33
2.7.1 Mitochondrial staining 33
2.7.2 Evaluation of mitochondrial morphology 34
2.7.3 Immunocytochemistry of Drp1 34
2.8 Epifluorescence and confocal laser scanning microscopy (CLSM) 35
2.8.1 Epifluorescence microscopy 35
2.8.2 Confocal laser scanning microscopy 35
2.9 Protein analysis 36
2.9.1 Protein sample preparation from HT-22 neurons 36
2.9.2 Immunoprecipitation of Drp1 37
2.9.3 Determination of protein amount 37
2.9.4 Polyacrylamid gel electrophoresis and western blot 38
2.10 RNA analysis 42
2.10.1 RNA sample preparation 42
2.10.2 Determination of RNA amount 42
2.10.3 One Step reverse transcriptase polymerase chain reaction (RT-PCR) 42
2.10.4 Agarose gel electrophoresis 43
2.11 Cerebral ischemia in mice 45
2.12 Statistical analysis 45

3 Results..46
3.1 Glutamate sensitivity of HT-22 cells 46
3.2 Oxidative stress results in pronounced mitochondrial fragmentation 48
3.3 The BH3-only protein Bid is a mediator of glutamate-induced mitochondrial fission 50
3.3.1 Bid inhibition prevents fission of mitochondria in glutamate-induced cell death 50
3.3.2 Mechanism of mitochondrial damage downstream of Bid 51
3.3.3 Specificity of the Bid inhibitor 55
3.4 BI-6c9 prevents Drp1 translocation to the mitochondria in glutamate-induced cell death 57
3.5 Drp1 as a mediator of glutamate-induced mitochondrial fission 58
3.5.1 SiRNA silencing of Drp1 attenuates glutamate-induced cell death and mitochondrial fragmentation in HT-22 cells 58
3.5.2 Novel pharmacological inhibitors of Drp1 provide protective effects in HT-22 cells 62
3.5.3 Drp1 gene silencing and pharmacological Drp1 inhibition prevent mitochondrial depolarization 67

3.5.4 Mdivi compounds mdiviC and E show protective effects on mitochondrial fragmentation in HT-22 cells 71

3.5.5 The negative isoform of Drp1 inhibitor mdiviG cannot prevent mitochondrial fission in HT-22 cells 72

3.5.6 Inhibition of Drp1 prevents tBid-induced mitochondrial fragmentation and neuronal cell death 73

3.6 The Role of Drp1 in primary neurons *in vitro* and *in vivo* 75

3.6.1 Mdivi compounds protect primary neurons against glutamate-induced excitotoxicity 75

3.6.2 Mdivi compounds protect primary neurons against oxygen glucose deprivation (OGD) *in vitro* 76

3.6.3 Mdivi compounds attenuate ischemic brain damage *in vivo* 77

3.7 Mitochondrial distribution and mobility 79

3.7.1 Tubulin structures are destroyed after glutamate toxicity in HT-22 cells 79

3.7.2 Cyclosporine A prevents mitochondrial fragmentation after glutamate-toxicity in HT-22 cells 81

3.7.3 Protein interacting partners of Drp1 in HT-22 cells after glutamate-toxicity 83

3.8 The Role of Drp1 and Bid in different models of oxidative stress 85

3.8.1 Bid inhibition does not prevent neuronal cell death by radical donors 85

3.8.2 4-HNE-induced cell death is not prevented by BI-6c9 86

3.8.3 NO toxicity and subsequent nitrosylation of Drp1 does not occur in glutamate-treated HT-22 cells 87

4 Discussion..91

4.1 Enhanced mitochondrial fission induced by glutamate in HT-22 cells 92

4.2 The Bcl-2 family proteins modulate mitochondrial dynamics 94

4.2.1 The Bcl-2 family proteins control mitochondrial dynamics in nonapoptotic cells 94

4.2.2 The Bcl-2 proteins control mitochondrial dynamics in apoptotic cells 94

4.2.3 Bid is a key regulator of mitochondrial fission in glutamate-induced cell death in HT-22 cells 95

4.3 The role of Drp1 in the oxidative stress model of HT-22 cells 98

4.3.1 Mitochondrial fission is Drp1-dependent after glutamate 98

4.3.2 Drp1 and Bcl-2 family proteins control mitochondrial fission in HT-22 cells 98

4.4 Two major structural changes in mitochondria correlate with glutamate-induced apoptosis 100

4.4.1 Mitochondrial fission and mitochondrial membrane permeabilization 100

4.4.2 The role of Drp1 in MOMP 102

4.5 The role of Drp1 in primary neurons 103
4.6 The role of Drp1 and Bid in other models of oxidative stress 106
    4.6.1 The effects of Drp1 and Bid inhibition on neuronal damage by radical donors 106
    4.6.2 The role of NO toxicity in HT-22 cells 107
4.7 Mdivi-1, the first inhibitor of mitochondrial dynamin-related protein 1 109
4.8 The therapeutic potential of small molecule inhibitors of Drp1 110

5 Summary 112

6 Zusammenfassung 114

7 Abbreviations 117

8 References 122

9 Publications 140

9.1 Original papers 140
9.2 Poster presentations 141
9.3 Oral presentations 143

10 Acknowledgements 144

11 Curriculum vitae.. 146

1 Introduction

1.1 Programmed cell death in neurons

Programmed cell death (PCD) is a cellular self-destruction mechanism that is essential for a variety of physiological processes in the central nervous system (CNS), such as developmental sculpturing of the brain, neural tissue homeostasis and the removal of dispensable cells. Further, PCD plays a prominent role in neuropathology and causes delayed and progressive neuronal loss after ischemic brain damage and in chronic neurodegenerative diseases (1-3). Programmed cell death in neurons can be triggered by different stress stimuli and may involve very distinct death signaling pathways. Depending on the nature and the strength of the insult, PCD is characterized by different morphological features, recognized as necrosis or apoptosis.

1.1.1 Necrosis

A neuron undergoing necrosis dies rapidly as a result of massive calcium (Ca^{2+}) influx, dysregulation of intracellular ion homeostasis, impaired protein function and loss of Adenosinetriphosphate (ATP). Later stages of necrosis are associated with mitochondrial swelling, cell swelling, and finally, rupture of the cell membrane (4). Such cellular disruption by necrosis is associated with inflammatory processes and the further release of several substances, such as glutamate, prostaglandins, histamines and lysosomal enzymes into the extracellular space, followed by substantial cell damage in the surrounding tissue (5;6).

1.1.2 Apoptosis

Apoptosis is the best described type of PCD, due to the highly conserved and uniform nature of apoptotic cell death. Apoptosis occurs during cell development in proliferating tissue and regulates adult cell turnover through replacement of senescent, excessive and unneeded cells. For example, during development apoptosis is required to avoid the accumulation of cellular debris in the extracellular space and subsequent inflammatory response. In contrast to the physiological role of apoptosis, its dysregulation has been widely observed to occur as either a cause or consequence of distinct pathological disorders ranging from cancer, where inhibition of apoptosis promotes cellular survival to malignant proliferation to neurodegenerative diseases, where apoptotic mechanisms cause progressive neuronal cell death (7;8). The term “apoptosis” was first used to describe a particular form of PCD by Kerr et al. in 1972 and was morphologically characterized by nuclear condensation (pyknosis) and DNA fragmentation, membrane blebbing and subsequent formation of apoptotic bodies (9). The resulting apoptotic cell fragments, which are surrounded by an intact plasma membrane, can be absorbed by other cells via phagocytosis. In contrast to necrosis, apoptosis does not induce inflammatory processes and is an active form of cell death depending on energy supply and apoptosis-inducing factors. For a long time, necrosis has been regarded as the passive and uncontrolled form of cell death. However, this paradigm has to be redefined based on recent findings, were morphological and biochemical features of necrosis and apoptosis were identified in the same cell. This newly discovered form of cell death was consequently named necroptosis indicating an apoptosis-necrosis continuum within a dying cell. Necroptosis involves tightly controlled signaling pathways typical for apoptotic cell death and, concomitantly, features of necrotic cell death, such as mitochondrial swelling and plasma membrane lysis (10). The role of necroptosis in neurological disorders is an emerging subject of ongoing research.

Apoptosis has been studied in great detail in a large variety of different cell types and tissues. As mentioned above, the physiological role of apoptosis in all organisms is the removal of damaged, senescent or mutated cells, thereby preserving the function and maintenance of various tissues without causing inflammatory responses to this ‘silent’ form of cell suicide. Especially in the nervous system, apoptotic mechanisms are required to remove dispensable or damaged cells, e.g. during development of the brain and the peripheral nerve fibers. In contrast to this important physiological role, dysregulation of apoptotic mechanism is the major reason for pathological neural demise in neurodegenerative diseases, as for example, Alzheimer’s disease (AD) and Parkinson’s disease (PD). Further, deregulated apoptotic pathways are also involved in delayed neuronal cell death following acute brain damage, e.g. caused by cerebral ischemia or traumatic brain injury (3;8;11-16).

1.1.2.1 Molecular pathways of apoptosis

On the biochemical level two apoptotic cascades exist: an extrinsic pathway that bypasses the mitochondria and an intrinsic pathway where mitochondria play a pivotal role (17).

The extrinsic pathway is activated by the binding of ligands at different death receptors like tumor necrosis factor (TNF), FAS (TNF receptor superfamily, member 6, CD95) or tumor necrosis factor related apoptosis inducing ligand (TRAIL), which can activate initiator caspases-1, -2, -8 or -10. Activation of caspases is a well-established biochemical hallmark of apoptosis (17). Caspases are cysteine proteases with an aspartyl-specificity. Under physiologic conditions, they reside in the cytosol as inactive precursors that are activated during apoptosis by autoproteolysis, other caspases or other proteases. Pro-caspase-1 or -8 have long pro-domains, such as the death effector domain (DED) or the caspase recruitment domain (CARD) which can interact with activating proteins containing death domains (DD) or other binding domains. In contrast to the initiator caspases, the so-called executing caspases (-3, -6, -7) have shorter prodomains with up to now unknown functions and cleave downstream substrates such as, for example, inhibitor of caspase-activated deoxyribonuclease (ICAD) and inhibitors of apoptosis (IAPs), among others (18).

Caspase-8 has multiple functions. It transforms the proapoptotic B-cell-lymphoma-2 (Bcl-2) protein Bcl-2 interacting domain death antagonist (Bid) to a truncated Bid (tBid), and, further activates effector caspases, such as caspase-3, which then releases nucleases like caspase-activated deoxyribonuclease (CAD) from its inactive form (ICAD) (19). Caspase-activated CAD translocates from the cytosol into the nucleus where it cleaves the nuclear deoxyribonucleic acid (DNA) into characteristic double-stranded internucleosomal fragments of 180 base pairs (bp) resulting in the typical DNA fragmentation. Such CAD-mediated DNA fragmentation is regarded as a major hallmark in late stages of the caspase-dependent signaling pathways, when the apoptotic death machinery reaches ‘the point of no return’ and ultimately cell death (20;21). Furthermore, caspase-8-mediated cleavage of Bid to tBid links the extrinsic caspase-dependent cascade to the intrinsic apoptotic pathways.

The intrinsic death pathway predominates in neurons and is initiated by trophic factor withdrawal, moderate overactivation of glutamate receptors, toxic increases in intracellular Ca^{2+} concentrations, oxidative stress (reactive oxygen species-ROS) and DNA-damage (3;22;23). Apoptotic trigger mechanisms involve the activation of kinases like c-Jun N-terminal kinases (JNKs) and transcription factors like p53 that transactivate the proapoptotic Bcl-2-family proteins Bcl-2-associated x protein (Bax) and Bcl-2 antagonist killer 1 (Bak) to the mitochondria where they form pores in the outer mitochondrial membrane (OMM). The increased permeability of the outer mitochondrial membrane is also involved in the formation of the large permeability transition pores (PTP) from the mitochondrial intermembrane space to the cytosol, which allows the release of cytochrom c (Cytc), apoptosis-inducing factor (AIF), Omi/HtrA2 or Smac/DIABLO. In the cytosol, Cytc binds to the apoptosis-protease activating factor (Apaf-1) and ATP to form the apoptosome, which then recruits and activates caspase-9. Caspase-9 cleaves and activates caspase-3 which, in turn, cleaves numerous protein substrates that execute the cell death process, including the

CAD as described before (24). The release of Omi/HtrA2 or Smac/DIABLO from the mitochondria are alternative mechanisms of caspase activation by blocking x-chromosomal linked inhibitor of apoptosis (XIAP) and other inhibitors of apoptosis (IAPs) which usually inhibit the activation of caspases (12;14;22;23;25;26).

In addition to the established caspase-dependent signaling pathways, emerging evidence suggests, that caspase-independent pathways mediated by AIF and Endonuclease G (EndoG) released from mitochondria play a major role in neuronal PCD, in particular in the adult brain. Upon mitochondrial release, AIF and EndoG rapidly translocates to the nucleus where they mediate DNA damage in a caspase- and ATP-independent manner (27). In neurons, acute brain damage after stroke or traumatic brain injury leads to excitotoxic cell death which exhibits apoptotic and necrotic features and does not require Bax/Bak activation (28). During acute brain injury, such as ischemic stroke, oxygen levels are rapidly reduced resulting in abrupt decrease of ATP production and rapid depolarization of the plasma membrane. ATP depletion causes the release of abnormally high amounts of glutamate into the synapses, which is followed by an overactivation of ionotropic glutamate receptors like N-methyl-D-aspartate-(NMDA), 2-amin-3-(3-hydroxy-5-methylisoxazol-4-yl) propionate (AMPA) or kainate receptors (29). This causes massive Ca^{2+}-influx, activation of neuronal nitric monooxide synthases (nNOS), mitochondrial dysfunction and the subsequent release of proapoptotic mitochondrial proteins like Cytc, AIF, EndoG and Smac/DIABLO (30-33). All of these mechanisms of excitotoxicity exacerbate the formation and accumulation of reactive oxygen species (ROS) and ultimately lead to cell death in a combine necrotic and apoptotic fashion.

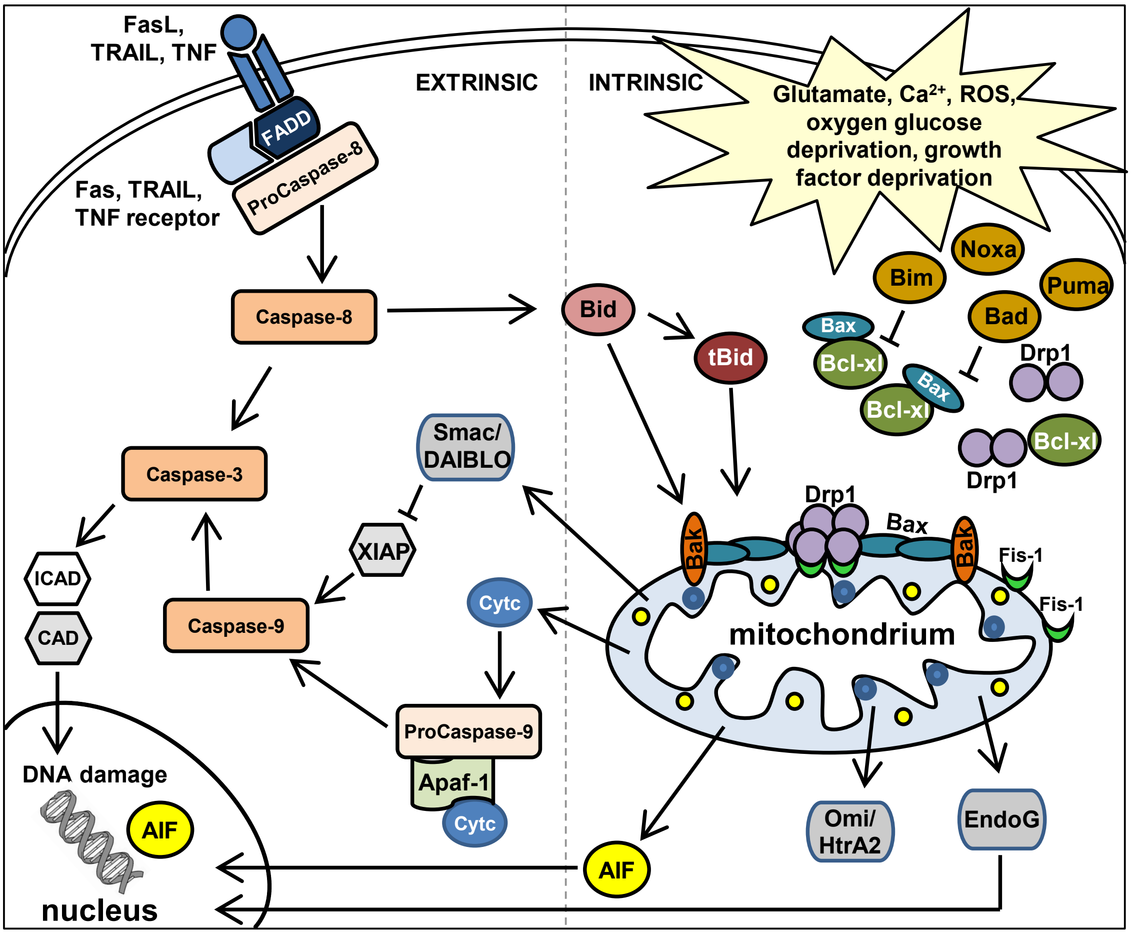
FasL,
TRAIL, TNF
FADD
ProCaspase-8
Fas, TRAIL,
TNF receptor
EXTRINSIC
INTRINSIC
Glutamate, Ca2+, ROS, oxygen glucose deprivation, growth factor deprivation
Noxa
Bim
Puma
Bad
Bax
Bcl-xl
Bax
Bcl-xl
Drp1
Drp1
Bcl-xl
Caspase-8
Bid
tBid
Caspase-3
Smac/
DAIBLO
XIAP
ICAD
CAD
Caspase-9
Cytc
Drp1
Bax
Bak
Bak
Fis-1
Fis-1
mitochondrium
ProCaspase-9
Apaf-1
Cytc
DNA damage
AIF
nucleus
AIF
Omi/
HtrA2
EndoG

Figure 1 Intrinsic and extrinsic apoptotic pathways in mammalian cells

Activation of intrinsic, mitochondria-dependent death signaling pathway leads to mitochondrial membrane permeabilization and subsequent release of AIF, Cytc, Smac/DIABLO, EndoG, Omi/HtrA2, apoptosome formation and caspase activation. Extracellular ligand binding to death receptors (Fas, TNF-R, etc.) triggers the extrinsic pathway that involves the activation of caspases. The intrinsic pathway is also triggered by caspase-8 which cleaves Bid to tBid. Activated tBid translocates to the mitochondria to induce mitochondrial damage and amplification of the death signaling. Both apoptotic signaling pathways converge at the level of effector caspases, such as caspase-3. Bcl-2 family members regulate apoptosis by modulating the release of proapoptotic mitochondrial proteins, such as Cytc. The proapoptotic proteins Bax and Bak interact at the outer mitochondrial membrane where they can form oligomeric pores. Bcl-2 and Bcl-xl are antiapoptotic Bcl-2 family proteins and can block the function of Bax and Bak. Further, the BH3-only Bcl-2 family proteins (Bim, Bid, Bad, Puma, Noxa, etc.) modulate the proapoptotic processes of Bax/Bak, e.g. by inhibiting the antiapoptotic Bcl-2 members. Enhanced intracellular Ca^{2+} concentrations promote mitochondrial translocation of the mitochondria-shaping protein Drp1. In the cytosol, Cytc, Apaf-1, and procaspase-9 interact to form the apoptosome that drives the activation of caspase-3. Upon release from mitochondria, AIF and EndoG translocate to the nucleus where they mediate DNA degradation. Smac/DIABLO or Omi/HtrA2 scavenge the inhibitors of apoptosis (IAPs) such as XIAP and, consequently, their release from mitochondria indirectly enhances activation of caspase-3 and 9. Caspase-3 cleaves many substrate proteins, for example endonucleases including caspase-activated DNAse (CAD) from its inactive form (ICAD) that translocates to the nucleus to cleave DNA into internucleosomal fragments.

1.1.3 Oxidative stress as mediator of neuronal apoptosis

Production of high levels of ROS as key mediators of oxidative stress has been linked to a variety of neurological disorders such as Alzheimer`s, Parkinson`s disease or stroke (34;35). Under physiological conditions, low levels of ROS are involved in signaling processes and functions as mediators in different processes, such as cellular growth and adaption responses (36). ROS include a broad range of diverse molecules such as oxygen free radicals (superoxide radicals, hydroxyl radicals), peroxides (hydrogen peroxides, lipid hydroperoxides), nitric oxide and peroxynitrite anions, which mediate oxidative stress (36). ROS induce damages in cellular membrane and can alter DNA and unsaturated lipids as well as membrane lipids. Further, at the mitochondrial level, ROS may directly or indirectly mediate the formation of mitochondrial membrane permeability (MMP) and consequently the release of apoptosis-inducing factors and activation of caspases. Therefore, ROS together with excitotoxic increases in intracellular Ca^{2+}, are important triggers of the intrinsic pathway in neuronal cell death (22;37;38). Excessive ROS formation in neurons can be caused by excessive glutamate, beta-amyloid plaques, oxygen glucose deprivation and massive NO formation (2;3;24;37). The mechanism of glutamate-induced oxidative stress is not fully understood. It has been shown that high levels of glutamate induce Ca^{2+}-dependent ROS formation, but recent findings suggested that glutamate can also mediate oxidative stress independently of ionotropic glutamate receptors (39;40). Therefore, it is of utmost interest to understand the cellular mechanisms of glutamate-induced oxidative stress, which is involved in neuronal apoptosis.

To investigate the mechanism of oxidative stress in neurons, immortalized HT-22 cells were used as a glutamate-sensitive neuronal cell line. These cells are derived from mouse hippocampus and are responsive to glutamate at millimolar (mM) concentrations. Since HT-22 cells do not express ionotropic glutamate receptors, glutamate-induced death is mediated by glutathione depletion, not by excitotoxicity. High extracellular glutamate concentrations block the glutamate-cystine-antiporter system Xc-, which normally mediates the cystine-uptake into the cells. Consequently, glutamate reduces the intracellular cystine levels that is a limiting factor for the cells' glutathione (GSH) synthesis (41-44). Glutathione serves as a radical scavenger that sequesters free radicals and ROS. Consequently, levels of ROS increase within a few hours after glutamate treatment of HT-22 neurons due to the breakdown of the glutathione pools in the cells. Later, the excessive ROS levels further increase the damage of intracellular structures (lipid membranes, proteins and DNA), mitochondria and the subsequent breakdown of the cellular ion homeostasis. Furthermore, an elevation of cytosolic Ca^{2+}, despite the absence of NMDA receptors, has been observed following ROS formation in glutamate-exposed HT-22 neurons (45). Enhanced ROS formation, increased Ca^{2+} and mitochondrial dysfunction are established features of apoptosis. All of these features are detectable in this model system of glutamate-induced oxidative stress in HT-22 cells. For this reason, this model system of glutamate toxicity serves as a valuable and applicable model to investigate molecular mechanisms of neuronal apoptosis induced by detrimental oxidative stress.

In the current thesis, the results obtained in these immortalized hippocampal neurons were always compared with similar experiments performed in primary neurons that express ionotrophic glutamate receptors (AMPA, NMDA receptors). This strategy enabled the comparison of the contribution of the newly identified mechanisms of mediating oxidative death pathways in HT-22 cells with paradigms of excitotoxicity that are triggered in primary neurons by increases in intracellular calcium and enhanced ROS production.

1.2 The role of Bcl-2 family proteins in neuronal cell death

It is well established that neurons undergo apoptosis via the intrinsic pathway, which involves damage of mitochondria (46;47). A critical step of mitochondrial damage is reached, when mitochondrial outer membrane permeabilization (MOMP) results in the release of mitochondrial proapoptotic factors (Cytc, AIF, Smac/DIABLO, Omi/HtrA2, EndoG) into the cytosol. Bcl-2 family proteins are essential regulators of MOMP and represent a protein family of pro- and antiapoptotic proteins (48). All members of this family share a close homology in characteristic regions named Bcl-2-homology (BH) domain. Bcl-2 proteins can be classified into three subtypes based on structural and functional features. To date, four BH-domains have been identified, termed BH1, BH2, BH3 and BH4 (49). Antiapoptotic Bcl-2 proteins consist of Bcl-2, Bcl-2 related long isoform (Bcl-xl), Bcl-w and myeloid cell leukemia 1 (Mcl-1) suppresses apoptosis and contains all four Bcl-2-homology domains (BH1-4). For instance, Bcl-2 and Bcl-xl can prevent the proapoptotic function of Bax by the formation of heterodimer complexes (50).

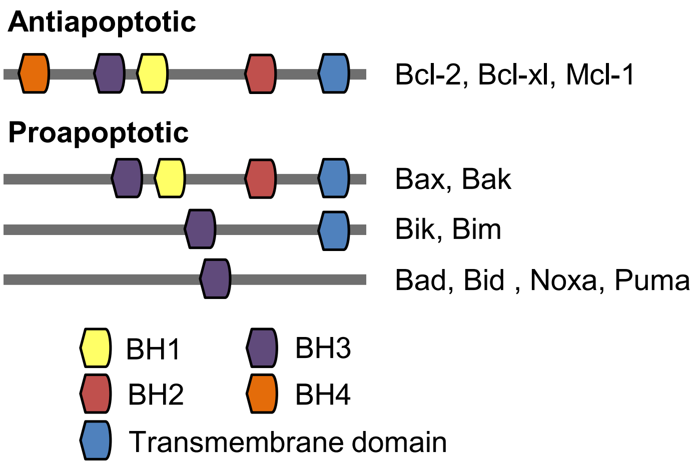

Figure 2 Proteins of the Bcl-2 family

Bcl-2 proteins can be classified into three subtypes based on structural and functional features. To date, four Bcl-2-homolgy (BH)-domains have been identified (BH1-4). The Bcl-2 family is divided into antiapoptotic effectors which include Bcl-2, Bcl-xl, Mcl-1. Proapoptotic “multi-domain” proteins include Bax and Bak and “BH3-only proteins” as direct activators of MOMP with Bid, Bim, Noxa, Puma, Bik (modified from Chipuk et al., 2010).

Some proapoptotic proteins such as Bax and Bak contain BH1-3-domains and are termed “multi-domain proteins”, whereas other proapoptotic members of the Bcl-2 family, like Bcl-2-interacting mediator of cell death (Bim), Bik, Noxa, Puma, Bid and Bcl-2 antagonist of cell death (Bad) share only one BH3-domain with the other members of the Bcl-2 protein family and are therefore named “BH3-only proteins”. These proteins are exclusively proapoptotic and act as sensors for damage by oxidative stress or growth factor deprivation. They are activated by a variety of stimuli such as transcriptional upregulation, limited proteolysis or dephosphorylation (51;52). How Bcl-2 family members interact to permeabilize the mitochondrial membrane remains controversial.

The multi-domain proapoptotic proteins Bax and Bak are thought to promote MOMP by oligomerization to form pores within the outer mitochondrial membrane (OMM). One route to Bax/Bak activation involves the displacement of the antiapoptotic Bcl-2 proteins from Bax/Bak due to binding of BH3-only proteins to the antiapoptotic proteins Bcl-xl and Bxl-2 (53). Another possible route to Bax/Bak activation is the direct, but possibly transient, interaction of BH3-only proteins, like Bid or Bad that provoke a conformational change of Bax/Bak followed by their oligomerization (54). Overall, the BH3-only-proteins appear to activate Bax and Bak indirectly by engaging, binding and neutralization of pro-survival Bcl-2 family proteins (Bxl-xl, Bcl-2).

1.3 Activation of Bid and the regulation of apoptosis

In healthy cells, most of the antiapoptotic multi-domain Bcl-2 family members are constitutively found in the OMM, like Bak. Bax is mostly localized in the cytosol as well as BH3-only proteins like Bid, Bad or Bim. During apoptosis, Bax and Bak undergo conformational changes, and at least two of the BH3-only proteins, Bid and Bim are capable of direct activation of Bax and Bak. The activated form of Bid (tBid) and Bim results in a recruitment, insertion and oligomerization of Bax in the OMM (55;56). The translocation of truncated Bid (tBid) to the mitochondria, where it interacts with Bax (57;58), has been identified as a major pathway in neuronal cell death triggered by death receptor signaling and after cerebral ischemia (59;60). A series of events leading to Bid-mediated activation of Bax has been elucidated in *in vitro* studies with isolated mitochondria or large unilamellar vesicles (54;61) and by Förster resonance energy transfer (FRET) analysis (55;56). The pivotal role of Bid in the activation of the intrinsic pathway of apoptosis was confirmed by several studies, where pharmacological inhibition of Bid and genetic Bid depletion exerted pronounced protection against apoptotic cell death. In particular, Bid knockout mice show less neuronal cell death after trauma compared to wild type mice (62), and Bid-deficient neurons were protected against oxygen glucose deprivation and cerebral ischemia (60;63).

In healthy cells, inactive full-length Bid is highly expressed and located in the cytosol where it can be cleaved and activated to tBid by caspase-8 cleavage. Caspase-8 is the most prominent activator of Bid, which itself gets activated by Fas or TNF death receptors. Several studies found enhanced caspase-8 activation after oxygen glucose deprivation (OGD) and cerebral ischemia in rodents (60;63). It is important to note that Bid can also be cleaved by caspases-1 and -2 as shown, for example, in models of cerebral ischemia and hypoxia for caspase-1. In addition to caspases, granzyme B, lysosomal hydrolases and calpains are able to cleave Bid (64;65). For example, calcium-triggered activation of calpains may cause Bid activation, and subsequent mitochondrial damage and release of proapoptotic mitochondrial proteins (66;67). In addition to the proposed direct or indirect activation of Bax and Bak, Bid is also capable of (directly) mediating mitochondrial damage, independent of these proapoptotic Bcl-2 proteins, through pore formation by tBid oligomers in the mitochondrial membrane (54;55;68;69).

Interestingly, truncation of Bid to tBid is only one of various mechanisms to activate the full apoptotic activity of BH3-only proteins. In epithelial cells, full-length Bid mediates apoptosis associated with loss of mitochondrial membrane potential and DNA damage without prior cleavage to tBid (70). Taken together, tBid and also activated full-length

Bid are key mediators of mitochondrial demise and subsequent cell death pathways. Therefore it is necessary to investigate the exact mechanism of Bid activation and its role in regulation of mitochondrial mechanisms during neuronal cell death for further understanding of key molecular mechanisms in neurodegenerative disorders.

1.4 Mitochondria in neurons

Mitochondria are semi-autonomous organelles present in all aerobic organisms that contain their own genome and protein synthesis machinery. The most prominent role of mitochondria is to supply the cell with metabolic energy in form of ATP (71). Furthermore, mitochondria are involved in many catabolic and anabolic reactions of different metabolites, e.g. phospholipids, the regulation of ROS metabolism and calcium homeostasis (72;73). In addition to their central role in various biochemical pathways, mitochondria are key regulators of development, aging and neuronal apoptosis (23). The multitude of different functions of mitochondria is reflected in their structure. Mitochondria consist of two membranes, the inner and the outer membrane, an intermembrane space and a matrix, which contains the mitochondrial DNA encoding proteins essential for the organelle’s replication and energy transduction.

Live cell microscopy studies showed, that mitochondria are highly dynamic organelles, which build large interconnected networks or appear as spherical small rounded organelles, depending on physiological conditions (74). The dynamic nature of mitochondria provides quality control mechanisms to stabilize mitochondrial function, to regulate the organelles size and number, and allows mitochondrial DNA (mtDNA) and protein exchange between mitochondria (75-78). Further, continuous movement of the organelles along the cytoskeleton throughout the length of axons and dendrites of neurons involves constant alterations of mitochondrial morphology and size (75;79;80). In fact, energy supply for ATP-dependent processes, like vesicle release, neurotransmitter synthesis, calcium buffering in synapses and dendritic spines, requires the mitochondria to travel over long distances from the cell body to these remote areas (74;81;82). Therefore, neurons are particularly sensitive to changes in mitochondrial dynamics and movements. Defects in mitochondrial fusion or division lead to an extensively interconnected and collapsed mitochondrial network and a complete loss of mtDNA (83). Thus, it is not surprising that alterations in mitochondrial dynamics significantly impair/affect neuronal function, and the prevalence of neuronal disease associated with mutations in mitochondrial fission/fusion genes underlines the important functional relationship between mitochondrial dynamics and neuronal function (46;84-86).

1.4.1 Mitochondrial dysfunction in neuronal apoptosis and neurodegeneration

Mitochondrial dysfunction is an early event in neurological diseases and defects in mitochondrial fission and fusion proteins are associated with a wide array of inherited or acquired neurodegenerative diseases, such as Charcot-Marie-Tooth 2A disease (CMT2A), dominant optic atrophy (DOA), Alzheimer’s disease or Parkinson`s disease (35;87;88). For example, mice lacking the dynamin-related proteins (Drps) that comprise the heart of the mitochondrial division and fusion machinery, such as dynamin-related protein 1 (Drp1), Mitofusin-1 and -2 (Mfn-1,-2), optic atrophy 1 (Opa1), exhibit deleterious developmental defects (88-90). Mutation in human Drp1 causes early infant mortality, and mutations in Mfn-2 or Opa1 cause two distinct types of neurodegenerative diseases CMT2A and DOA, respectively. Furthermore, the mitochondrial network becomes extensively fragmented into smaller, more numerous organelles in caspase-independent manner during apoptosis triggered by oxidative stress (91-93), or after critical changes in energy demands and fluctuations of intracellular calcium levels (94). Fission and fusion defects may limit mitochondrial motility, decrease energy production, promote oxidative stress, and lead to accumulating mtDNA defects, thereby promoting neuronal dysfunction and cell death.

It is not clear why the mitochondrial network is disrupted during apoptosis, but it has been proposed, that this may be due to neutralization of the function of one or more members of the Bcl-2 family that may contribute to the mitochondrial morphogenesis in healthy cells (93). Indeed, Youle and colleagues found that Bax/Bak-deficient cells have constitutive defects in mitochondrial morphology and contain mitochondria that are significantly smaller than mitochondria in wildtype cells (26). In addition, Bax and Bak colocalize with mitochondrial fusion and fission GTPases. For example, Drp1 seems to control the outer mitochondrial membrane permeabilization by interaction with Bax. In addition, Bak can interact with mitofusins thereby blocking fusion and inducing fragmentation. In neurons, toxic concentrations of nitrogen monoxide (NO) display Bax foci on mitochondria undergoing fission. In contrast, inhibition of Drp1 delays this fission, Bax foci formation and loss of neurons (95;96), which suggests a functional link between the progression of apoptosis and Drp1-mediated mitochondrial fission. Interestingly, mitochondrial fusion also plays a role in the regulation of apoptosis. Loss of Mfn-1 and Mfn-2 has profound effects on mitochondrial structure and function, leading to mitochondrial fragmentation and swelling, loss of mtDNA, cristae disorganization, and enhanced sensitivity to apoptotic stimuli (97).

It has also been suggested that mitochondrial fusion and fission occurs as a consequence of apoptosis in association with permeabilization of mitochondrial outer membrane and subsequent loss of intermembrane space proteins like Opa1, AIF, and Smac/DIABLO (98;99). Some investigators reported that mitochondrial fission promoted Cytc release and therefore steered caspase activation during apoptosis (85;86). In contrast, however, other findings showed that Bax/Bak-induced mitochondrial fission can be uncoupled from Cytc release. Overall, the large majority of data suggests, that cell death-associated fragmentation of mitochondria is a consequence rather than a cause of apoptosis signaling and reflects potential of yet unknown interactions or connections between members of Bcl-2 family and the machinery regulating mitochondrial morphology (26;85;93;100).

Irrespective of the functional role, apoptosis-induced mitochondrial fragmentation is widely accepted as an established feature of apoptosis in essentially all cell types and in response to most, if not all, apoptotic stimuli (51;85;100). Not only mitochondrial networks undergo fragmentation during apoptosis, but these fragmented mitochondria also become clustered around the nucleus and the dynamic mitochondrial movement appears to cease (92;93). It is not clear exactly how these phenomena are regulated, but in apoptotic cells mitochondria likely become uncoupled from their normal attachment points on the cytoskeleton, an observation that awaits further investigation.

Given the importance of mitochondrial dynamics for cellular function, regulation and cell death, it is not surprising that aberrant mitochondrial dynamics have been associated with prevalent human diseases, including AD, PD, Huntington`s disease, amyotrophic lateral sclerosis (ALS) and diabetes. In these cases, fragmentation of the mitochondrial network has been observed in patient samples and experimental disease models, suggesting a shift in division/fusion balance towards division. The cause of this shift is unclear and could be the result of direct activation of mitochondrial division, inhibition of mitochondrial fusion or both. In the cases of mitochondrial-fusion linked diseases, namely Charcot Marie Tooth 2A or dominant optic atrophy, it is clear, that the disease-associated alterations of mitochondrial morphologies are at least in part due to a direct shift towards division as a result of attenuated fusion. The link between increased mitochondrial division and disease states or apoptosis signaling proposes the mitochondrial fission machinery as an attractive target for therapeutics in the treatment of an impressive array of diseases from neurodegenerative disorders to more acute conditions such as cerebral stroke or myocardial infarction.

1.4.2 Regulation of mitochondrial fission and fusion

The current knowledge of the mechanisms regulating mitochondrial dynamics indicates that fission and fusion of mitochondria are under control of highly conserved dynamin-related GTPases (76). Specifically, in mammalian cells mitochondrial outer and inner membrane fusion is mediated by mitofusin-1 and -2 (Mfn-1, -2) and optical atrophy 1 (Opa1), respectively (97;101).

Mfn-1 and -2 are localized to mitochondrial outer membranes where they interact with each other to promote tethering and fusion of neighboring mitochondria (102). Opa1 is localized in the mitochondrial intermembrane space and during fusion, Opa1 cooperates with mitofusins to reorganize the inner membrane cristae (89;98).

Mitochondrial fission is mainly mediated by Drp1 and Fis-1 (103-106). Mitochondrial fission is a multistep process initiated by the enhanced recruitment of Drp1 protein from the cytoplasm to the mitochondrial surface, followed by protein oligomerization around the organelle in a punctuated distribution pattern, which become fission sites (107;108).

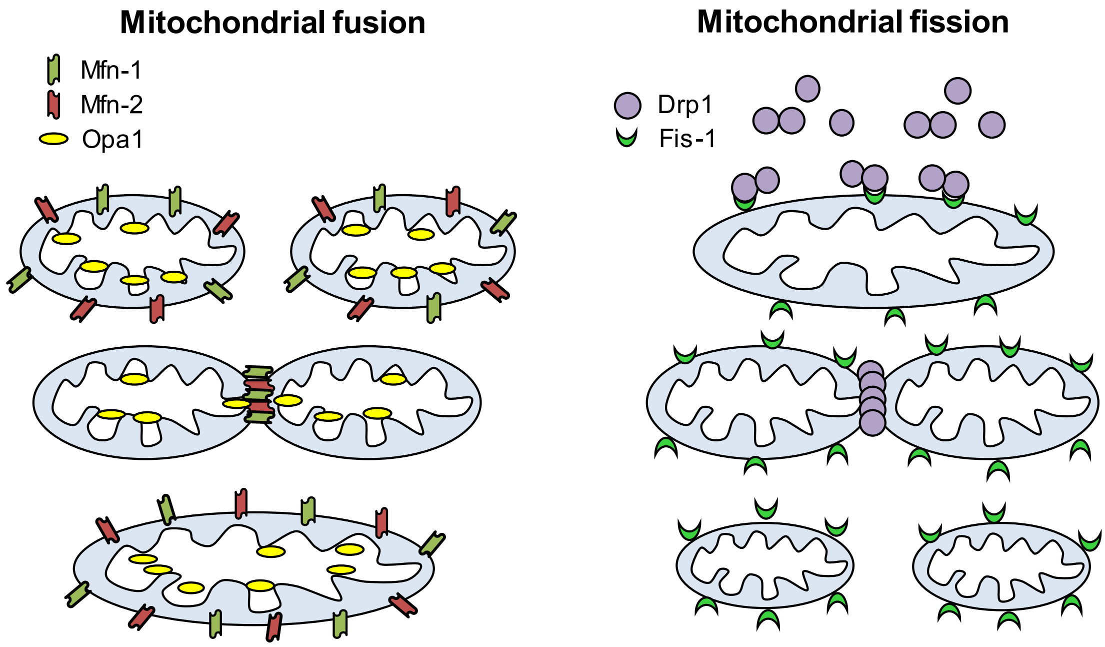

Figure 3 Molecular regulation of mitochondrial dynamics

Proteins involved in mitochondrial fusion (*left panel*) and fission (*right panel*) mechanism. *Left panel*: Mitochondrial outer membrane located Mfn-1 and Mfn-2 in association with Opa1 promote mitochondrial fusion of the outer and inner mitochondrial membrane to produce longer mitochondria. *Right panel*: Dynamin-related protein 1 (Drp1) is found in the cytoplasm and forms oligomers and translocates after diverse apoptotic stimuli to the mitochondrial outer membrane. The Drp1 oligomers interact with outer mitochondrial membrane bound Fis-1 and encircles on specific fission sites on mitochondria to separate the daughter organelles.

Drp1 is mainly distributed in a diffuse manner throughout the cytosol in cultured cells, which suggests that it is predominantly unassembled (104). In response to a certain apoptotic stimuli, such as increase in Ca^{2+} levels or initiation of apoptosis, mitochondrial targeting and assembly of Drp1 is greatly enhanced and consequently fission increased. While the mechanism underlying regulation of Drp1 assembly are unclear, it is still evident that regulation of assembly can be used as a means to regulate mitochondrial function (85;109).

In addition, mitochondrial fission is dependent on non-dynamin-related protein factors like Fis-1, Endophilin B1, mitochondrial fission factor (Mff), ganglioside-induced differentiation associated protein 1 (GDAP) or other outer mitochondrial membrane proteins. Fis-1 is distributed evenly at the outer mitochondrial membrane where it may act as a mitochondrial Drp1 receptor (103;105). It has been suggested that the mitochondrial outer membrane proteins Fis-1 and Mff and the proapoptotic Bcl-2 family protein Bax and Bcl-xl (100;110) function as positive regulators of Drp1 to promote mitochondrial fission, however, the mechanisms that promote and regulate the recruitment of cytosolic Drp1 to mitochondria are largely unknown (46;103;105;111;112). In addition to these potential protein regulators of mitochondrial division, the function of Drp1 is also influenced by post-translational modifications. Phosphorylation, S-nitrosylation, ubiquitination and sumolyation have all been identified to regulate Drp1 function (113-124). It is likely known that a distinct combination of post-translational modifications and protein effectors regulate the activity of Drp1 in different physiological and pathological contexts.

While the mitochondrial division machinery is influenced by many factors, Drp1 is the most obvious target of small molecule modulators as it is the highly conserved, core mechanical component of the division protein complex. In addition, Drp1 is a promising target for small molecule effectors, in the sense that there are many critical functional features of the protein, such as GTP binding, GTP hydrolysis and self-assembly which is mediated by conformational changes linked to the GTPase cycle. Therefore, small molecule effectors that target the different functional facets of Drp1 and thus either positively or negatively affect distinct stages of Drp1-driven mitochondrial division can be identified. Finally, given the increasing number of Drp1 interacting proteins that have been implicated in division, it may be possible to identify tissue specific or context-specific inhibitors of mitochondrial division by targeting Drp1 effector interactions. These strategies may protect neurons from enhanced mitochondrial fission and from irreversible damage and cell death.

1.4.2.1 The first inhibitor of mitochondrial Drp1

The laboratory of Jodi Nunnari, UC Davis, USA identified dynamin-related protein (Dnm1, yeast; Drp1, human) as the first small molecule effector of the mitochondrial division protein Drp1 in a growth-based assay in yeast (125). Afterwards, Dnm1 was also demonstrated to target Drp1 in mammalian cells. This derivative of quinazolinone, called **m**itochondrial **div**ision **i**nhibitor 1 (mdivi-1) act as a mixed type inhibitor to attenuate the dynamin-related protein (Drp) assembly in the early stages of division by preventing the polymerization of higher order structures. Mdivi-1 selectively targets the unassembled pool of the mitochondrial division dynamin-related protein, and its binding creates and stabilizes an assembly-deficient conformation (Figure 4). Assembly of the division dynamin-related protein is critical for its function. Thus, mdivi-1 acts as an efficacious inhibitor of mitochondrial division in cells and inhibits MOMP (125).

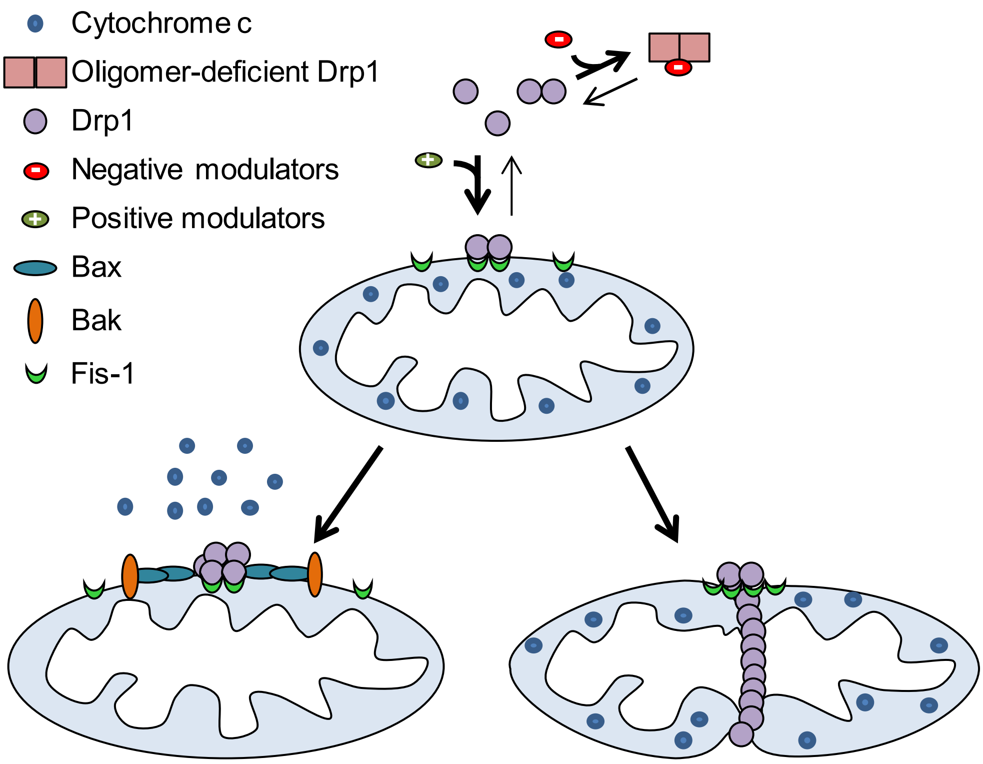

Figure 4 Modulation of Drp1-mediated mitochondrial division and potentiation of apoptosis by negative and positive effectors

Negative effectors, like mdivi-1, may block Drp1 assembly or Drp1 function and thus attenuate mitochondrial division and/or mitochondrial outer membrane permeabilization (MOMP). Positive effectors, like phosphorylation, protein interactions with Bax or Fis-1 may stimulate Drp1 assembly and/or function, and depending on the distinct set of effectors, which is defined by biological circumstances, mitochondrial division and/or MOMP can be induced.

Given the conservation of the Drp super family members; it is remarkable that mdivi-1 also displays a high degree of selectivity for the mitochondrial division dynamins, as it has no effect on other Drps, such as the endocytic dynamin or the mitochondrial fusion dynamins. This selectivity is encouraging for the division dynamin protein as a therapeutic target in different models of neurological diseases (109). This promising result makes this compound interesting to investigate the role of Drp1 in more detail. In particular, these substances make Drp1 as prime target to prevent mitochondrial fragmentation in different models of neurodegenerative diseases and acute brain damage by cerebral ischemia. In the present study, different isoforms of mdivi-1 compound were applied for the first time in neurons to elucidate the role of Drp1-induced mitochondrial fragmentation in neuronal cell death.

1.5 Aims of the thesis

The relevance of enhanced mitochondrial fragmentation in neuronal cell death emerged in the last couple of years, but until now very little is known about the regulatory mechanisms, the key mediators upstream and the processing which leads to mitochondrial fragmentation in neuronal cell death.

In particular, it has been established that proapoptotic Bcl-2 protein family members such as Bax, Bak and Bid mediate mitochondrial dysfunction and associated death signaling pathways in neurons, and a number of recent findings suggested that such intrinsic death pathways are associated with extensive mitochondrial fragmentation. Therefore, the present thesis investigated the mitochondrial morphology dynamics and their regulation in a model of glutamate toxicity in immortalized HT-22 neurons. Furthermore, a major aim of this study was to elucidate whether BH3-only protein Bid was involved in the regulation of mitochondrial dynamics and associated in mitochondrial cell death pathways after glutamate-mediated oxidative stress. In this thesis, the established Bid inhibitor BI-6c9 was applied to elucidate the particular role of this BH3-only protein in mitochondrial fission in the model of glutamate-induced cell death.

Previous investigations on mechanisms of mitochondrial dynamics highlighted the pivotal role of Drp1. The observation that enhanced mitochondrial fission is linked to neurodegeneration and apoptotic pathways revealed the possibility that Drp1 is a therapeutic target for the prevention of neuronal cell death. For this reason, the present thesis emolyed siRNA approaches and novel small molecule inhibitors of Drp1 (125) to address whether Drp1 plays a major role in neuronal cell death after glutamate toxicity and oxygen-glucose deprivation (OGD*)* in cultured neurons. In addition, potential protein interactions between Drp1 and other regulators of apoptosis and mitochondrial damage were addressed, as well as the potential role of Drp1 in other models of oxidative stress. Finally, to further substantiate the therapeutic potential of Drp1 inhibition based on findings in models of neuronal cell death *in vitro*, the applications of the Drp1 inhbitior were expanded to a model of ischemic brain damage *in vivo*.

2 Material and methods

2.1 Chemicals and reagents

All standard chemicals were obtained from Sigma-Aldrich (Taufkirchen, Germany) and Roth (Karlsruhe, Germany), if not described otherwise. All buffers and solution were prepared using demineralized, ultrapure water that was prepared with the SG Ultra Clear UV plus pure water system (VWR, Darmstadt, Germany). For media and solutions that were used in the cell culture the ultrapure, demineralized water was sterilized using a steam autoclave (Systec V-40, Systec GmbH, Wettenberg, Germany). All media and solutions that were used in cell culture were sterilized by filtration using 0.22 µm filter sets (Sarstedt, Nümbrecht, Germany).

2.2 Cell culture materials

Sterile plastic ware was used as follows

Table 1 Sterile plastic ware

Plastic ware	Ordering number	Company
T75 flasks	658 175	Greiner, Frickenhausen, Germany
T175 flasks	660 175	Greiner, Frickenhausen, Germany
6-well plates	657 160	Greiner, Frickenhausen, Germany
24-well plates	662 160	Greiner, Frickenhausen, Germany
96-well plates	655 180	Greiner, Frickenhausen, Germany
12-well plates	655 180	Greiner, Frickenhausen, Germany
48-well plates	655 180	Greiner, Frickenhausen, Germany
IbiTreat 8-well	80826	Ibidi, Munich, Germany
15 ml-tubes	188 271	Greiner, Frickenhausen, Germany
50 ml-tubes	227 261	Greiner, Frickenhausen, Germany
Sterile filter 0.22 µm	291-3320	Nalgene, Thermo Fisher Scientific, Roskilde, Denmark
0.5-, 1.5-, 2-ml tubes	72.704, 72.706, 72.695	Sarstedt, Nümbrecht, Germany
Cell scraper	83.1830	Sarstedt, Nümbrecht, Germany

The E-plates and the xCELLigence System for the impedance measurements were obtained from Roche, Applied Science (Penzberg, Germany).

2.3 Inducers and inhibitors of apoptosis

2.3.1 Inducers of apoptosis

Glutamate stock solution was prepared by solving DL-glutamic acid monohydrate (Sigma-Aldrich, Taufkirchen, Germany) to a stock concentration of 100 mM in Earl's balanced salt solution (1x EBSS) or Dulbeccos's modified eagle medium (DMEM; PAA Laboratories GmbH; Cölbe, Germany). The pH was adjusted to 7.2 with concentrated sodium hydroxide solution (NaOH). The stock solution was stored at -20 °C and diluted with DMEM or 1x EBSS to final concentrations ranging from 1 mM to 5 mM in DMEM for HT-22 neurons and at a final concentration of 20 - 30 µM in 1x EBSS for primary rat neurons.

For treatment with hydrogen peroxide (H_2O_2, Sigma-Aldrich, Taufkirchen Germany), H_2O_2 (stock with a concentration of 30 %) was diluted with DMEM to concentrations of 500 - 700 µM. The solutions were always freshly prepared.

Sodium nitropusside (SNP, Sigma-Aldrich, Taufkirchen, Germany) was dissolved in DMEM immediately before treatment of the cells and diluted to concentrations of 20 - 600 µM.

Glucose oxidase (GO, Sigma-Aldrich, Taufkirchen, Germany) has been used to achieve a continuous production of H_2O_2. Before treatment, glucose oxidase was dissolved in sodium acetate solution (50 mM, pH 5.1, Merck, Darmstadt, Germany) and diluted to concentrations of 1 - 20 mM.

4-Hydroxynonenal-dimethylacetat (4-HNE, Sigma-Aldrich, Taufkirchen Germany) was dissolved in 1 mM cold HCl according to the manufacture`s protocol and diluted to concentrations of 5 - 30 µM with DMEM.

DEA/NO,2-(N,N-Diethylamino)-diazenolate-2-oxide-diaethylammonium salt (DEANO-NOate, Enzo Life Science, Lörrach, Germany) was dissolved in 96 % Ethanol to a concentration of 100 mM and stored at -20 °C for at most 1 week. This stock solution was diluted to concentrations of 500 µM - 2 mM in DMEM immediately before the treatment.

2.3.2 Inhibitors of apoptosis

Derivates of **m**itochondrial **div**ision **i**nhibitor 1 (mdivi-1) named A, B, C, E and G (kindly provided by Jodi Nunnari, UC Davis, California, USA and from Enzo Life Science, Lörrach, Germany) were dissolved in DMSO at stock concentrations of 10 mM (Figure 5). Mdivi-1 compounds were applied to the cell culture medium at final concentrations of 50 - 75 µM in HT-22 neurons and 25 µM in primary neurons, respectively. In order to analyze the toxicity of the solvents of the different chemical substances and inhibitors, the vehicle controls were always treated with medium containing the highest concentration of the solvent that was present at the highest applied concentrations of the active compounds during the experiment.

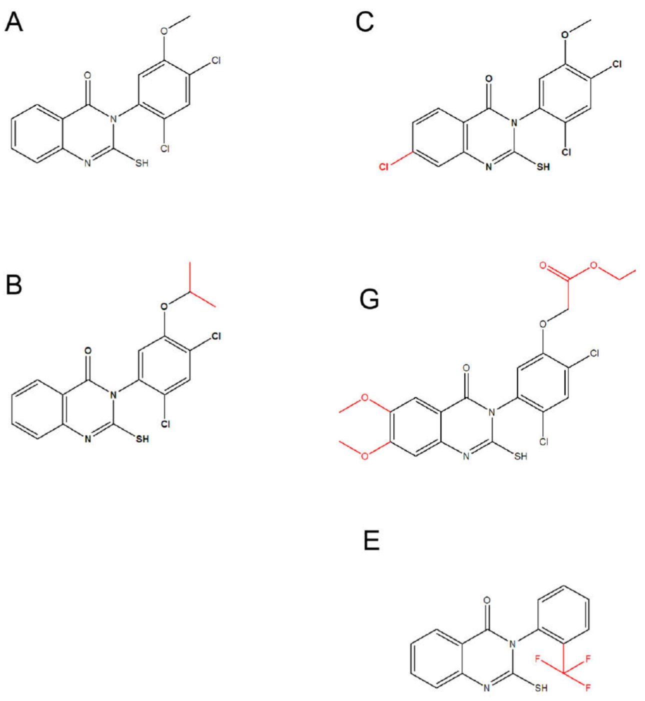

Figure 5 The chemical structure of mdivi-1 representitive compounds A, B, C, E and G

Mdivi-1 is a derivative of quinazolinone. Compounds A and B have the highest efficacy, compounds C and E a moderate and mdiviG no efficacy to block mitochondrial dynamin-related protein GTPase activity. The structural differences between each molecule and mdiviA are highlighted in red (adopted from Cassidy-Stone et al., 2008 (125)).

Bid inhibitor BI-6c9 (Sigma-Aldrich, Taufkirchen, Germany) was dissolved in dimethyl sulfoxide (DMSO) to a stock concentration of 10 mM (Figure 6). It was used at a final concentration of 10 µM in DMEM and 1x EBSS for applications in HT-22 neurons and primary rat neurons, respectively.

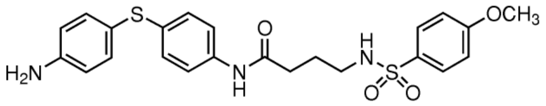

Figure 6 The chemical structure of the Bid inhibitor BI-6c9

2.3.3 Transfection reagents

Lipofectamine 2000 and Opti-MEM I (both obtained from Invitrogen, Karlsruhe, Germany) was used to form DNA- or siRNA transfection complexes. Lipofectamine 2000 (Invitrogen, Karlsruhe, Germany) was used at a final concentration of 1.5 µl/ml in antibiotic-free DMEM medium to complex DNA plasmids or siRNA.

2.3.3.1 Plasmid vectors

The mitoGFP (mGFP) vector was a kind gift from Andreas Reichert (Goethe University Frankfurt, Frankfurt, Germany). The tBid vector was generated as described previously (126). The plasmid pcDNA 3.1+ control vector was obtained from Invitrogen (Karlsruhe, Germany). All the plasmids were amplified using a QIAGEN Plasmid Plus Midi (Qiagen, Hilden, Germany) according to the manufacturer’s protocol. Prior to use, the plasmid DNA-concentrations were determined in a NanoVue Plus Spectrophotometer (Implem, GE Healthcare Europe GmbH, Freiburg, Germany), and digestion by restriction enzymes with subsequent gel electrophoresis analysis was performed.

2.3.3.2 SiRNA

Drp1 siRNA (On-target Plus siRNA Pool) and nonfunctional mutant siRNA (scrambled siRNA, 5’-AAG AGA AAA AGC GAA GAG CCA-3’) were purchased from Dharmacon (Thermo Scientific, Bonn, Germany). For RT-PCR, Drp1 primers were purchased from Eurofins MWG Operon (Ebersberg, Germany). (See also 2.10.3).

2.3.4 Primary antibodies

All primary antibodies were diluted in Tris-buffered saline with Tween 20 (TBST). The dilution of the Drp1-antibody (BD Bioscience Laboratories, Heidelberg, Germany) was 1:500, of AIF-antibody (Santa Cruz, Santa Cruz, California, USA) 1:500, α-tubulin-antibody (Sigma-Aldrich, Taufkirchen, Germany) was diluted 1:20,000, Tyrosine-nitrosylation, Bid, Bcl-xl, Bax, Bak-antibodies (Cell Signaling, Danvers, Massachusetts, USA and New England Biolabs GmbH, Frankfurt, Germany) were diluted 1:1,000. Fis-1-antibody (Enzo Life Science, Lörrach, Germany) was used at a dilution of 1:1,000, and anti-actin antibodies (Cell Signaling, Danvers, Massachusetts, USA, and New England Biolabs GmbH, Frankfurt, Germany) were used at dilution of 1:10,000.

2.3.5 Secondary antibodies

All secondary antibodies were purchased from Vector Labs (Burlingame, California, USA). Horse radish peroxidase (HRP) labeled anti-mouse IgG (H+L), anti-goat IgG (H+L) and anti-rabbit IgG (H+L) secondary antibodies were used for western blot at dilutions of 1:2,000 - 1:5,000 in TBST. Biotinylated anti-goat, anti-mouse and anti-rabbit IgG (H+L) antibodies were used for immunocytochemistry in a 1:200 dilution in phosphate buffered saline (1x PBS) containing 3 % horse serum (Invitrogen, Karlsruhe, Germany).

2.3.6 Kits

Following kits were used in this work and applied following the manufacturer's instructions:

Table 2 Kits

Kit	Company	
Annexin-V-FITC Detection Kit	Promokine	Heidelberg, Germany
Bodipy (581/591 C11)	Invitrogen	Karlsruhe, Germany
JC-1	Invitrogen	Karlsruhe, Germany
Lipofectamine 2000	Invitrogen	Karlsruhe, Germany
NucleoSpin RNA II Kit	Machery & Nagel	Düren, Germany
Pierce BCA Kit	Perbio Science	Bonn, Germany
QIAGEN Plasmid Plus Midi	Qiagen	Hilden, Germany
ViaLight® HS Kit ATP-detection	Lonza	Köln, Germany

2.4 Cell culture methods

2.4.1 Cell culture and induction of neuronal cell death

2.4.1.1 Cell culture media of HT-22 neurons

Dulbecco’s modified eagle medium with 4.5 g/l glucose and sodium pyruvate (DMEM) for culturing HT-22 neurons was prepared as described in Table 3. All reagents were obtained from PAA (Cölbe, Germany).

Table 3 Dulbecco’s modified eagle medium (DMEM)-Medium

DMEM + 4.5 g/l glucose + sodium pyruvate	500	ml
10 % FCS Gold	50	ml
L-alanyl-L-glutamine 200 mM	5	ml
Penicillin/Streptomycin 100x	5	ml

Table 4 1x Trypsin/EDTA (1x TE)

0.05 % Trypsin	100	mg
0.02 % EDTA	40	mg
1x PBS ad	200	ml

All reagents for 1x TE were obtained from Sigma Aldrich (Taufkirchen, Germany).

Glutamate (1 - 5 mM) was added to the serum containing medium and cell viability was evaluated 12 - 18 h later.

2.4.1.2 Induction of neuronal cell death in HT-22 neurons

HT-22 neurons were obtained from Gerald Thiel with kind permission of David Schubert (Salk Institute, San Diego, California, USA). The HT-22 line was originally selected from HT-4 cells based on glutamate sensitivity. HT-4 cells were immortalized from primary hippocampal neurons using a temperature-sensitive SV-40 T antigen (127). They were cultured in T75 flasks and split 1:10 - 1:20 every 3 - 4 days. This was performed as follows: growth medium was replaced by 2 ml 1x PBS containing 0.05 % trypsin and 0.02 % ethylenediaminetetraacetic acid disodium salt (EDTA) (1x TE, Invitrogen, Karlsruhe, Germany). Afterwards, cells were incubated 2 - 5 min. at 37 °C. After detaching of the cells, trypsin was inhibited by adding serum containing growth medium. The cells were centrifuged at 1,000 x g; the cell pellet was resuspended in fresh growth medium. Then cells were seeded in 6-well plates with a density of 2.5 x 10^5 cells per well, in 24-well plates with a density of 6 - 8 x 10^4 cells per well or in 96-well plates with a density of 7 - 8 x 10^3 cells per well for further treatment. Induction of apoptosis was performed 24 h after seeding of the cells. Growth medium was removed and replaced by medium containing inhibitors and inducers of apoptosis. Between 3 h and 18 h later, cells were analyzed following standard procedures for flow cytometry, epifluorescence microscopy, protein or RNA analysis. To harvest cells for flow cytometry, epifluorescence microscopy or protein analysis, 100 µl of 1x TE was used per well for a 24-well plates. For analysis by epifluorescence microscopy after respective treatments, the cells were fixed with 4 % paraformaldehyde (PFA) and stained with the fluorescent DNA-binding dye 4',6-diamidino-2-phenylindole dihydrochloride (DAPI, Sigma-Aldrich, Taufkirchen, Germany).

2.4.1.3 Cell culture medium of primary embryonic cortical neurons of rat

For culturing of primary embryonic rat cortical neurons, cell culture dishes were coated one day before preparation with 5 % polyethylenimine (PEI). Coating was performed by incubation with 5 % PEI for 2 h at room temperature. The dishes were washed twice with bidest water and dried under UV-light. Cell dishes were filled up with MEM+ and incubated overnight in the cell incubator with 37 °C and 5 % CO_2.

Table 5 5 % PEI

Boric acid	3.1	mg
Borax	4.75	mg
PEI	1	ml
Bidest H_2O ad	1000	ml

Primary rat embryonic cortical neurons were cultured in neurobasal medium with 2 % (v/v) B-27 supplement. All mediums were obtained from Invitrogen (Karlsruhe, Germany). Chemical substances were obtained from Sigma-Aldrich (Taufkirchen. Germany).

Table 6 Neurobasal medium (NB)

Neurobasal	500	ml
HEPES 4-(2-hydroxyethyl)-piperazine-1-ethanesulfonic acid	0.573	g
L-glutamine	0.088	g
Gentamycin sulfate (10 mg/ml)	0.5	ml
2 % (v/v) B-27 50x	10	ml

Additional following mediums were used:

Table 7 Eagle's minimum essential medium (MEM)

MEM - Phenolrot	4.695	mg
1 mM HEPES-	4.75	mg
26 mM $NaHCO_3$	1.1	g
40 mM Glucose	5	g
20 mM KCl	0.605	g
1 mM Na-pyruvate	0.6	g
1.2 mM L-glutamine	0.088	g
10 % (v/v) FCS	1000	ml
10 % (v/v) gentamycin sulfate	0.5	ml
Bidest H_2O	450	ml

Table 8 Hank's balanced salt solution (1x HBSS) pH 7.2

10x HBSS	50	Ml
HEPES	0.573	g
Gentamycin sulfate (10 mg/ml)	0.5	ml
2 % (v/v) B-27 50x	10	ml
Bidest H_2O ad	500	ml

Table 9 1x EBSS pH 7.2, obtained as 10x solution from Invitrogen (Karlsruhe, Germany)

NaCl	6.8	g
KCl	0.4	g
$CaCl_2$ x $2xH_2O$	0.264	g
Cl_2 x 7 H_2O	0.2	g
$NaHCO_3$	2.2	g
NaH_2PO_4 x H_2O	0.14	g
Glucose	1	g
Bidest H_2O ad	1000	ml

In 6 to 10 day-old primary neurons, the culture medium was replaced with Earl's balanced salt solution (1x EBSS) medium immediately before glutamate treatment (20 - 30 µM, 18 - 24 h). At 6 - 8 days *in vitro* (DIV), these neurons express NMDA receptors and are therefore susceptible to glutamate-induced excitotoxicity. For oxygen glucose deprivation (OGD), glucose-free 1x EBSS medium supplemented with gentamycin (5 mg/l) was prepared.

2.4.1.4 Induction of neuronal cell death in primary rat neurons

Embryonic hippocampal or cortical cultures: brains were removed from embryonic day 17 Sprague-Dawley rats (Charles River Laboratories, Sulzfeld, Germany) and hippocampi and cortices separated and each dissociated by mild trypsinization and trituration as follows. Isolated hippocampi and cortices were separately incubated for 15 min. in a solution of 1 mg/ml trypsin (Sigma, Taufkirchen, Germany) in Ca^{2+}- and Mg^{2+}-free 1x HBSS (made from 10x HBSS, Invitrogen, Karlsruhe, Germany) at 37 °C. The separated hippocampi and cortices were then rinsed with fresh 1x HBSS, exposed for 2 min. with 1 mg/ml trypsin inhibitor (Sigma, Taufkirchen, Germany), and then washed twice with 1x HBSS. Cells were mechanically dissociated by trituration using a 10 ml standard glass pipette (VWR International GmbH, Darmstadt, Germany). The triturated cells were centrifuged at 1,000 x g for 5 min. at room temperature. The supernatant was removed and the cells were again triturated in MEM+ before counting in a cell counting chamber (Neubauer Zählkammer). The cells were then seeded onto 96-well-plates with 8 or 16 x 10^4/cm^2 cells, 35 mm polyethylenimine (PEI)-coated culture dishes (for survival analysis) with or without containing glass coverslips (for immunocytochemistry) with 4 or 5 x 10^4/cm^2 cells or 60 mm culture dishes (for immunoblot analysis) with 8 x 10^4/cm^2 cells containing 1 ml or 2 ml MEM+, respectively. After 4 h of incubation, the MEM+ was replaced with NB+-Medium and after five days in culture the medium was exchanged. Since cultures of primary neurons develop functional glutamate receptors after 6 - 8 days in culture, experimental treatments were performed with 8 - 10-day old cultures in 1x EBSS. Apoptosis was induced by glutamate (20 - 30 µM) in 1x EBSS and quantified 18 - 24 h later. Cells were treated with mdiviA or mdiviB 25 µM in 1x EBSS. After 18 to 24 hours the neurons were fixed with 4 % PFA and stained with the fluorescent DNA-binding dye DAPI (Sigma-Aldrich, Taufkirchen, Germany). Living and pyknotic cells were counted using a fluorescence microscope (DMI6000B, Leica, Wetzlar, Germany) without knowledge of the treatment history. For the quantification of apoptotic cells, five hundred cells from five areas per cell culture dish were counted in total and experiments were performed at least three times with n=5 per treatment condition.

2.4.1.5 Oxygen glucose deprivation (OGD)

Oxygen glucose deprivation (OGD) in neuronal cultures is an *in vitro* model for cerebral ischemia that is based on the application of medium without glucose and the deprivation of oxygen by exposure to a mixture of 5 % carbon dioxide (CO_2) and 95 % nitrogen (N_2) in an air-tight chamber. The air-tight chamber is located in an incubator to obtain a temperature of 37 °C and linked to a gas bottle containing the mixture of 5 % carbon dioxide and 95 % N_2. The oxygen concentration is controlled by an oxygen sensor (Oxy 3690 MP, Greisinger electronic, Regenstauf, Germany) that also regulates the influx of the mixture. To prevent the desiccation of the dishes, a cup filled with ultrapure water was placed in the air-tight chamber. All dishes were opened when they were placed in the chamber to ensure rapid oxygen deprivation in the samples. Validation of the chamber and the protocol was performed by using the NMDA receptor antagonist MK-801, because it has been shown that NMDA glutamate receptor inhibition by MK-801 significantly reduced OGD-induced neuronal cell death (128).

Primary cortical or hippocampal neurons were seeded onto 35-mm culture dishes with $5 \times 10^4/cm^2$ cells. At day 8 or 9 in culture the dishes were separated into two groups, one for the OGD chamber and one control group. First, all dishes were washed twice with 1x EBSS without glucose. For OGD the cells were treated with mdiviA or mdiviB 25 µM in 1x EBSS without glucose and transferred to the chamber containing 5 % carbon dioxide (CO_2) and 95 % N_2 for 4 h. The analogue treatment in 1x EBSS containing glucose or neurobasal was applied to the control cells in the regular oxygen-containing incubator. After four hours of OGD, the 1x EBSS +/- glucose was replaced by NB+-medium containing glucose to all dishes and the cells were incubated for another 18 - 24 hours. For counting analysis of cell death, cells were fixed with 4 %

PFA and stained with the fluorescent DNA-binding dye DAPI (Sigma-Aldrich, Taufkirchen, Germany). Living and pyknotic cells were counted using a fluorescence microscope (DMI6000B, Leica, Wetzlar, Germany) without knowledge of the treatment history. For the quantification of apoptotic cells, five hundred cells from five areas per cell culture dish were counted in total and experiments were performed at least three times with n=5 per treatment condition.

2.4.2 Transfection protocols

HT-22 neurons were transfected in 24-well plates 24 hours after seeding at a density of 6 - 7 x 10^4 cells per well. Antibiotic containing growth medium was replaced by 900 µl antibiotic free DMEM per well.

2.4.2.1 DNA-transfection

Lipofectamine 2000 (Invitrogen, Karlsruhe, Germany) and the respective DNA plasmids were dissolved separately in Opti-MEM I (Invitrogen, Karlsruhe, Germany). After 10 min. of equilibration at room temperature each DNA solution was combined with the respective volume of the Lipofectamine 2000 solution, mixed gently, and allowed to form plasmid liposomes for further 20 min. at room temperature. The transfection mixture was added to the antibiotic-free cell culture medium to a final concentration of 1 µg DNA and 1.5 µl/ml Lipofectamine 2000 in HT-22 neurons. Controls were treated with 100 µl/ml Opti-MEM I only, and vehicle controls with 1.5 µl/ml Lipofectamine 2000. Cells were transfected for at least 24 h before further treatment.

2.4.2.2 SiRNA-transfection

For siRNA transfections, Lipofectamine 2000 (Invitrogen, Karlsruhe, Germany) and Drp1 siRNA or non-functional scrambled siRNA were dissolved separately in Opti-MEM I (Invitrogen, Karlsruhe, Germany). After 10 min. of equilibration at RT, each siRNA solution was combined with the respective volume of the Lipofectamine 2000 solution, mixed gently, and allowed to form siRNA liposome complexes for further 20 min. at room temperature. The transfection mixture was added to the antibiotic-free cell culture medium to a final concentration 60 - 80 nM siRNA and 1.5 µl/ml or 2 µl/ml Lipofectamine 2000 in HT-22 cells. Controls were treated with 100 µl/ml Opti-MEM I only, and vehicle controls with 1.5-2 µl/ml Lipofectamine 2000.

2.4.3 Morphological cell viability analysis

For morphological analysis of cell viability, transmission light microscopy of living HT-22 neurons or primary neuronal cultures growing as monolayers was performed using an Axiovert 200 microscope (Carl Zeiss, Jena, Germany) equipped with a Lumenera Infinity 2 digital camera (Lumenera Corporation, Ottawa, Canada). Light was collected through a 10 x 0.25 NA objective (Carl Zeiss, Jena, Germany), and images were captured using phase contrast. Digital image recording and image analysis were performed with the INFINITY ANALYZE software (Lumenera Corporation, Ottawa, Canada). Light was collected through 5 x 0.12 NA. 10 x 0.25 NA or 32 x 0.40 NA objective (Carl Zeiss, Jena, Germany), and images were captured using phase contrast.

2.5 Cell viability assays

For cell viability assays, HT-22 neurons were grown in 96-well plates. Primary rat hippocampal neurons were grown in 35 mM dish. For the Annexin-V and JC-1 assay, HT-22 neurons were cultured in 24-well plates. MitoTracker DeepRed staining was performed in cells cultured on Collagen A-coated Ibitreat µ-slide 8-well plates (Ibidi GmbH, Munich, Germany) immediately before confocal microscopic analysis.

2.5.1 MTT-assay

Metabolic activity of HT-22 neurons was determined by using a 3-(4,5- Dimethylthiazol-2-yl)-2,5-diphenyltetrazolium bromide (MTT) reduction assay in 96-well plates: To each well 10 µl of a 5 mg/ml MTT solution (Sigma-Aldrich, Taufkirchen, Germany) in sterile 1x PBS buffer were added (final concentration/well: 0.5 µg/ml). Cells were incubated at 37 °C for 1 h, medium was removed and the samples were frozen at -80 °C for at least one hour. Afterwards, 100 µl of DMSO was added to solve the MTT dye and samples were incubated at 37 °C for 30 min. under constant shaking. Absorbance was measured at 570 nm (versus the reference wavelength 630 nm) using a microplate reader (Fluostar OPTIMA, BMG Labtech, Offenburg, Germany), and cell viability levels were expressed as percentage of absorption levels in untreated control cells (100 % viability). For statistical analysis the experiments were repeated at least three times.

2.5.2 ATP-assay

Adenosinetriphosphate (ATP) can be used to assess the functional integrity of living cells since all cells require ATP for survival and their energy-dependent specialized functions. Any form of cell injury results in a rapid decrease of cytoplasmic ATP-levels. The detection of ATP is based on a bioluminescent assay. The bioluminescent assay utilizes the enzyme luciferase which catalyzes the formation of light from ATP and luciferin according to the following reaction:

$$\text{ATP} + \text{Luciferin} + \text{O}_2 \xrightarrow[\textbf{Mg}^{2+}]{\textbf{Luciferase}} \text{Oxyluciferin} + \text{AMP} + \text{PPi} + \text{CO}_2 + \text{LIGHT}$$

For endpoint analysis of total ATP levels the ViaLight HS Kit (Lonza,Cologne, Germany) was used following the manufacturer’s instructions. HT-22 cells were seeded in white 96-well plates (Greiner, Frickenhausen, Germany) for luminescence measurements. Twenty four hours after seeding, the cells were damaged with glutamate 3 - 5 mM and treated with Drp1-inhibitors (75 µM) or BI-6c9 (10 µM). ATP levels were detected 3 - 18 hours after the onset of glutamate exposure by detection of luminescence. Briefly, the culture plate was allowed to cool down to room temperature for at least 5 minutes. In this time all reagents were prepared following the manual instructions. First, 100 µl of “nucleotide releasing reagent” (NRR) was added to each well and incubated for 5 minutes. The microplate reader (Fluostar OPTIMA, BMG Labtech, Offenburg, Germany) was primed with the “ATP monitoring reagent” (AMR) control solution and the software programmed to dispense automatically 20 µl into the appropriate wells and immediate measurement of the luminescence. The ATP release levels were expressed as percentage of luminescence levels in treated control cells (100 % ATP-release). For statistical analysis the experiments were repeated at least three times.

2.5.3 DAPI /Hoechst 33342 staining

At different time points after the onset of the different treatment conditions, cultured primary neurons were fixed for 15 min. in 1 ml of a 1x PBS solution containing 4 % PFA. The fixed primary neurons were stained for 15 min. in 35 mm-dishes with the fluorescent DNA binding dye 4’, 6-diamidino-2-phenylindole dihydrochloride (DAPI) or Hoechst 33342 (1 µg/ml in 1x PBS). After removing the fluorecent dyes, cells were washed twice with 1x PBS and kept in 1 ml 1x PBS. Stained nuclei were visualized under epifluorescence illumination (DMI6000B, Leica, Wetzlar, Germany with A4 (340 nm excitation and 510 nm barrier) filter) using a 40x objective. Neurons with condensed and fragmented nuclei were considered apoptotic. For the quantification of apoptotic cells, five hundred cells from five areas per cell culture dish were counted in total and experiments were performed at least three times with n=5 per treatment condition without knowledge of the treatment history. For statistical analysis the experiments were repeated at least three times.

2.5.4 Real-time measurements with xCELLigence System

The xCELLigence System (Roche, Penzberg, Germany) monitors cellular events in real time by measuring the electrical impedance between micro-electrodes integrated into the bottom of custom made tissue culture plates (E-plates). Since cells have a very high electrical resistance, the detected impedance increases with the area of the E-plate's well bottom covered by the cells. HT-22 cells were seeded at a density of 4,500 cells per well in 96-well E-plates (Roche, Penzberg, Germany). The electrical impedance, which is displayed as cell index (CI) as function of the time, was used to monitor the kinetics of cellular growth, cell viability and changes of cell morphology in a large number of tissue culture wells simultaneously throughout the experiments. It is important to note that the system is very sensitive to changes in temperature and therefore the medium was never removed completely to prevent a persistent breakdown of the impedance (129). At twenty-four hours after seeding of the HT-22 cells, cells were treated with glutamate or dependent on the experiment, with different compounds or siRNA. For statistical analysis the experiments were repeated at least three times.

2.6 Flow cytometric measurements

2.6.1 Annexin-V-FITC staining

Apoptotic cells were detected after labeling with Annexin-V and subsequent flow cytometry. Annexin-V binds in the presence of calcium to phosphatidylserine, which appears on the cell surface in early phases of apoptosis (130). Apoptotic cell death was detected by Annexin-V/Propidium iodide staining and subsequent flow cytometry analysis. Cells were harvested 14 h after glutamate-treatment by using 1x TE, washed once in 1x PBS and stained according to the manufacturer's protocol (Annexin-V-FITC Detection Kit, PromoKine, Promocell, Germany). Apoptotic and necrotic cells were determined using FACScan (BD Bioscience, Heidelberg, Germany). Annexin-V-FITC was excited at 488 nm and emission was detected through a 530 ± 40 nm band pass filter. Propidium iodide was excited at 488 nm and fluorescence emission was detected using a 680 ± 30 nm band pass filter. To exclude cell debris and doublets, cells were appropriately gated by forward versus side scatter and pulse width, and 1×10^4 gated events per sample were collected. Surviving cells did not show any staining whereas Annexin-V staining indicated apoptosis and cells positive for both Annexin-V and propidium iodide were regarded necrotic. The experiments were repeated at least three times.

2.6.2 Analysis of mitochondrial membrane potential with JC-1

Mitochondrial membrane potential of HT-22 neurons was determined by 5, 5', 6, 6'-tetrachloro-1, 1', 3, 3'-tetraethylbenzimidazolylcarbocyanine iodide (JC-1) reduction. HT-22 neurons were stained with JC-1 (Mitoprobe, Invitrogen, Karlsruhe, Germany) according to the manufacturer's protocol and analyzed by subsequent flow cytometry or epifluorescence microscopy. After glutamate treatment (12 h), JC-1 was added to each well of the different treatment conditions to a final concentration of 2 µM for 30 min. Living-control cells received vehicle (DMSO, 0.1 % final concentration) and damage-control cells were treated with carbonyl cyanide m-chlorophenylhydrazone (CCCP) 15 min. before staining to induce mitochondrial membrane depolarization. Detached cells in the medium were collected and combined with the attached cells harvested with standard Trypsin/EDTA (1x TE, Sigma-Aldrich, Taufkrichen, Germany) in 1x PBS. Trypsin incubation was stopped by adding 1 ml serum containing medium to each well. Cells were centrifuged at 1,000 x g for 5 min. at room temperature, washed once with 1x PBS, and kept in 0.5 ml 1x PBS on ice until analysis of JC-1 fluorescence using a FACScan (BD Bioscience, Heidelberg Germany). JC-1 green fluorescence indicating mitochondrial uptake of the dye was excited at 488 nm and emission was detected using a 530 ± 40 nm band pass filter. JC-1 red fluorescence indicating intact mitochondrial membrane potential was excited at 488 nm and emission was detected using a 613 ± 20 nm band pass filter. To exclude cell debris and doublets, cells were appropriately gated by forward versus side scatter and pulse width, and 1×10^4 gated events per sample were collected from 3 - 4 independent samples per treatment condition and the experiments were repeated at least three times.

2.6.3 Evaluation of oxidative stress/lipid peroxidation with Bodipy

Bodipy is a sensitive fluorescent reporter for lipid peroxidation, undergoing a shift from red to green fluorescence emission upon oxidation of the phenylbutadiene segment of the fluorophore. This oxidation-dependent emission shift enables fluorescence ratio imaging of lipid peroxidation in live cells. For detection of cellular lipid peroxidation, HT-22 neurons were seeded out in 24-well plates with 7×10^5 cells per well. After respective treatments the cells were loaded with 2 µM BODIPY 581/591 C11 for 60 min. in 1 ml DMEM per well. Cells were then harvested with standard Trypsin/EDTA (1x TE, Sigma-Aldrich, Taufkrichen, Germany) in 1x PBS with 100 µl/well. Trypsin incubation was stopped by adding 1 ml serum containing medium to each well. Cells were centrifuged at 1 000 x g for 5 min. at room temperature, washed with 1x PBS and resuspended in 1 ml 1x PBS. Detection of lipid peroxidation was performed by flow cytometry on a FACScan (BD Bioscience, Heidelberg, Germany) by using 488 nm UV line argon laser for excitation and lipid peroxidation emission was recorded on channels FL1 at 530 nm (green) and FL2 at 585 nm (red). To exclude cell debris and doublets, cells were appropriately gated by forward versus side scatter and pulse width, and 2×10^4 gated events per sample were collected from 3 - 4 independent samples per treatment condition and the experiments were repeated at least three times.

2.7 Immunocytochemistry

2.7.1 Mitochondrial staining

For detection of mitochondrial morphology changes during cell death, HT-22 neurons were transfected with the mGFP plasmid, respectively. Twenty-four hours after transfection HT-22 cells were seeded in ibidi µ-slide 8-well plates (Ibidi, Munich, Germany) at a density of 1.7×10^4 cells per well for endpoint analysis on a fluorescence microscope (DMI6000B, Leica, Wetzlar, Germany). Alternatively, mitochondria were visualized by MitoTracker Green / DeepRed according to the manufacturer’s protocol (Invitrogen, Karlsruhe, Germany). To 50 µg MitoTracker Green or DeepRed (Invitrogen, Karlsruhe, Germany) 74.4 µl DMSO were added. The resulting 1 mM solution was diluted 1:10,000 in DMEM and 300 µl were added to HT-22 neurons or primary rat cortical neurons after their respective treatment in Collagen A-coated Ibitreat µ-slide 8-well plate. Cells were incubated for 20 min. at 37 °C with the staining medium. Afterwards, the staining medium was replaced with DMEM and mitochondria were visualized using an epiflourescence (DMI6000B, Leica, Wetzlar, Germany) or confocal laser scanning microscope at an excitation wavelength of 488 nm (Axiovert 200, Carl Zeiss, Jena, Germany). Light was collected through a 40 x 1.3 NA, 63 x 1.4 NA or 100 x 1.3 NA oil immersion objective. MitoTracker Green fluorescence was excited at a wavelength of 488 nm and emission was detected using a 560 nm long pass filter. MitoTracker DeepRed fluorescence was excited at a wavelength of 620 nm band pass filter and emissions were detected using 670 nm long pass filter (red).

2.7.2 Evaluation of mitochondrial morphology

HT-22 cells were transfected with mGFP as described before. After 24 h the cells were reseeded on ibidi µ-slide 8-well plates (ibidi GmbH, Munich, Germany) and after additional 24 hours treated for 18 hours with glutamate (3 or 5 mM) and different mdivi compounds (75 µM) or BI-6c9 (10 µM), respectively. Endpoint pictures were taken after fixation with 4 % PFA and DAPI counterstaining of the nuclei 18 h after onset of treatment. Counting of three different types of mitochondrial states was performed in at least four independent experiments with five hundred cells. Three categories of mitochondrial morphology states were defined as follows: healthy cells display category 1, mitochondria form a tubular network. These mitochondria are equally distributed throughout the cytosol. Cells containing large round mitochondria distributed throughout the cytosol are defined as category 2. These cells do not show apoptotic features, e.g. shrunken nuclei, and are not detached. In contrast, damaged and dying cells contain smaller round heterogeneous mitochondria located close to the nucleus. These mitochondria are defined as category 3. For the quantification of mitochondrial morphology, five hundred cells per well/treatment condition were counted in total and experiments were performed at least three times without knowledge of the treatment history. For statistical analysis the experiments were repeated at least three times. For automated analyses of mitochondrial morphology changes, mitochondrial length was also calculated by ImageJ software (NIH, Bethesda, USA) from at least six independent pictures per experimental condition (92).

2.7.3 Immunocytochemistry of Drp1

For detection of Drp1 localization during apoptosis, HT-22 neurons were seeded in ibidi µ-slide 8-well plates (Ibidi GmbH, Munich, Germany) at a density of 1.7 x 10^4/well. After 24 hours cells were respectively treated and fixed for endpoint analysis with 4 % PFA. Culture medium was removed and cells were washed once with 1x PBS. Afterwards, cells were fixed in 1 ml 4 % PFA for 20 min., washed once in 1x PBS and then membranes were permeabilized by exposure for 5 min. to 0.4 % Triton X-100 (Sigma-Aldrich, Taufkirchen, Germany) in 1x PBS, and cells were placed in blocking solution (3 % horse serum (Invitrogen, Karlsruhe, Germany) in 1x PBS) for 30 minutes. Cells were then exposed to a polyclonal anti-Drp1 antibody (1:100 in block solution, BD Bioscience Laboratories, Heidelberg, Germany), overnight at 4 °C and subsequent 2.5 hours at room temperature, followed by an incubation for 2 hours with biotinylated anti-mouse IgG antibody (1:200, Vector Labs, Burlinghame, CA. USA) and 30 min. in the presence of streptavidin oregon green 514 conjugate (Invitrogen, Karlsruhe, Germany) according to the manufacturers protocol. The specificity of Drp1 immune reactivity was controlled by emission of the primary antibody in parallel staining of negative controls. Mitochondria were counterstained with Mitotracker DeepRed as described above. Images were acquired using a confocal laser scanning microscope (Axiovert 200, Carl Zeiss, Jena, Germany) equipped with an UV and an argon laser delivering light at 364 nm and 488 nm, respectively. Light was collected through a 63 x 1.4 NA oil immersion objective. Mitotracker DeepRed fluorescence was excited at 620 nm and emission was achieved by using the 690 nm long pass filter. Fluorescence of oregon green was excited at a wavelength of 488 nm and emission was detected using a 505 nm long pass filter. For digital imaging the software LSM Image Browser 4.2.0 (Carl Zeiss, Jena, Germany) was used.

2.8 Epifluorescence and confocal laser scanning microscopy (CLSM)

2.8.1 Epifluorescence microscopy

Imaging of mitochondrial morphology, JC-1-stained HT-22 neurons or DAPI-stained primary rat hippocampal neurons were performed using a DMI6000B fluorescence microscope, equipped with a DCF360FX-camera (Leica, Wetzlar, Germany). JC-1 green fluorescence was excited using a 480 ± 40 nm band pass filter, and emission was collected using a 527 ± 30 nm band pass filter (Filter L5, Leica, Wetzlar, Germany). JC-1 red fluorescence was excited using a 620 ± 60 nm band pass filter, and fluorescence emission was collected using a 700 ± 75 nm band pass filter (Filter Cy5, Leica, Wetzlar, Germany). DAPI fluorescence was excited using 360 ± 40 nm band pass filter, and emission was collected using a 470 ± 40 nm band pass filter (Filter A4, Leica, Wetzlar, Germany). For digital imaging the software LAS AF (Leica, Wetzlar, Germany) was used.

2.8.2 Confocal laser scanning microscopy

For detection of mitochondrial morphology changes and Drp1 localization during apoptosis, HT-22 neurons were immunostained as described before. Endpoint pictures were taken after fixation with 4 % PFA and DAPI counterstaining of the nuclei between 5 h to 17 h after onset of treatment. Images were acquired using a confocal laser scanning microscope (Axiovert 200, Carl Zeiss, Jena,Germany) equipped with an UV and an argon laser delivering light at 364 nm and 488 nm, respectively. Light was collected through a 40 x 1.3 NA, 63 x 1.4 NA or 100 x 1.3 NA oil immersion objective. Fluorescence of Mitotracker Green or Mitotracker DeepRed fluorescence was excited at 488 nm and 543 nm and emissions were observed using 505 - 530 nm band pass (green) or were excited at 514 nm and emission was achieved by using the 630 nm long pass filter (red), respectively. Fluorescence of oregon green was excited at a wavelength of 488 nm and emission was detected using a 505 nm long pass filter. DAPI fluorescence was excited at 364 nm and emission was achieved by using the 385 nm. For digital imaging the software LSM Image Browser 4.2.0 (Carl Zeiss, Jena, Germany) was used.

2.9 Protein analysis

For protein extraction and subsequent analysis, HT-22 neurons were grown at a density of 7 x 10^4 cells per well in 24-well plates or 2 x 10^5 cells per well in 6-well plates. Primary rat neurons were cultured in PEI-coated 60 mm culture dishes at a density of 2.5 x 10^6 cells per dish. Important to note for protein analysis every step was performed at 4 °C.

2.9.1 Protein sample preparation from HT-22 neurons

For western blot analysis, HT-22 neurons were harvested as described using 1x TE solution to detach cells. At least four wells per condition were pooled. Cells were washed in 1x PBS and lysed with 50 - 150 µl with protein lysis buffer. Protein extracts were kept on ice for 15 min. and then extracts were centrifuged at 15,000 x g for 15 min. at 4 °C to remove insoluble membrane fragments. The supernatants were stored at -80 °C until further use.

Table 10 Protein lysis buffer pH 7.8

0.25 M D-Mannitol	4.56	g
0.05 M Tris-base	0.788	g
1 mM EDTA	0.038	g
1 mM EGTA	0.038	g
Bidest H_2O ad	100	ml

The pH 7.8 was adjusted by concentrated HCl. This stock-buffer was stored in 10 ml aliquots in -20 °C. For 10 ml of working solution, the stock buffer was supplemented with:

DTT (100 mM)	0.1	ml
Triton X-100	0.1	ml
1 tablet/10 ml Complete mini protease inhibitor cocktail		
1 tablet/10 ml phosphatases inhibitor		

Complete mini protease inhibitor cocktail tablets and phosphatase inhibitor tablets contain a cocktail of several reversible and irreversible protease inhibitors and phosphatase inhbitors (Roche, Mannheim, Germany).

2.9.2 Immunoprecipitation of Drp1

The immunoprecipitation of Drp1 was performed by pull-down of Drp1 from total protein lysates according to the manufacturer's protocol (Invitrogen, Karlsruhe, Germany). Briefly, magnetic Dynabeads Protein A were prepared for each condition to effectively bind the Drp1-antibody (7.5 µg, BD Biocience Laboratories, Heidelberg, Germany). The Drp1-antibody is added to the Dynabeads Protein A for 30 min. to bind the Dynabeads via their Fc-region. For all washing steps the tube was placed on a Dynamagnet, where the beads migrate to the side of the tube facing the magnet and allow for easy removal of the supernatant. To avoid co-elution of the antibody and to increase the binding capacity of the antibody on the Dynabeads, crosslinking reaction with BS^3 was performed according to the manufacturer's protocol. The bead-bound antibody is now ready for immunoprecipitation. For immunoprecipitation of Drp1, 2.5 mg of total protein lysate of each treatment condition was incubated for one hour at room temperature (RT) followed by a second hour at 4 °C. The elution of Drp1 with its binding partners was performed by adding 70 µl of 2.5x sodium dodecyl sulfate (SDS) -sample buffer and afterwards boiling of this Dynabead-protein lysat-mix for 10 min. at 95 °C. Dynabeads were removed from the solution and the supernatant removed. The supernatant was stored at -80 °C. 30 µl of the eluat was loaded on a SDS-gel to detect protein-interaction partners of Drp1 by western blotting analysis. The regular protein lysate with 30 µg of protein per treatment condition was used as a control in the SDS-PAGE.

2.9.3 Determination of protein amount

Protein determination is one of the most common operations performed in biochemical research. The principle of the bicinchoninic acid (BCA)-assay is similar to the Lowry procedure, in that both rely on the formation of a Cu^{2+} protein complex under alkaline conditions, followed by reduction of the Cu^{2+} to Cu^{1+} by proteins (Biuret-reaction). The amount of reduction is proportional to the protein present. BCA forms a purple blue complex with Cu^{1+} in alkaline solutions. Responsible for this color reaction of the BCA are the macromolecular structures of the protein, the amount of peptides and the four amino acids cysteine, cystine, tryptophan and tyrosine. This provides a basis to monitor the reduction of alkaline Cu^{2+} by proteins and thus determine the protein concentration in biochemical samples and cell extracts (131).

Protein amounts in extracts were determined with the Pierce BCA kit (Perbio Science, Bonn, Germany). To this end, 5 µl of each sample were diluted in 95 µl 1x PBS. A standard curve containing 0 - 200 µg bovine serum albumin (Perbio Science, Bonn, Germany) per 100 µl, 5 µl of the respective lysis buffer and 1x PBS ad 100 µl was prepared. Then, 200 µl of a 1:50 mixture of reagent B : reagent A (Perbio Science, Bonn, Germany) was added to each sample. Samples were incubated for 30 min. at 60 °C; 100 µl of each sample were pipetted into a 96-well plate (Nunc, Wiesbaden, Germany). Absorption at 590 nm was determined using a microplate reader (Fluostar OPTIMA, BMG Labtech, Offenburg, Germany) and protein amounts of the test samples were calculated from the standard curve.

2.9.4 Polyacrylamid gel electrophoresis and western blot

Sodium dodecyl sulfate polyacrylamide gel electrophoresis (SDS-PAGE) is a technique widely used in biochemistry and molecular biology to separate proteins according to their electrophoretic mobility (a function of length of polypeptide chain or molecular weight). SDS gel electrophoresis of samples having identical charge per unit mass due to binding of SDS results in fractionation by size (132).

For SDS gel electrophoresis following solutions were used:

Table 11 0.5 M Tris pH 6.8

Tris-HCl	7.88	g
Bidest dH_2O ad	100	ml

The pH 6.8 was adjusted by concentrated HCl.

Table 12 1.5 M Tris pH 8.8

Tris-HCl	23.6	g
Bidest dH_2O ad	100	ml

The pH 8.8 was adjusted by concentrated HCl.

Table 13 10 % Ammoniumpersulfat (APS)

Ammoniumpersulfat	1	g
Bidest dH_2O ad	10	ml

Table 14 10 % Sodium dodecyl sulfate (SDS)

Sodium dodecyl sulfate (SDS)	1	g
Bidest dH_2O ad	10	ml

Table 15 Running gel 12.5 % and 15 %

1.5 M Tris	2.5	ml
30 % Acrylamid/Bis solution 37,5:1	3.34 or 5	ml
SDS	0.1	ml
10 % APS	0.05	ml
TEMED	0.01	ml
Bidest dH_2O ad	10	ml

Table 16 Stacking gel 3.5 %

0.5 M Tris	2.5	ml
30 % Acrylamid/Bis solution 37,5:1	1.2	ml
SDS	0.1	ml
10 % APS	0.05	ml
TEMED	0.01	ml
Bidest dH_2O ad	10	ml

Table 17 1x Electrophoresis buffer

Tris base	3	g
Glycine	14.4	g
SDS	1	g
Bidest dH_2O ad	1000	ml

Table 18 5x SDS-loading buffer

1 M Tris-HCl pH 6.8	7	ml
Glyerol	3	ml
SDS	1	g
D,L-dithiotreitol (DTT)	0.93	g
β-Mercaptoethanol	0,1	ml
Bromophenol blue sodium salt	1.2	mg

For Western Blot analyses following buffers were used:

Table 19 1x Transfer buffer

Tris base	3	g
Glycine	14.4	g
Methanol	100	ml
Bidest dH_2O ad	1000	ml

Table 20 1x TBS/Tween 20

Tris base	2,42	g
Sodium chloride	29,2	g
Methanol	100	ml
Tween 20	0,5	ml
Bidest dH_2O ad	1000	ml

Table 21 5 % Blocking buffer

non-fatty milk powder	5	g
TBST ad	100	ml

Table 22 Stripping buffer

Glycine	15	g
SDS	1	g
Tween 20	10	ml
Bidest dH_2O ad	1000	ml

The pH was adjusted to 2.2 by concentrated HCl.

An amount of 20 - 30 µg protein of each sample was filled up to 40 µl with bidest water. Afterwards, 8 µl of 5x SDS-loading buffer were added and boiled at 95 °C for 5 minutes. Then samples were loaded onto the gel and 10 µl of PageRuler™ Plus Prestained Ladder (Fermentas, St. Leon-Rot, Germany) were used on each gel as molecular weight marker. The electrophoresis was performed at 60 V for 20 min. and subsequent 125 V for one hour per 2 gels in electrophoresis buffer. After electrophoresis, proteins were blotted onto a polyvinylidenfluorid membrane (PVDF, Bio-Rad, Munich, Germany) according to the Bio-Rad protocol at 15 V for 90 minutes.

PVDF-Membrane was activated in methanol 2 min. and afterwards incubated for 10 min. in 1 x transfer buffer before blotting. In addition the two thick filter paper and the gels were also pre-incubated in 1x transfer buffer before blotting. The blotting was performed in a Trans-Blot SD semi-dry transfer cell (Bio-Rad, Munich, Germany) using extra thick filter paper (Bio-Rad, Munich, Germany) and 1x transfer buffer containing methanol. The blots were washed with TBST and blocked for 1 h in 5 % blocking buffer. Then blots were probed with an appropriate primary antibody in 5 % blocking solution at 4 °C overnight. Membranes were then exposed to the appropriate HRP-conjugated secondary antibody in 5 % blocking solution for one hour followed by washing three times with TBST for 15 min. binding was detected by chemiluminescence using HRP-Juice (PJK GmbH, Kleinblittersdorf, Germany).

Detection was performed using the Chemidoc-XRS System (Bio-Rad, Munich, Germany). Equal protein loading and quality was controlled by re-probing the membrane with the monoclonal anti-α-tubulin or anti-actin antibodies (Sigma-Aldrich, Taufkirchen, Germany) and the respective secondary antibodies. Chemidoc software (Bio-Rad, Munich, Germany) was used for quantification of western blot signals.

2.10 RNA analysis

For RNA extraction and subsequent analysis HT-22 neurons were grown at a density of 7 x 10^4 cells per well in 24-well plates.

2.10.1 RNA sample preparation

For RT-PCR analysis, HT-22 neurons were harvested in 1x PBS and then centrifuged at 1,000 x g at 4 °C for 10 min., the pellet was washed once in 1x PBS, and afterwards centrifuged again. NucleoSpin RNA II Kit was used for total RNA extraction according to the manufacturer’s protocol (Macherey und Nagel, Düren, Germany). Briefly, samples were dissolved in Nucleospin SDS-containing cell lysis buffer RA1 and β-mercaptoethanol (Merck, Darmstadt, Germany). To separate insoluble cell fragments, samples were filtered through Nucleospin Filter units. Ethanol was added to the filtrate and the sample was loaded onto a Nucleospin RNA II column. Salt and DNA were removed by membrane desalting buffer and a subsequent DNAse reaction, respectively. The membrane was washed with Nucleospin buffer RA2 and RA3. Finally, the purified RNA was eluted from the column with RNAse-free water. The RNA samples were stored at -80 °C until further use.

2.10.2 Determination of RNA amount

To determine the RNA amount in the samples, 4 µl were diluted in 156 µl RNAse-free water (Sigma-Aldrich, Taufkirchen, Germany). The RNA concentration was determined by UV absorption measurements, using NanoVue Plus Spectrophotometer (Implem, GE Healthcare Europe GmbH, Freiburg, Germany) at a wavelength of 260 nm. The quality of the purified RNA was determined at the reference wavelength of 280 nm. An OD of 1 at 260 nm represents a concentration of 40 µg/ml RNA.

2.10.3 One Step reverse transcriptase polymerase chain reaction (RT-PCR)

One-step RT-PCR was performed with SuperscriptIII One Step RT-PCR (Invitrogen, Karlsruhe, Germany). Primers for Drp1 and GAPDH were used as follows:

Table 23 Forward and reverse Primer sequence for Drp1 and GAPDH

Primer	Sequence
Drp1 forward	5`-ACAGGAGAAGAAAATGGAGTTTGAAGCAG-3`
Drp1 reverse	5`-AACAAATCCTAGCACCACGCAT-3`
GAPDH forward	5`-CGTCTTCACCACCATGGAGAAGGC-3`
GAPDH reverse	5`-AAGGCCATGCCAGTGAGCTTCCC-3

PCR for GAPDH and Drp1 was performed as follows: cDNA-synthesis at 60 °C for 30 min.; initial denaturation 95 °C for 2 min., amplification by 26 cycles of 30 s at 95 °C, 1 min. at 57 °C and 2 min. at 70 °C. The final extension was performed at 70 °C for 10 min. RT-PCR products were visualized under UV illumination after electrophoresis on a 1.5 % agarose gel containing ethidium bromide or SybrGold (Invitrogen Karlsruhe, Germany).

2.10.4 Agarose gel electrophoresis

Analysis of PCR amplification products was performed by fluorescence detection after agarose gel electrophoresis. To this end, 10 µl of each sample were mixed with 6x bromphenol blue containing loading buffer and were loaded onto a 1.5 % agarose gel containing ethidium bromide or SybrGold. The gel was prepared by dissolving 0.6 g agarose (Sigma-Aldrich, Taufkirchen, Germany) in 40 ml 1x TBE boiling everything up to 100 °C and adding 2 µl of a 0.5 mg/ml SybrGold or 5 µl of stock solution ethidium bromide (1 % in water) (Invitrogen, Karlsruhe, Germany) solution after cooling down to about 70 °C. The electrophoresis was performed for 70 min. at 80 V. 10 µl of 1,000 bp DNA-ladder (Fermentas, St. Leon-Roth, Germany) were used as a size marker. PCR amplification products were detected under UV light (excitation 260 nm) by photographing the emission light (560 nm) of ethidium bromide in the Chemidoc System (Bio-Rad, Munich, Germany).

Table 24 6x DNA loading buffer

0.5 M EDTA	2.4	ml
Glycine	12	ml
Bromphenol blue	0.04	g
Bidest dH_2O	5.6	ml

Table 25 1x TBE buffer

Tris-base	10.8	g
Boric acid	5.5	g
Disodium EDTA	0.75	g
Bidest dH_2O ad	1000	ml

Table 26 1.5 % Agarose gel

Agarose	0.6	g
1x TBE buffer	40	ml

2.11 Cerebral ischemia in mice

The middle cerebral artery occlusion (MCAo) experiments were performed in a blinded and randomized manner by Uta Mamrak (Ludwig-Maximillians-University, Munich, Germany). Male C57BL/6 mice (body weight, 18 - 22 g; Charles River, Wilmington, MA, USA) were subjected to transient MCAo as described previously (60;133). The Drp1 inhibitors mdiviA and B were injected i.p. at doses of 1 and 3 mg/kg body weight prior to the induction of MCAo. Surgery was performed in isoflurane/N_2O anesthesia (1.5 % isoflurane, 68.5 % N_2O, 30 % O_2). A silicone coated nylon monofilament was inserted into the internal carotid artery and gently pushed forward until blood flow in the MCA territory decreased to less than 20 % of baseline as determined by laser Doppler fluxmetry. Twenty four hours after MCAo animals were perfusion fixed with 4 % PFA. Thereafter brains were removed, post fixed in 4 % PFA over night, dehydrated, and embedded in paraffin. Twelve-fifteen sections (10 µm, 500 µm apart), including the middle cerebral artery territory, were stained with cresyl violet for quantification of infarct area. For each experimental group, 8 - 11 animals were used. Statistical analysis was performed using the Mann-Whitney-U-test. For determination of neuronal function mice were examined at one and 24 hours after reperfusion. The neuroscore was determined by the following criteria: 0: no deficit; 1: paralysis of the contralateral forepaw; 2: circling to the contralateral side; 3: loss of righting reflex; 4: no spontaneous motor activity.

2.12 Statistical analysis

All data are given as means ± standard deviation (SD) and means ± standard deviation of the mean (SEM) as indicated. For statistical comparison between two groups Mann-Whitney-U-test was used. Multiple comparisons were performed by analysis of variance (ANOVA) followed by Scheffé's post hoc test or Bonferroni test, as indicated. Calculations were performed with the Winstat standard statistical software package (R. Fitch Software, Bad Krozingen, Germany).

3 Results

3.1 Glutamate sensitivity of HT-22 cells

HT-22 neurons are immortalized hippocampal mouse neurons. This is an adhesive cell line with spindle shaped morphology that does not exhibit dendrites or axons. In these cells, glutamate (1 - 5 mM) induces toxicity by inhibition of the Xc-transporter and the subsequent glutathione (GSH) depletion mediates lethal oxidative stress and cell death in dose- and time-dependent manner (Figure 7A, B). After exposure to glutamate, HT-22 neurons round up and detach from the well bottom (Figure 7A). The glutamate toxicity was confirmed by endpoint measurements using the MTT assay and real-time analysis of the electrical impedance using the xCELLigence System (Figure 7A, B, C).

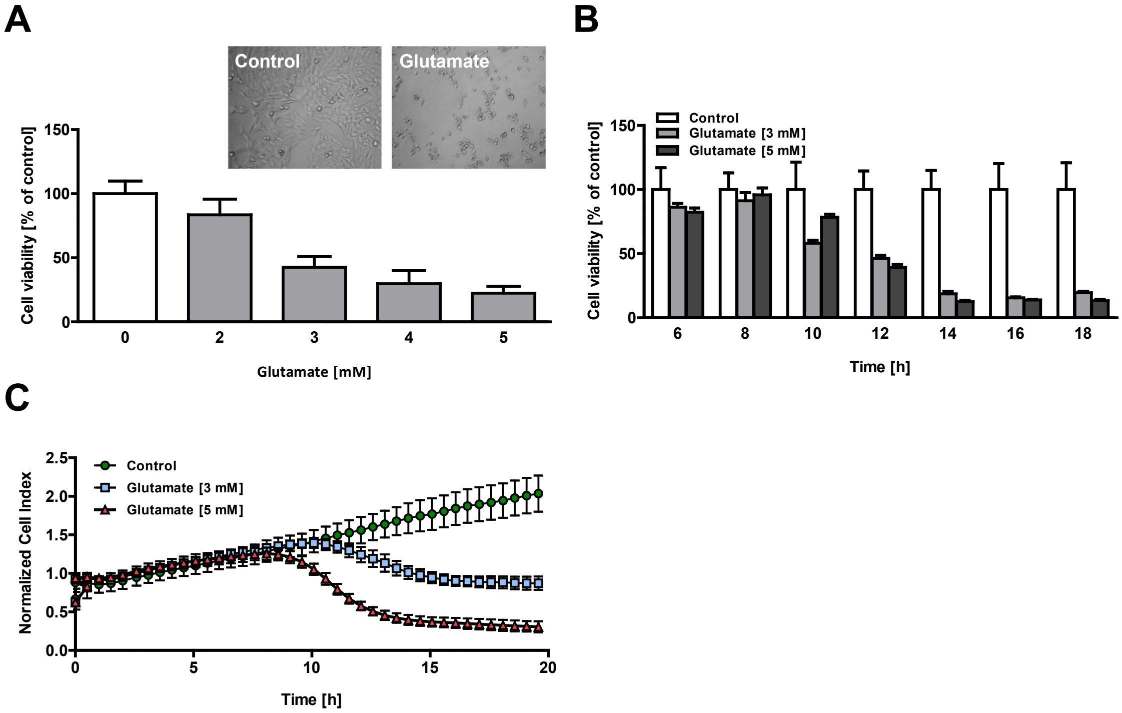

Figure 7 Glutamate-induced toxicity leads to loss of cell viability in HT-22 cells

HT-22 cells were seeded in 96-well plates with a density of 7,000 cells per well. **A**, Glutamate (1 - 5 mM) reduced cell viability of HT-22 neurons in a concentration-dependent manner as evaluated by MTT assay 18 h after onset of glutamate treatment (n=8). **B**, MTT assay evaluated glutamate-toxicity in a time-dependent manner with 3 and 5 mM in HT-22 cells for 6 - 18 h (n=8). **C**, HT-22 cells were seeded in 96-well E-plates with a density of 4,500 cells per well. Attaching and proliferation of the cells were observed over 48 h. After 24 h, cells were treated with glutamate 3 and 5 mM and real time detection of cellular impedance was done with xCELLigence System (Roche, Penzberg, Germany). HT-22 cells showed reduction of cell viability after 8 - 10.5 h glutamate treatment. After initiation of cell death, HT-22 cells died within 3 - 5 h (n=8). The experiments were repeated three times and the results presented as mean ± S.D.

Treatment of HT-22 cells with glutamate at concentrations of 3 mM and 5 mM resulted in a decrease of the Normalized Cell Index (NCI) between 8 and 10.5 h later, indicating progressive cell death (Figure 7B, blue and red graphs, glutamate 3 mM and 5 mM, respectively). It is interesting to note that, once started, the loss of cellular impedance was observed within a relatively small and constant time window of 3 - 5 h, suggested that cell death and detaching of the cells occurred rapidly and in a highly synchronized manner. In contrast, the control groups showed an increase of NCI, which was the cause of their normal growth (Figure 7B, green graph). It is important to note that sensitivity to glutamate toxicity varies in HT-22 neurons depending on their density and passage number. Therefore, experiments were always performed at different glutamate concentrations between 1 - 5 mM, and representative results are mostly shown from individual experiments where the respective glutamate concentration induced at least 50 % cell death as detected with the MTT assay. Glutamate-induced cell death was accompanied by a decrease of total ATP levels in the HT-22 cells. Glutamate (5 mM) led to a decrease of approximately 50 % of total ATP levels 6 h after induction of cell death (Figure 8A). The supposed increase of lipid peroxidation/ROS afer glutamate challenge was measured at different time points after onset of glutamate treatment using the fluorescent dye Bodipy (BODIPY® 581/591 C11 Invitrogen, Karlsruhe, Germany) followed by FACS analyses. The results obtained from cells exposed to glutamate for 6 h, 8 h and 17 h showed a time-dependent increase of lipid peroxidation/ROS formation. Glutamate induced a first increase of lipid peroxidation within 6 - 8 h after glutamate exposure, followed by a more pronounced, secondary accumulation at 17 h after glutamate treatment (Figure 8B).

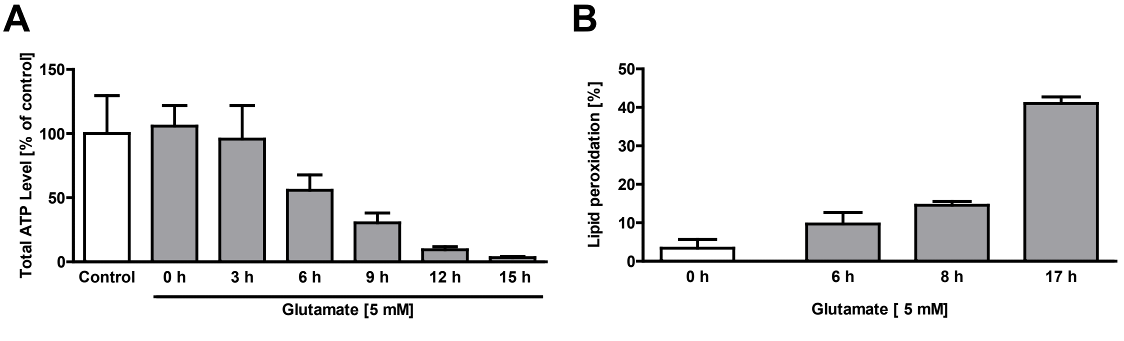

Figure 8 Glutamate-induced toxicity leads to ATP depletion and lipid peroxidation in HT-22 cells

A, HT-22 cells were seeded in 96-well plates with a density of 7,000 cells per well. ATP levels were determined by luminescence measurements. Total ATP levels are decreased after 6 h with glutamate (5 mM) in HT-22 cells (n=8). **B**, Glutamate induced the production of lipid peroxides. Glutamate treatment (5 mM) was performed for 6 - 17 h. After the addition of 2 µM Bodipy for 60 min., fluorescence was quantified by FACS analysis. Lipid peroxidation increased two fold 6 h after glutamate treatment with 5 mM. A second increase of lipid peroxidation was observed after 17 h (n=3). The experiments were repeated three times and the results presented as mean ± S.D.

3.2 Oxidative stress results in pronounced mitochondrial fragmentation

As described before, exposure of HT-22 neurons to glutamate resulted in enhanced lipid peroxidation and ROS formation in a time-dependent manner (Figure 8B). This ROS formation was associated with a significant change in mitochondrial morphology. For further quantification of mitochondrial fission in HT-22 cells, three categories of mitochondrial morphology were defined (Figure 9A). Healthy HT-22 cells predominantly expose category 1 mitochondria that form a tubular network. These mitochondria are equally distributed throughout the cytosol. Cells containing large round mitochondria distributed throughout the cytosol are defined as category 2 and these cells are still viable and do not show apoptotic features, such as, for example, pyknotic nuclei, and they are adherent to the well bottom. In contrast, damaged and dying cells show small rounded mitochondria of different sizes that are predominantly accumulated close to the nucleus. Cells containing such fragmented mitochondria are defined as category 3. To quantify mitochondrial morphology, cells were transfected with mGFP as described before and used for experiments 24 h after they were seeded out in 8-well ibidi slides. Mitochondrial categories were evaluated with five hundred cells per well without knowledge of the treatment history. In addition, mitochondrial length was quantified in six photomicrographs using the ImageJ image analysis software (Figure 9B).

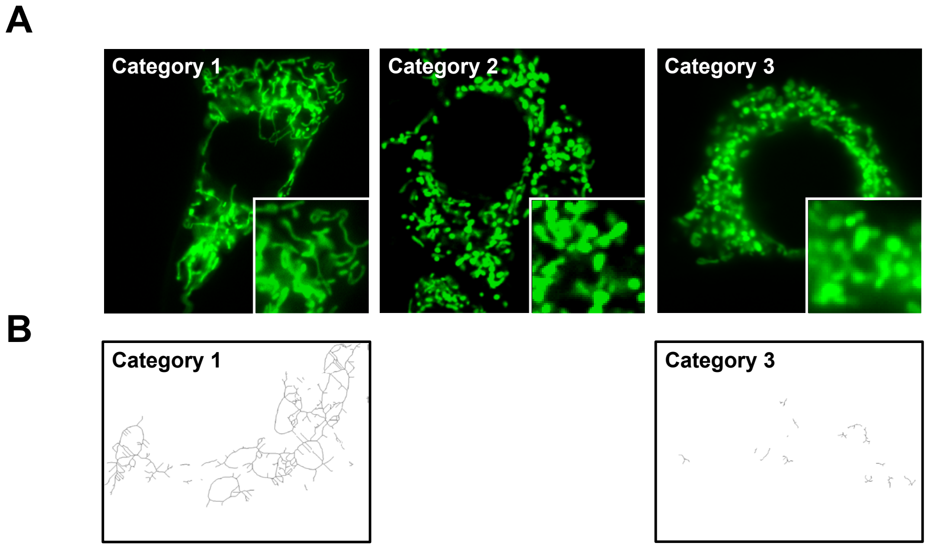

Figure 9 Classification of different morphology categories of mitochondria in HT-22 cells

A, Fluorescence photomicrographs (63x objective) showed mitochondria-targeting (mGFP)-transfected HT-22 cells which have different mitochondrial morphology structures. Category 1: elongated, tubulin-like, category 2: intermediate, category 3: fragmented. Magnifications for each category show mitochondrial morphology for each category in detail. **B**, Photomicrographs of analyzed mitochondria of categories 1 and 3 by ImageJ program.

As mentioned before mitochondria were organized as a tubular network under control conditions, however, after exposure to glutamate the mitochondrial network broke up in short tubules and small round fragments (Figure 10A). These changes resulted in a significant shortage of mitochondrial length (Figure 10B) and in an evident shift of mitochondrial morphology three hours after glutamate treatment from category 1 into categories 2 and 3 (Figure 10C). These changes, which are well in line with the definition of mitochondrial fission, were associated with a decrease of cell viability from 100 % to 20 % (Figure 7). The evaluation of the kinetics of this process of the organelle`s fragmentation showed that mitochondrial fragmentation started 3 - 4 h after glutamate exposure (Figure 10C) and was associated with increased ROS formation and lipid peroxidation (Figure 8B). The following decline of cell viability occurred 8 - 12 h after onset of the glutamate challenge, i.e. several hours after mitochondrial fission and at time points where mitochondrial depolarization became evident.

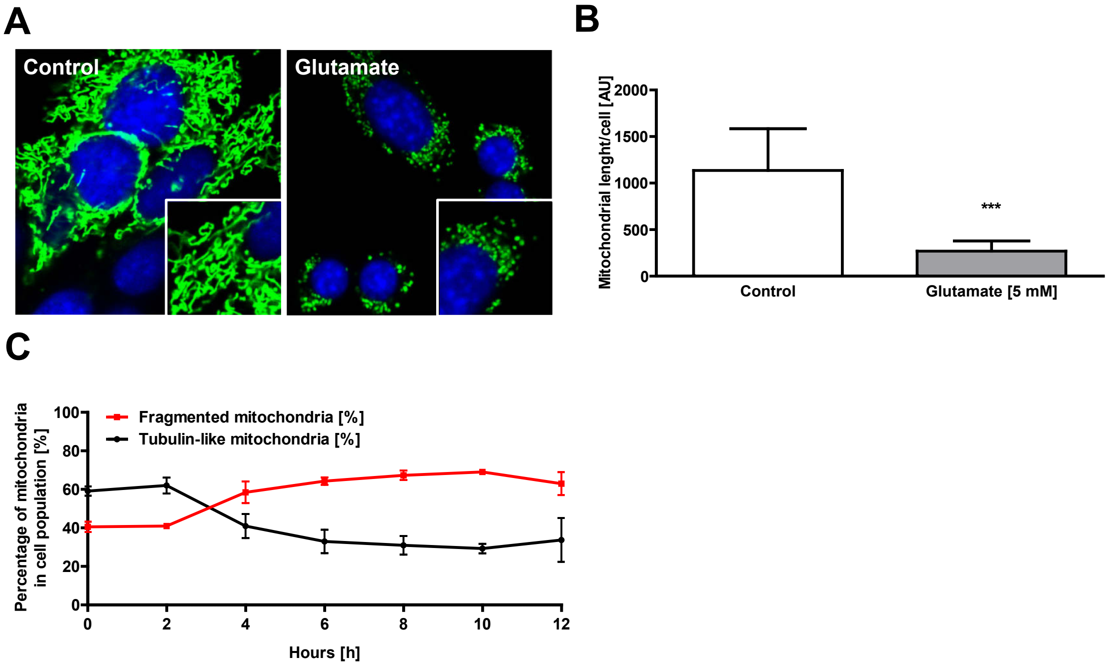

Figure 10 Oxidative stress induces pronounced fragmentation of mitochondria in HT-22 neurons

A, Fluorescence photomicrographs (63x objective) showed changes of mitochondrial morphology in HT-22 cells transfected with mGFP (green) and DAPI-stained nucleus (blue) treated with glutamate (5 mM) for 18 h. **B**, Mitochondrial length measurements of control and glutamate-treated HT-22 cells. Six Pictures were quantified as absolute values (AU) by the ImageJ program. **C**, Time-dependent shifting of mitochondria category 1 (tubulin-like) over 12 h to mitochondria category 3 (fragmented) in culture of HT-22 neurons. The increase of fragmented mitochondria of category 2 and 3 started 3 - 4 h after glutamate treatment (3 mM). The experiments were repeated three times and the results presented as mean ± S.D.

3.3 The BH3-only protein Bid is a mediator of glutamate-induced mitochondrial fission

3.3.1 Bid inhibition prevents fission of mitochondria in glutamate-induced cell death

It has been established that proapoptotic Bcl-2 protein family members such as Bax, Bak and Bid mediated mitochondrial dysfunction and associated death signaling in neurons (99;134;135), and a number of recent findings suggested that such intrinsic death pathways are associated with extensive mitochondrial fragmentation (3;13;51;57;136;137). The present study investigated, whether Bid is involved in the regulation of mitochondrial dynamics and associated with mitochondrial cell death pathways after induction of oxidative stress in HT-22 cells. Translocation of the proapoptotic Bcl-2 family member Bid to mitochondria results in AIF translocation to the nucleus and cell death, as previously evaluated in HT-22 cells expressing Bid-red fusion protein and AIF-GFP (39). To confirm the essential role of Bid in the regulation of mitochondrial dynamics, the specific Bid inhibitor BI-6c9 was applied in glutamate-induced neuronal death.

In the current experiments, the highly specific Bid inhibitor BI-6c9 blocked fission of mitochondria in glutamate-exposed HT-22 cells and prevented the shift of mitochondrial morphology from tubular, network-like structures (category 1) to small, round shaped and highly fragmented organelles (categories 2 and 3). Thus, in BI-6c9 treated cells, mitochondrial morphology was restored almost to control levels (Figure 11A and B). The preservation of mitochondrial morphology by BI-6c9 was associated with a normalization of mitochondrial membrane potential (Figure 14), suggesting that mitochondrial morphology is closely linked to mitochondrial function and that ROS-induced mitochondrial damage and loss of function are not the result of unspecific membrane damage, but of specific Bid-mediated cell death signaling.

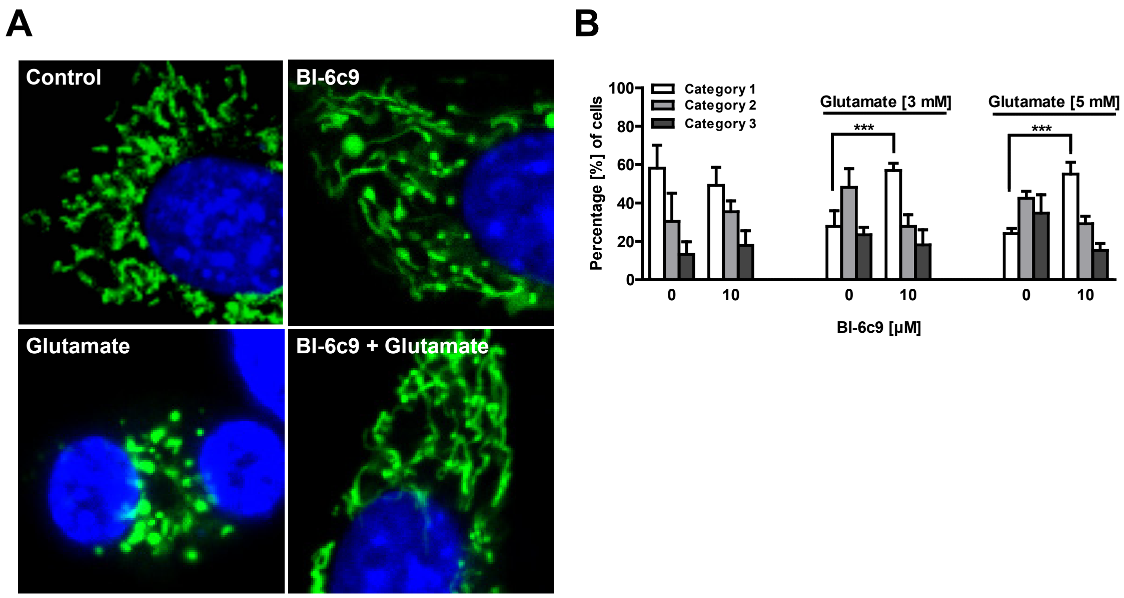

Figure 11 Bid inhibitor BI-6c9 prevents Bid translocation to mitochondria and mitochondrial fission

A, Fluorescence photomicrographs (63x objective) of mGFP-transfected and DAPI-stained HT-22 cells showed that Bid inhibitor BI-6c9 (10 µM) prevented fission of mitochondria in glutamate-exposed (5 mM, 18 h) HT-22 cells. **B**, Quantification of mitochondrial morphology of five hundred cells per condition. Category 1: elongated, tubulin-like, category 2: intermediate, category 3: fragmented. ***$p<0.001$ compared with glutamate 3 and 5 mM-treated cells (ANOVA, Scheffé's-test). The experiments were repeated three times and the results presented as mean ± S.D.

3.3.2 Mechanism of mitochondrial damage downstream of Bid

3.3.2.1 Restoration of mitochondrial morphology and function – effect on cell viability

Inhibition of Bid did not only result in the preservation of mitochondrial morphology and function, but also preserved cell viability in glutamate-treated HT-22 cells as demonstrated by the MTT assay and the novel xCELLigence System (Figure 12). While exposure to glutamate resulted in a reduction of cell viability from 100 % to 20 %, inhibition of Bid by BI-6c9 restored cell viability at almost baseline levels (Figure 12A). The protective effect of Bid inhibition could be confirmed by the real-time analysis of the electrical impedance using the xCELLigence System (Figure 12B). The NCI started to decrease after the treatment of HT-22 cells with glutamate at concentrations of 3 mM between 5.5 h and 7 h later, which indicated a progressive cell death (Figure 12B, red graph, glutamate 3 mM). The loss of cellular impedance in glutamate treated cells was observed within a relatively small and constant time window of 2 - 3 h, suggesting that cell death and detaching of the cells occurred rapidly and in a highly synchronized manner. Inhibition of Bid by BI-6c9 resulted in a complete protection of this delayed, glutamate-induced loss of the NCI and, hence, inhibition of cell death as also confirmed by the MTT assay. These data indicate that glutamate-induced ROS production induced specific, Bid-mediated cell death signaling, which result in a delayed loss of mitochondrial morphology and function, and ultimately cell death.

Photomicrographs confirmed the essential role of Bid in glutamate-induced neuronal death. HT-22 neurons exposed to glutamate for 17 h showed typical morphology of dying cells: the neuronal cells appear shrunken, rounded and detach from the culture dish (Figure 13A). HT-22 cells treated with the Bid inhibitor BI-6c9 retained their normal spindle-shaped morphology and were completely rescued from glutamate-induced cell death as determined by the MTT assay (Figure 12A). Cells treated with the Bid inhibitor alone, showed enhanced metabolic activity. In addition to the protective effect of BI-6c9 on cell viability, the Bid inhibitor also prevented significantly HT-22 cells from ATP depletion (Figure 13B).

Overall, these results reveal a major upstream role for Bid in mitochondrial damage, energy depletion, and subsequent execution of cell death in this model of glutamate-induced oxytosis.

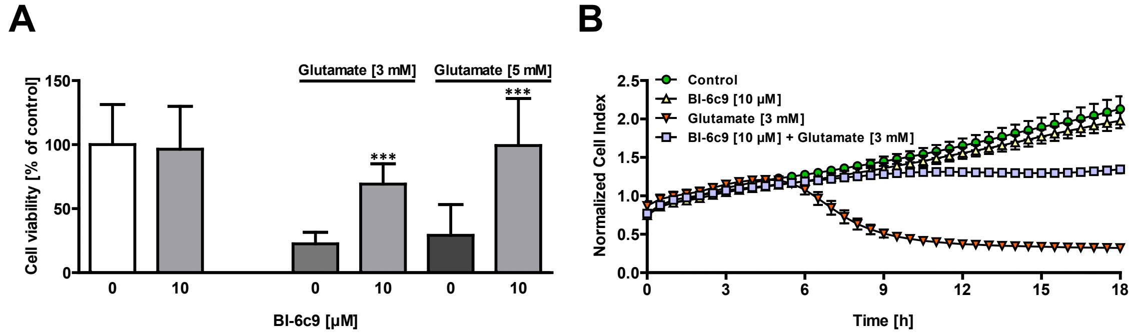

Figure 12 Bid inhibitor BI-6c9 protects HT-22 cells against glutamate-induced cell death

A, Quantification of glutamate-induced (3 and 5 mM, 17 h) sever cell damage and the protective effect of BI-6c9 (10 µM) by the MTT assay. HT-22 cells were seeded in 96-well plates with a density of 7,000 cells per well (n=8). ***p<0.001 compared to glutamate (3 and 5 mM)-treated cells (n=8) (ANOVA, Scheffé's-test). **B**, HT-22 cells were seeded in 96-well E-plates with a density of 4,500 cells per well and treated 24 h later with 3 mM glutamate for 20 h. Real time detection of cellular impedance was done with xCELLigence System (Roche, Penzberg, Germany). BI-6c9 showed an exerted persistent protective effect. All experiments were repeated three times and the results presented as mean ± S.D.

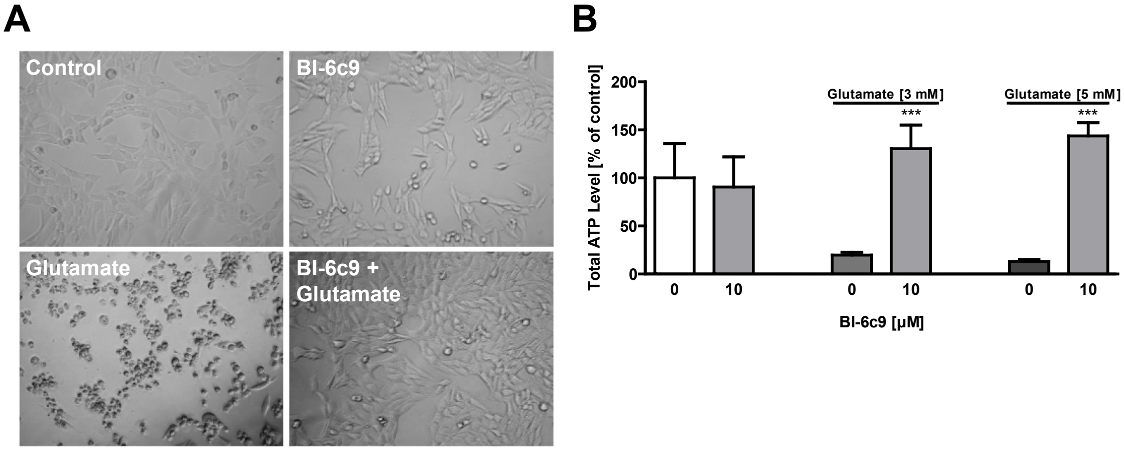

Figure 13 Bid inhibitor BI-6C9 protects HT-22 cells against glutamate-induced cell death and ATP depletion

A, Photomicrographs (10x objective) showed morphological evidence for severe damage of HT-22 cells 17 h after glutamate (3 mM) exposure. Glutamate-treated cells lose their spindle-like morphology, shrink and detach from the culture well bottom; in contrast, cells pretreated with the Bid inhibitor BI-6c9 (10 µM) are fully protected against glutamate-induced death and are not different from the controls. **B**, HT-22 cells were seeded in 96-well plates with a density of 7,000 cells per well. ATP levels were determined by luminescence measurements after glutamate (3 and 5 mM, 15 h) challenge. Bid inhibitor BI-6c9 (10 µM) prevents the glutamate-induced loss of ATP (n=8). ***p< 0.001 compared to glutamate 3 and 5 mM-treated cells (ANOVA, Scheffé's-test). All experiments were repeated three times and the results presented as mean ± S.D.

3.3.2.2 Mitochondrial membrane potential

Since Bid is supposed to act upstream of mitochondrial damage, the involvement of Bid in the breakdown of mitochondrial membrane potential was examined. Staining with JC-1 was used to evaluate the effect of Bid inhibition on glutamate-induced breakdown of the mitochondrial membrane potential. Glutamate treatment caused a significant loss of JC-1 red fluorescence, i.e. loss of mitochondrial membrane potential after glutamate treatment within 12 h (Figure 14A, B).

In the HT-22 neurons, glutamate was as effective as carbonyl cyanide chlorophenylhydrazone (CCCP) inducing mitochondrial membrane depolarization (Figure 14B). Treatment with the Bid inhibitor BI-6c9 prevented glutamate-induced breakdown of the mitochondrial membrane potential after 12 h. Further, the results presented here confirmed that depolarization of the mitochondrial outer membrane is an important key event of mitochondrial apoptosis induced by oxidative stress. Pharmacological inhibition of Bid prevented mitochondrial outer membrane depolarization, mitochondrial membrane integrity which was associated with preserved mitochondrial morphology and enhanced neuronal survival. Glutamate-induced mitochondrial fission in HT-22 neurons is associated with depolarization of the mitochondrial membrane, and both events are apparently Bid dependent.

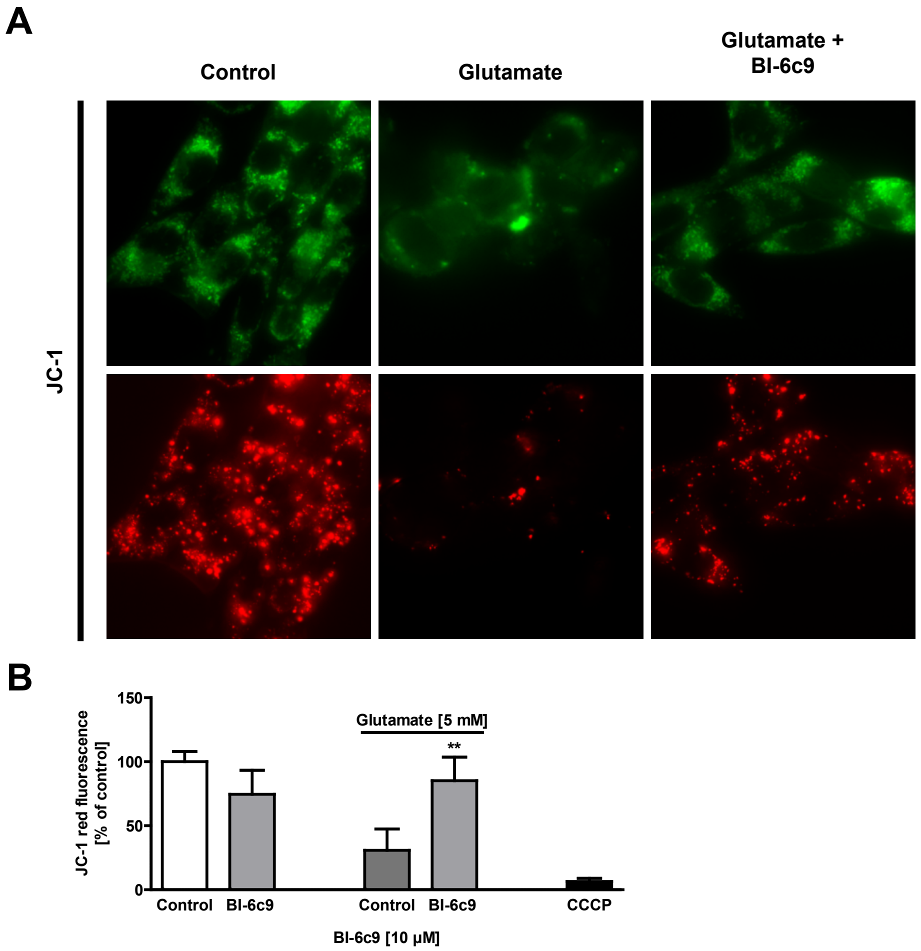

Figure 14 Bid inhibitor BI-6c9 prevents glutamate-induced mitochondrial depolarization

A, Mitochondrial membrane potential was analyzed by JC-1 fluorescence: upper panels showed epifluorescence photomicrographs (40x objective) indicating equal cellular uptake of JC-1 by green fluorescence, lower panels depicted mitochondria exposing red fluorescence. Glutamate-treated (5 mM, 12 h) HT-22 cells showed significantly reduced red fluorescence compared to controls whereas BI-6c9 (10 µM) prevented the breakdown of the mitochondrial membrane potential as indicated by preservation of the red JC-1 fluorescence. **B**, FACS analyses of n=3 per group revealed a decrease of the red JC-1 fluorescence to 30 % of control levels 12 h after glutamate treatment (5 mM) which is prevented by BI-6c9. Glutamate treatment was as effective as the positive damage-control CCCP, which causes a fast breakdown of the mitochondrial membrane potential. **p<0.01 compared to glutamate-treated cells (ANOVA, Scheffé's-test). The experiments were repeated three times and the results presented as mean ± S.D.

3.3.3 Specificity of the Bid inhibitor

The presented data demonstrated a role for the proapoptotic BH3-only protein Bid in enhanced mitochondrial fragmentation in the oxytosis model systems of HT-22 cell. Oxytosis, or oxidative glutamate toxicity, is a particular type of oxidative stress caused by exposure of neurons to glutamate. This happens most commonly *in vivo* due to stroke, which leads to the release of glutamate from dead and dying neurons. Oxytosis leads to a distinct mode of cell death separate from that caused by excitotoxicity. When neurons are exposed to high levels of extracellular glutamate, the normal function of the cystine/glutamate antiporter Xct is inhibited. In recent studies it was additionally demonstrated, that Bid is involved in the loss of MOMP and release of mitochondrial AIF, thereby mediating delayed neuronal death after cerebral ischemia (60;134). The specificity of BI-6c9 in the presently used culture system was confirmed in HT-22 neurons transfected with a tBid expression vector. Overexpression of tBid reduced cell viability by approximately 70 %, whereas cells pretreated with the Bid inhibitor BI-6c9 were significantly protected from tBid-induced cell death (Figure 15A).

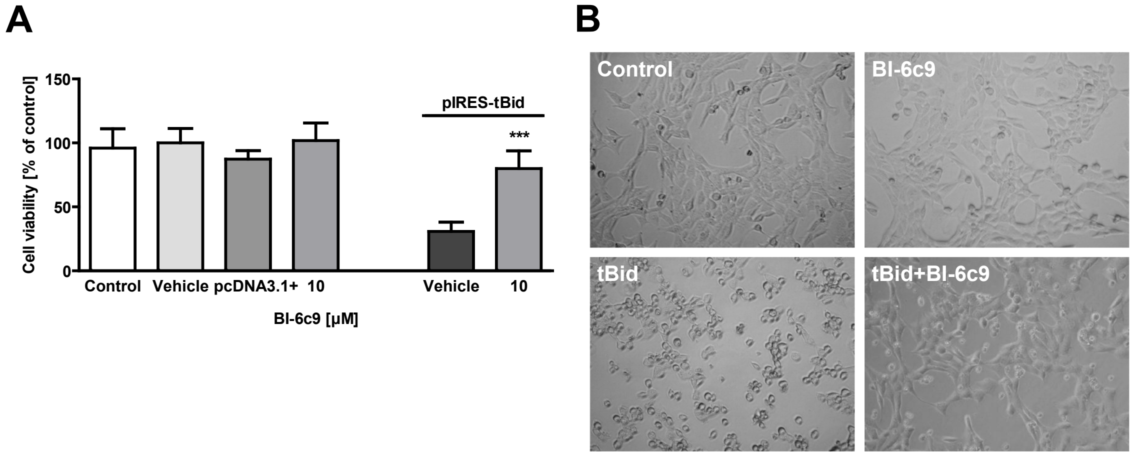

Figure 15 Inhibition of Bid by BI-6c9 prevents tBid-induced cell death

A, HT-22 neurons were pretreated with BI-6c9 (10 µM, 1 h) before transfection with a tBid expressing plasmid (pIRES-tBid) with the Lipofectamine 2000 protocol. MTT assay was used to determine the cell viability 14 h after tBid toxicity. Bid inhibitor BI-6c9 (10 µM, 1 h pretreatment) attenuated tBid toxicity. ***p<0.001 compared to tBid-transfected cells (n=8) (ANOVA, Scheffé's-test). **B**, Photomicrographs (10x objective) showed morphological evidence for severe damage of HT-22 cells 14 h after tBid toxicity. Similar to the glutamtate-treated cells, tBid toxicity induced loss of their spindle-like morphology, shrink and detach from the culture well bottom; in contrast, cells pretreated with the Bid inhibitor BI-6c9 (10 µM, 1 h pretreatment) are fully protected against tBid-induced death and are not different from the controls. The experiments were repeated three times and the results presented as mean ± S.D.

Photomicrographs confirmed the essential role of Bid in tBid-induced neuronal death. HT-22 neurons exposed to tBid for 14 h showed typical morphology of dying cells: the neuronal cells appear shrunken, rounded and detach from the culture dish (Figure 15B). HT-22 cells pretreated with the Bid inhibitor BI-6c9 retained their normal spindle-shaped morphology and were completely rescued from tBid-induced cell death as determined by the MTT assay (Figure 15A, B).

Additionally, this study revealed that glutamate-induced mitochondrial fragmentation also depended on tBid, since Bid inhibition by BI-6c9 prevented tBid-induced mitochondrial fission and preserved cell viability (Figure 16A, B). HT-22 cells transfected with tBid induced mitochondrial fragmentation, while treatment of BI-6c9 in combination with tBid preserved the tubulin-shaped mitochondrial morphology (Figure 16A). Quantification of mitochondrial morphology confirmed that BI-6c9 reduced the number of fragmented, shorter mitochondria of categories 2 and 3 in tBid-transfected HT-22 cells (Figure 16B).

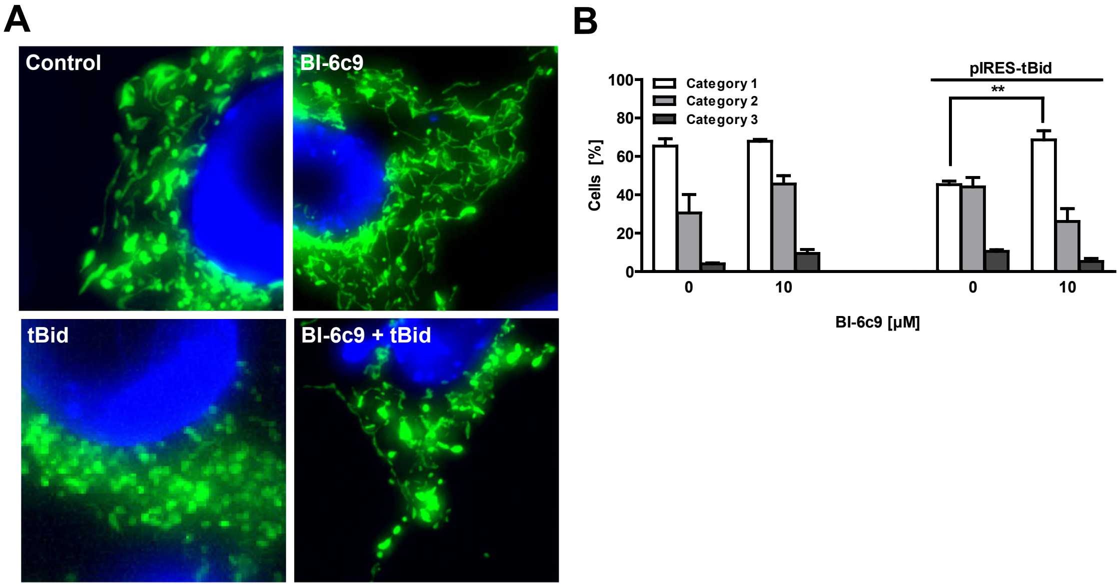

Figure 16 Inhibition of Bid by BI-6c9 prevents tBid-induced mitochondrial fragmentation in neuronal cell death

A, HT-22 neurons were pretreated with BI-6c9 (10 µM, 1 h) before cotransfection with an mGFP and a tBid expressing plasmid (pIRES-tBid) with the Lipofectamine 2000 protocol. Fluorescence photomicrographs (63x objective) of HT-22 cells showed tBid-induced mitochondrial fission and the Bid inhibitor BI-6c9 (10 µM) prevented fission of mitochondria in tBid-induced toxicity after 14 h in HT-22 cells (nucleus - in blue (DAPI)). **B**, Quantification of mitochondrial morphology of five hundred cells per condition. Category 1: elongated tubulin-like, category 2: intermediate, category 3: fragmented. **p<0.01 compared to glutamate (5 mM)-treated cells (ANOVA, Bonferroni-test). The experiments were repeated three times and the results presented as mean ± S.D.

It is important to note that overexpression of tBid may only partly reflect the mechanism of Bid-mediated death signaling, since Bid cleavage could not be detected in significant amounts in HT-22 cells after the glutamate challenge. However, BI-6c9 prevents translocation of full-length Bid to mitochondria, tBid-induced mitochondrial fission, tBid-mediated AIF release and cell death, suggesting that this model system is appropriate to mimic mechanisms mediating Bid-dependent neurotoxicity.

3.4 BI-6c9 prevents Drp1 translocation to the mitochondria in glutamate-induced cell death

There are a lot of speculations as to how Bcl-2 proteins are capable of regulating fission and fusion mechanisms of mitochondria. There is evidence that Bax, Bcl-xl and Bid are interact with Drp1, the main regulator of mitochondrial fission. Drp1 translocates after an apoptotic stimuli to the mitochondria, oligomerize and interacts on specific fission sites with the mitochondrial outer membrane to induce fragmentation of mitochondria (26;55;96;100;112;122;137). The initial data in this presented study upon the role of Bid in glutamate-induced neurotoxicity, suggested that Bid is a key regulator of glutamate-induced mitochondrial fission in HT-22 cells. But the exact mechanism, how Bid is involved and interacts with the mitochondrial fragmentation machinery in neuronal cell death is currently under consideration. Though, these data raised the questions, firstly, does Drp1 translocation occur in this model system of oxidative stress and secondly, can Bid influence the Drp1 translocation to induce enhanced fission after glutamate-induced toxicity in HT-22 cells. Experiments addressing these questions were performed by immunocytochemistry.

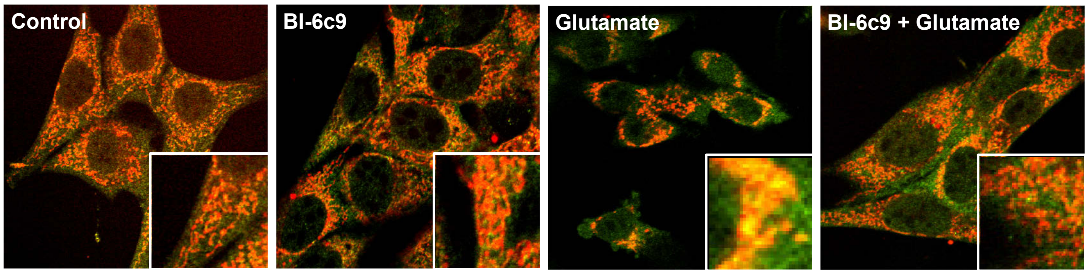

Figure 17 BI-6c9 inhibits glutamate-induced translocation of Drp1 to the mitochondria and prevents mitochondrial fission in HT-22 cells

HT-22 cells were cultured for 24 h in 8-well-ibidi-plates and treated with 3 mM glutamate and BI-6c9 (10 µM) for 17 h. Immunostaining of Drp1 revealed that Drp1 (green) translocation to the mitochondria (red) occured after glutamate stimulus. This is shown by overlapping of the fluorescence in yellow. Interestingly, BI-6c9 inhibited the translocation of Drp1 to the mitochondria and therefore mitochondrial fragmention.

This immunocytochemistry analysis revealed, that Drp1 (green) translocated to the mitochondria (red), where Drp1 formed clusters associated with mitochondria after glutamate treatment, concomitant with changes of mitochondrial shapes from tubulin-like structures to round fragmented bodies with perinuclear distribution (Figure 17). In control cells, mitochondria (red) are distributed as tubulin-like structures and Drp1 (green) is diffusely distributed in the cytosol. Treatment with the Bid inhibitor BI-6c9 prevented Drp1 translocation to the mitochondria and Drp1 clustering and the mitochondrial morphology was protected after glutamate toxicity, respectively.

In conclusion, glutamate toxicity induces a Drp1-dependent fragmentation, mitochondrial depolarization, accompanied with the movement of the mitochondria in the vicinity of the nucleus and decrease of cell viability in HT-22 cells. Bid inhibition can prevent these events and seems to interact with Drp1 in a direct or indirect manner. To reveal the direct interaction of Bid and Drp1, immunoprecipitation analysis was performed in this thesis (Figure 39). The analysis showed no direct interaction of Drp1 with Bid which suggests, that they interact indirectly with each other via other proteins, such as Bax or until now unknown mechanisms. This has to be investigated in greater detail in future studies.

3.5 Drp1 as a mediator of glutamate-induced mitochondrial fission

3.5.1 SiRNA silencing of Drp1 attenuates glutamate-induced cell death and mitochondrial fragmentation in HT-22 cells

The current knowledge on mechanisms regulating mitochondrial dynamics indicates that fission and fusion of mitochondria are under control of highly conserved dynamin-related GTPases (76). Specifically, in mammalian cells, mitochondrial outer and inner membrane fusion is mediated by mitofusin-1 and -2 (Mfn-1, -2) and optical atrophy 1 (OPA1), respectively (97;101). Mitochondrial fission is mediated by dynamin-related protein 1 (Drp1) (103-106). It has been suggested that the outer membrane proteins Fis-1 and Mfn-2 and the proapoptotic Bcl-2 family protein Bax (100) function directly or indirectly as Drp1 receptors to promote mitochondrial fission, however, the mechanisms that promote and regulate the recruitment of cytosolic Drp1 to mitochondria are largely unknown (46;103;105;111;112).

The observation, that enhanced mitochondrial fission is linked to neuronal apoptotic cell death raises the possibility that Drp1 may serve as a target to get more insight into the whole mechanism of mitochondrial fission. Further, Drp1 may exert as a novel therapeutic target for the prevention of neuronal cell death. In the present thesis, siRNA and novel small molecule inhibitors of Drp1 (125) were used to address, whether Drp1 plays a major role in neuronal cell death after glutamate toxicity and oxygen-glucose deprivation (OGD) *in vitro*.

The approach of Drp1 siRNA significantly reduced the expression of Drp1 mRNA and protein in cells as assessed by RT-PCR and western blot analysis, respectively. These analyses indicated that the Drp1-targeting siRNA significantly reduced the expression of Drp1 by >60 % in the HT-22 cells (Figure 18A).

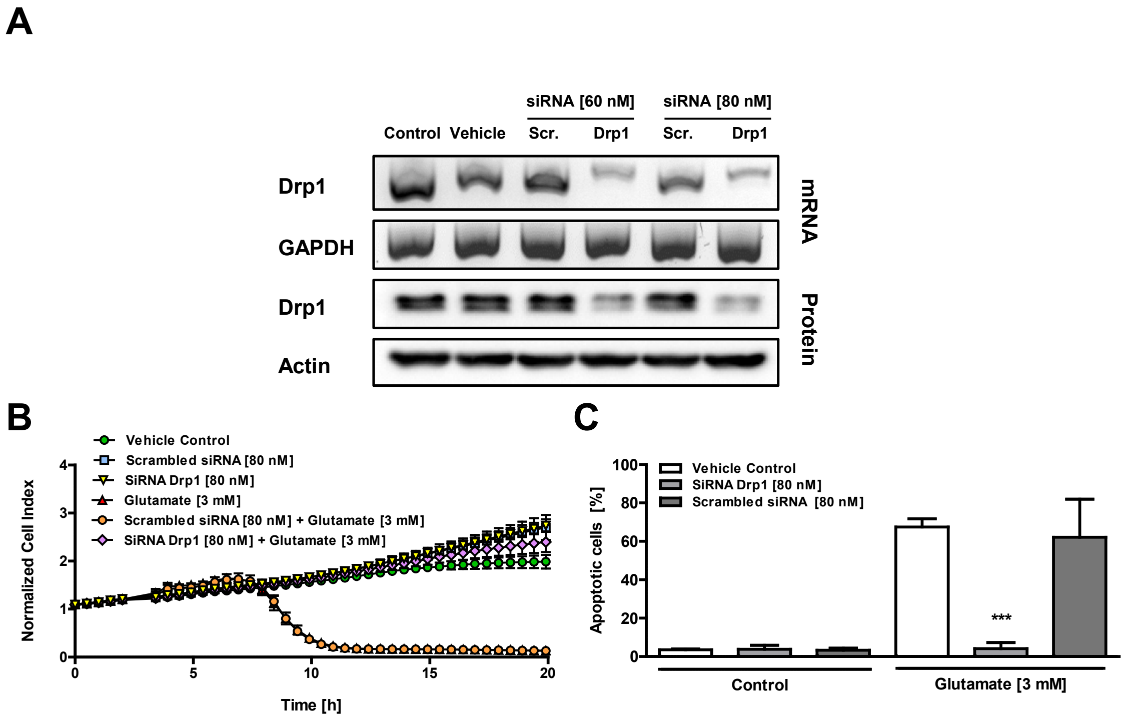

Figure 18 SiRNA silencing of Drp1 attenuates glutamate-induced neuronal cell death in HT-22 cells
A, RT-PCR analysis of Drp1 mRNA (*upper panels*) and western blot analysis of Drp1 protein (*lower panels*) in HT-22 cells pretreated with 60 nM and 80 nM Drp1 siRNA for 48 h. RT-PCR with primers specific for glyceraldehyde-3-phosphate-dehydrogenase (GAPDH) and anti-β-Actin-Antibody used as controls for respective analyses is shown. Quantification of the relative protein expression showed a reduction of 60 % and 70 %. **B**, After 24 h Drp1 siRNA transfected HT-22 cells were seeded out for additional 24 h in 96-well E-plates with 4,500 cells per well and treated with 3 mM glutamate for 20 h. Real time detection of cellular impedance was done with xCELLigence System (Roche, Penzberg, Germany). Glutamate-induced death did not differ in vehicle- or srambled siRNA treated cells, whereas Drp1 siRNA exerted a persistent protective effect. ***$p<0.001$ compared to glutamate 5 mM-treated cells (n=8) (ANOVA, Scheffé's-test). **C**, FACS analysis of HT-22 cells after FITC-Annexin-V labeling to detect apoptotic cells. Exposure to glutamate (3 mM, 14 h) results in enhanced Annexin-V binding of apoptotic HT-22 cells compared to controls. Silencing of Drp1 by siRNA (80 nM) significantly reduced glutamate-induced apoptosis. ***$p<0.001$ compared to glutamate 3 mM-treated cells (n=3) (ANOVA, Scheffé's-test). The experiments were repeated three times and the results presented as mean ± S.D.

In addition, silencing of Drp1 enhanced cell viability in glutamate-treated HT-22 cells as detected by real time measurements of cellular impedance (Figure 18B) and FACS analysis of apoptotic cells after FITC-Annexin-V-staining (Figure 18C). Specifically, both assays indicated that glutamate treatment significantly reduced cell viability and that a similar decrease in cell survival was observed in cell populations treated with glutamate or scrambled siRNA. In contrast, cell viability was comparable to control cells, when cells were treated with both, glutamate and Drp1 siRNA (Figure 18B, C).

These results indicate that Drp1 is a suitable target of therapeutic strategies for neuroprotection against glutamate toxicity.

As shown before, glutamate-toxicity involved enhanced mitochondrial fragmentation in the model of HT-22 cells (92). Under control conditions, mitochondria were primarily organized in an evenly distributed tubular network in HT-22 cells, indicating a balance between mitochondrial fusion and fission events (Figure 19A, B).

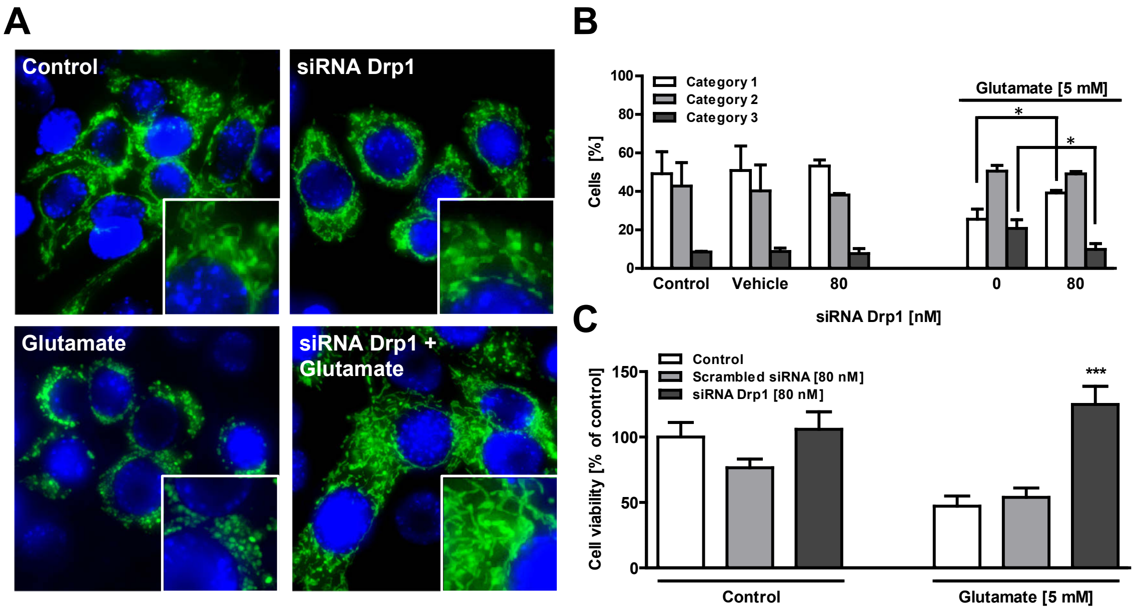

Figure 19 SiRNA silencing of Drp1 attenuates glutamate-induced mitochondrial fragmentation in HT-22 cells

A, Fluorescence photomicrographs (63x objective) of mGFP-transfected and DAPI-stained HT-22 cells showed that Drp1 siRNA (80 nM, 48 h) prevented fission of mitochondria in glutamate-exposed (5 mM, 18 h) HT-22 cells. **B**, Quantification of mitochondrial morphology of five hundred cells per condition: category 1: elongated tubulin-like, category 2: intermediate, category 3: fragmented mitochondria. $^{*}p<0.05$ compared to glutamate 5 mM-treated cells (ANOVA, Bonferroni-test). **C**, HT-22 cells were seeded out in 96-well plates with 7,000 cells per well. Silencing of Drp1 attenuated glutamate (5 mM, 17 h)-induced cell death as determined by MTT assay (n=8). $^{***}p<0.001$ compared to glutamate 5 mM-treated cells (ANOVA, Scheffé's-test). The experiments were repeated three times and the results presented as mean ± S.D.

In contrast, after exposure to glutamate, mitochondria were presented in cells as short tubules and round fragments with a perinuclear located phenotype of mitochondria, as indicated in the quantification analysis by the number of cells that contained long tubular structures (category 1) versus fragmented mitochondria (category 3) (Figure 19A, B). The approach of Drp1 siRNA, but not the control scrambled siRNA, attenuated mitochondrial fragmentation and preserved mitochondrial length in glutamate-treated cultures (Figure 19A, B, Figure 20A, B), indicated that glutamate-induced fragmentation of mitochondria is Drp1 dependent (Figure 19B). In addition, silencing of Drp1 enhanced cell viability in glutamate-treated HT-22 cells as detected by the MTT assay (Figure 19C). In contrast, control scrambled siRNA could not attenuate cell viability after glutamate-induced damage in HT-22 cells (Figure 18B, C, Figure 19C).

Overall, all shown cell viability assays and the quantification of mitochondrial morphology confirmed the protective effect of silencing of Drp1. The presented data indicate that glutamate-induced mitochondrial fragmentation is Drp1 dependent and accentuate Drp1 as a suitable target for therapeutic strategies of neuroprotection against glutamate toxicity.

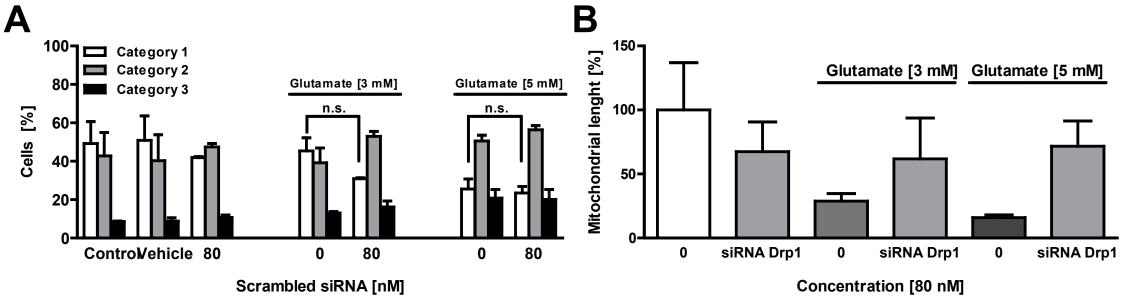

Figure 20 Scrambled siRNA has no effect on mitochondrial morphology

A, Quantification of mitochondrial morphology of five hundred cells per condition. HT-22 cells transfected with scrambled siRNA (80 nM, 48 h) and treated with glutamate (3, 5 mM) for 18 h. Category 1: elongated tubulin-like, category 2: intermediate, category 3: fragmented. N.s. (ANOVA, Bonferroni-test). **B**, Mitochondrial length measurements of treated HT-22 cells by ImageJ. Six Pictures were quantified as absolute values (AU) by the ImageJ program. The experiments were repeated three times and the results presented as mean ± S.D.

3.5.2 Novel pharmacological inhibitors of Drp1 provide protective effects in HT-22 cells

3.5.2.1 MdiviA rescues HT-22 cells from glutamate-induced mitochondrial fragmentation and neuronal cell death

On the basis of the promising results from the siRNA approach, the next step was applying the specific Drp1 inhibitor mdivi-1 (derivative A: mdiviA, Figure 5), which based on previously published work target Drp1 (125) to test the therapeutic potential of Drp1 inhibition in the model of glutamate-induced neuronal cell death. MdiviA preserved the tubular mitochondrial morphology and completely rescued HT-22 cells from glutamate-induced mitochondrial fragmentation (Figure 21A, B). Quantification of mitochondrial morphology confirmed the effect of mdiviA, showing that the Drp1 inhibitor increased the overall mitochondrial length and thus shifted the majority of mitochondria into category 1 in the cells (Figure 22D, Figure 21B).

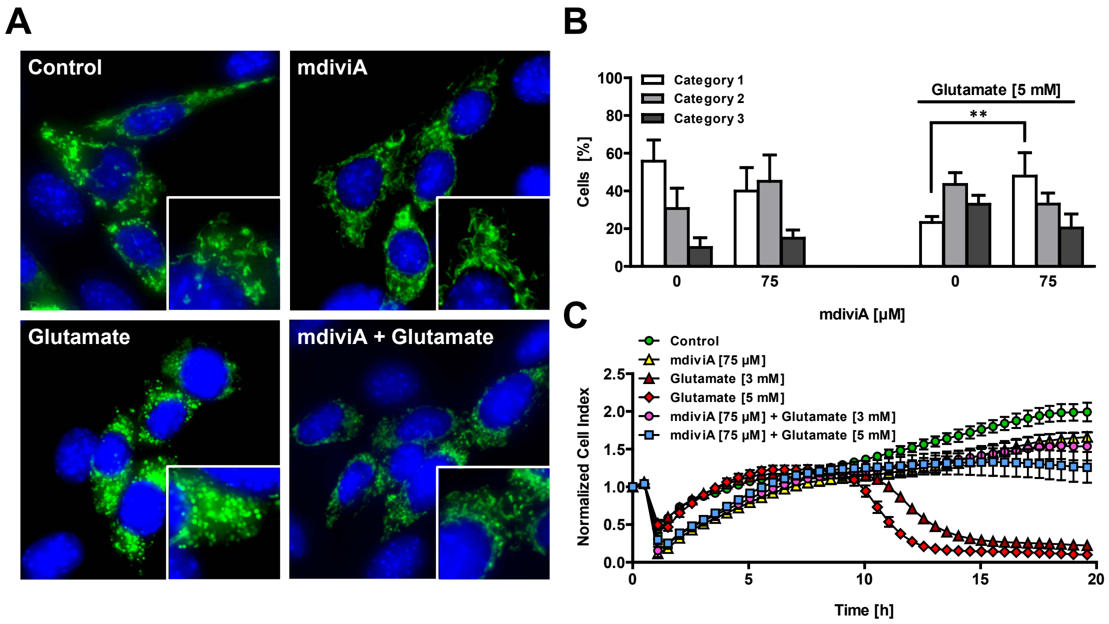

Figure 21 The novel pharmacological inhibitor of Drp1, mdiviA, protects HT-22 cells against glutamate toxicity

A, Fluorescence photomicrographs (63x objective) of mGFP-transfected and DAPI-stained HT-22-cells showed that Drp1 inhibitor mdiviA (75 µM) prevented fission of mitochondria in glutamate-exposed (5 mM, 18 h) HT-22 cells. **B**, Quantification of mitochondrial morphology of five hundred cells per condition. Category 1: elongated tubulin-like, category 2: intermediate, category 3: fragmented. **p<0.01 category 1 mdiviA + glutamate compared to glutamate 5 mM-treated cells (ANOVA, Bonferroni-test). **C**, HT-22 cells were cultured for 48 h in 96-well E-plates with 4,500 cells per well and treated 24 h after seeding with 3 mM and 5 mM glutamate and mdiviA (75 µM) for 18 h (n=8). Real time detection of cellular impedance was performed with xCELLigence System (Roche, Penzberg, Germany). The experiments were repeated three times and the results presented as mean ± S.D.

Inhibition of Drp1 by mdiviA did not only preserve mitochondrial morphology, but also enhanced cell viability of glutamate-treated HT-22 cells as detected by the MTT assay and real time measurements of cellular impedance. While glutamate significantly reduced cell viability to 50 - 20 % of control levels, inhibition of Drp1 by mdiviA preserved cell survival almost to baseline levels in MTT analysis (Figure 22A). Measurements of cellular impedance revealed that adding of glutamate at concentrations of 3 mM and 5 mM resulted in an immediate decline of normalized cell index (NCI) as a result of the temperature drop during the handling of the cells.

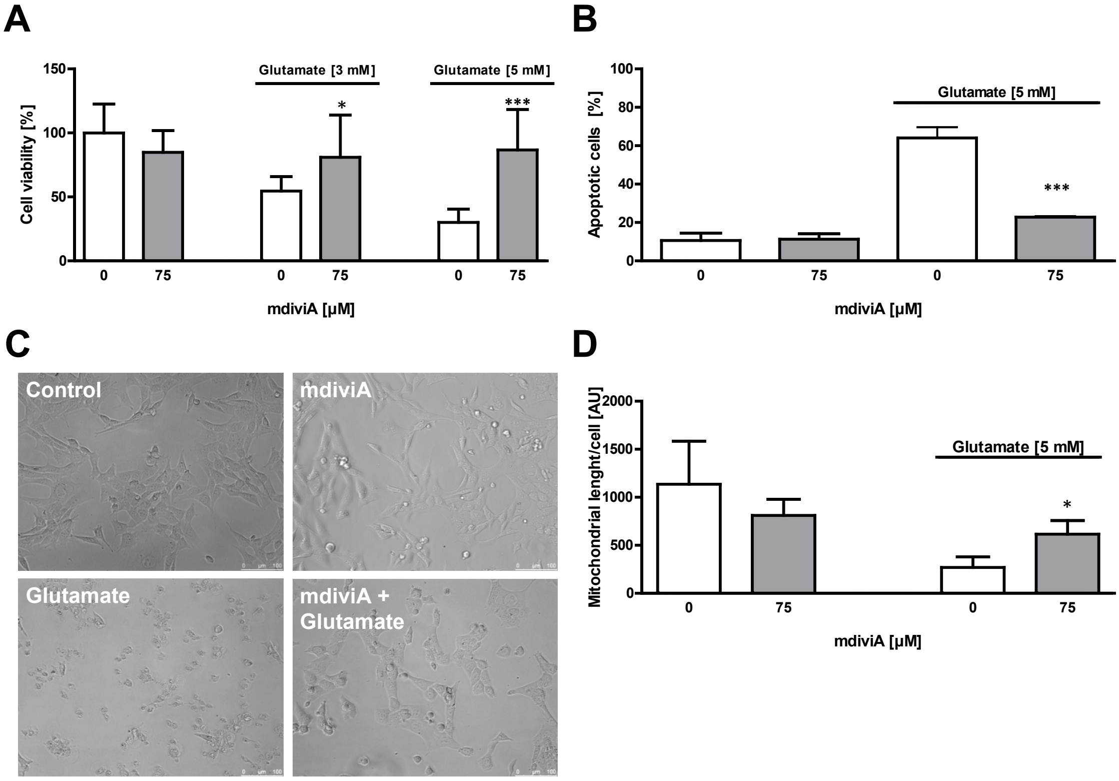

Figure 22 MdiviA prevents mitochondrial length and neuronal cell death

A, HT-22 cells were cultured in 96-well plates with 7,000 cells per well and MTT assay was used to determine the cell viability 18 h after glutamate (3 and 5 mM) treatment. Drp1 inhibitor mdiviA (75 µM) attenuated glutamate-induced cell death in HT-22 cells (n=8). **B**, FACS analysis of HT-22 cells after FITC-Annexin-V labeling to detect apoptotic cells (n=3). Exposure to glutamate (5 mM, 14 h) resulted in enhanced Annexin-V binding of apoptotic HT-22 cells compared to controls. MdiviA (75 µM) significantly reduced glutamate-induced apoptosis. **C**, Photomicrographs (10x objective) showed morphological evidence for severe damage of HT-22 cells 17 h after glutamate-toxicity. Glutamate-treated cells lost of their spindle-like morphology, shrink and detach from the culture well bottom; in contrast, cells pretreated with the Drp1 inhibitor mdiviA (75 µM, 17 h) are fully protected against glutamate-induced death and are not different from the controls. **D**, Mitochondrial length measurements of treated HT-22 cells by ImageJ. Six pictures were quantified as absolute values (AU) by the ImageJ program. ***p<0.001, *p<0.05 compared to glutamate (5 mM)-treated cells (ANOVA, Scheffé's-test). The experiments were repeated three times and the results presented as mean ± S.D.

The NCI returned to baseline levels over the following 7 h of incubation in all control cultures and mdivi-treatment groups, whereas only the glutamate-treated cells showed a decrease of the NCI indicating progressive cell death in these cultures that became detectable between 8 h and 10 h after onset of 5 mM and 3 mM glutamate exposure, respectively (Figure 21C). Inhibition of Drp1 by mdiviA resulted in a complete protection of this delayed glutamate-induced loss of the NCI, and this protective effect against glutamate toxicity was also confirmed by FACS analysis of apoptotic cells after FITC-Annexin-V-staining (Figure 22B).

Photomicrographs confirmed the essential role of Drp1 in the glutamate-induced neuronal death. HT-22 neurons exposed to glutamate for 17 h showed typical morphology of dying cells: the neuronal cells appear shrunken, rounded and detach from the culture dish (Figure 22C). HT-22 cells pretreated with the Drp1 inhibitor mdiviA retained their normal spindle-shaped morphology and were completely rescued from glutamate-induced cell death as determined by the MTT assay and FACS analysis (Figure 22A, B).

Here, these data confirm that glutamate-induced mitochondrial fragmentation depends on Drp1, since Drp1 inhibition by mdiviA prevented glutamate-induced mitochondrial fission and preserved cell viability.

3.5.2.2 MdiviA inhibits glutamate-induced translocation of Drp1 to the mitochondria, and prevents lipid peroxidation and energy depletion

It has been observed that Drp1 assembly and recruitment to mitochondria is stimulated during apoptosis (85;138;139). To gain further insight into Drp1-mediated mitochondrial division in HT-22 cells, the alterations of Drp1 distribution in the cells after glutamate exposure were examined. Consistent with the observations on mitochondrial morphology changes, glutamate treatment caused an increase in Drp1 clusters associated with mitochondria (Figure 23A). In contrast, in cells treated with mdiviA, the majority of Drp1 remained diffusely distributed in the cytoplasm despite the glutamate challenge similar to control cells. Consistent with the previous results, mitochondria in cells treated with mdiviA appeared as a tubular network, in sharp contrast to mitochondrial fragmentation present in cells undergoing glutamate-induced cell death (Figure 21A, Figure 22A).

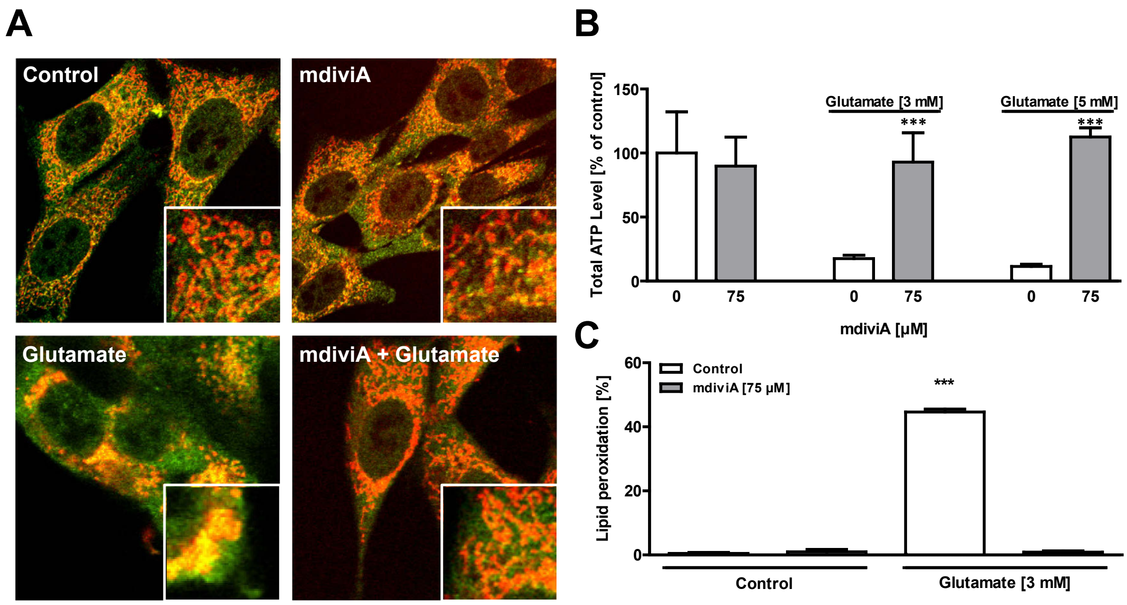

Figure 23 MdiviA inhibits glutamate-induced translocation of Drp1 to the mitochondria, prevents energy depletion and lipid peroxidation

A, HT-22 cells were cultured for 24 h in 8-well-ibidi-plates and treated with 3 mM glutamate and mdiviA (75 µM) for 14 h. Immunostaining of Drp1 revealed that Drp1 (green) translocation to the mitochondria (red) occured after glutamate stimulus. This is shown by overlapping of the fluorescence in yellow. MdiviA inhibited the translocation of Drp1 to the mitochondria. **B**, HT-22 cells were cultured in white 96-well plates with 7,000 cells per well and ATP-luminescence measurements treated with 3 mM and 5 mM glutamate and mdiviA (75 µM) at 14 h (n=8). **C**, Fluorecence detection of lipid peroxidation by Bodipy assay, quantified by FACS analysis (n=3). ***p<0.001 compared to glutamate (3, 5 mM)-treated cells (ANOVA, Scheffé's-test). The experiments were repeated three times and the results presented as mean ± S.D.

These results suggest, that mdiviA attenuated mitochondrial division during glutamate-induced oxytosis by blocking Drp1 recruitment to mitochondria, consistent with previously published work indicating that this compound inhibits Drp1 translocation during STS-induced cell death (85;125). In addition to the protection against cell death, mdiviA also prevented HT-22 cells from ATP depletion (Figure 23B) and reduced significantly lipid peroxidation after glutamate toxicity (Figure 23C).

3.5.2.3 The second isoform of the specific inhibitor of Drp1, mdiviB, also preserves cell viability

Another novel specific Drp1 inhibitor and mdivi-1 derivative, mdiviB (125), was applied to confirm the essential role of Drp1 in glutamate-induced neuronal death. The structure of mdiviB is modified by two additional methyl groups to the mdiviA structure (Figure 5).

In line with the previous results, HT-22 cells treated with mdiviB also preserved the tubulin-shaped mitochondrial morphology, while mitochondrial fragmentation associated with glutamate toxicity was completely blocked by the Drp1 inhibitor (Figure 24A). Quantification of mitochondrial morphology confirmed that mdiviB mediated an increase of tubulin-like mitochondria representing category 1 compared to glutamate-treated HT-22 cells, which mainly showed fragmented, shorter mitochondria of categories 2 and 3 (Figure 24B, C). Moreover, mdiviB restored the cell viability assessed by the MTT assay. Glutamate-reduced cell viability to 20 % of control levels, whereas inhibition of Drp1 by mdiviB significantly preserved the viability in glutamate-treated cells (Figure 25A, C). Analysis of Annexin-positive cells by FACS analysis confirmed the protective effect of mdiviB (Figure 25B).

Overall, these results reveal a major upstream role for Drp1 in mitochondrial damage, energy depletion and subsequent execution of cell death in glutamate-induced oxytosis in HT-22 cells.

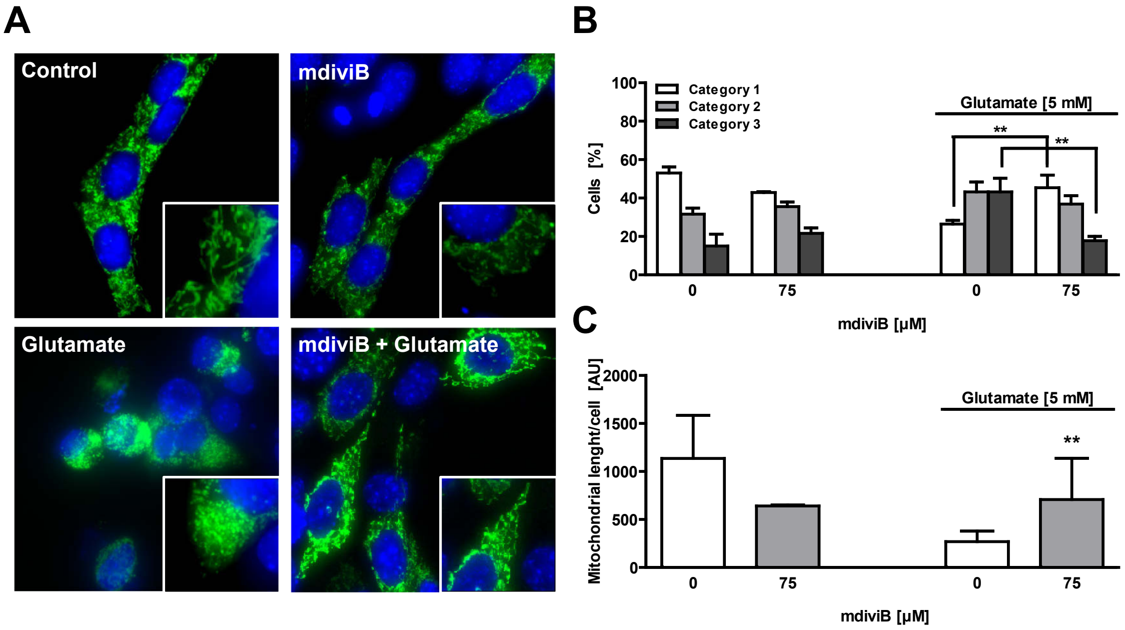

Figure 24 The second isoform of the specific inhibitor of Drp1, mdiviB prevents mitochondrial fission

A, Fluorescence photomicrographs (63x objective) of mGFP-transfected and DAPI-stained HT-22 cells showed that Drp1 inhibitor mdiviB (75 µM) prevented fission of mitochondria in glutamate exposed (5 mM, 18 h) HT-22 cells. **B**, Quantification of mitochondrial morphology of five hundred cells per condition. Category 1: elongated tubulin-like, category 2: intermediate, category 3: fragmented. **p<0.01 compared to glutamate (5 mM)-treated cells (ANOVA, Bonferroni-test). **C**, Mitochondrial length measurements of treated HT-22 cells by ImageJ. Six Pictures were quantified as absolute values (AU) by the ImageJ program. **p<0.01 compared to glutamate (5 mM)-treated cells (ANOVA, Scheffé's -test). The experiments were repeated three times and the results presented as mean ± S.D.

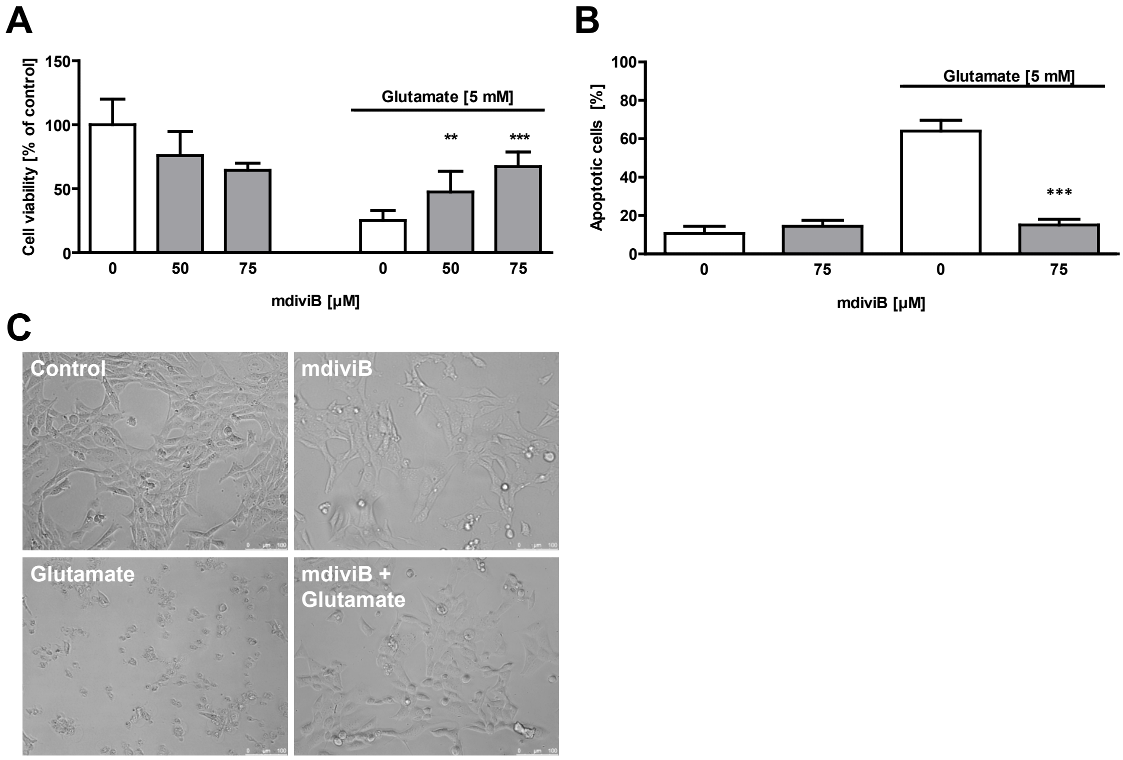

Figure 25 The second isoform of the specific inhibitor of Drp1, mdiviB preserves cell viability

A, HT-22 cells were cultured in 96-well plates with 7,000 cells per well and MTT assay was used to determine the cell viability 18 h after glutamate treatment (5 mM). Drp1 inhibitor mdiviB (50, 75 µM) attenuated glutamate-induced cell death in a concentration-dependent manner (n=8). **B**, FACS analysis of HT-22 cells after FITC-Annexin-V labeling to detect apoptotic cells. Exposure to glutamate (5 mM, 14 h) resulted in enhanced Annexin-V binding of apoptotic HT-22 cells compared to controls (n=3). MdiviB (75 µM) significantly reduced glutamate-induced apoptosis. ***p<0.001, **p<0.01 compared to glutamate (5 mM)-treated cells (ANOVA, Scheffé's-test). **C**, Photomicrographs (10x objective) showed morphological evidence for severe damage of HT-22 cells 17 h after glutamate-toxicity. Glutamate-treated cells loose of their spindle-like morphology, shrink and detach from the culture well bottom; in contrast, cells pretreated with the Drp1 inhibitor mdiviB (75 µM, 17 h) are fully protected against glutamate-induced death and are not different from the controls. The experiments were repeated three times and the results presented as mean ± S.D.

3.5.3 Drp1 gene silencing and pharmacological Drp1 inhibition prevent mitochondrial depolarization

Loss of mitochondrial membrane potential (MMP) is a major feature of glutamate-induced cell death that is associated with mitochondrial fragmentation and precedes the fatal release of AIF and execution of caspase-independent cell death (39;92).

In line with previous experiments in HT-22 cells, JC-1 fluorescence, which measures MMP, showed significant loss of red fluorescence signal, indicated that there was a decrease in MMP within 12 h after glutamate treatment, similar to that observed after treatment with the mitochondrial uncoupler CCCP (Figure 26 and Figure 27). In contrast, Drp1 siRNA significantly attenuated the glutamate-induced breakdown of the mitochondrial membrane potential and similar effects were detected after using the Drp1 inhibitors mdiviA and mdiviB (Figure 26B, Figure 27B).

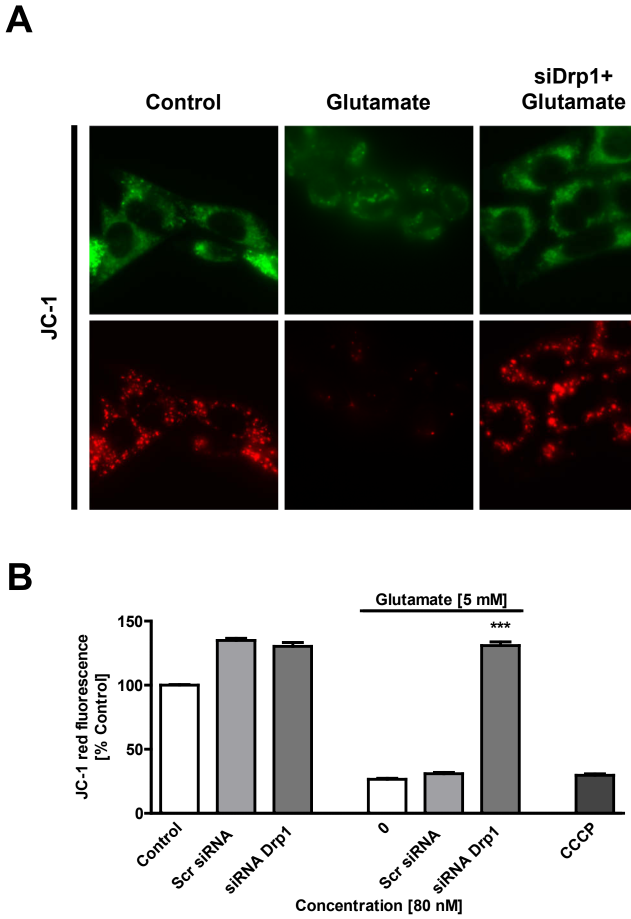

Figure 26 Inhibition of Drp1 prevents glutamate-induced mitochondrial depolarization

A, Mitochondrial membrane potential was analyzed by JC-1 fluorescence: upper panels showed epifluorescence photomicrographs indicating equal cellular uptake of JC-1 by green fluorescence; lower panels depicted intact mitochondria exposing red fluorescence. Glutamate treated (5 mM, 12 h) HT-22 cells show significantly reduced red fluorescence compared to controls whereas siRNA of Drp1 (80 nM) prevented the breakdown of the mitochondrial membrane potential as indicated by preservation of the red JC-1 fluorescence. **B**, FACS analyses of n=3 per group revealed a decrease of the red JC-1 fluorescence to 30 % of control levels 12 h after glutamate-treatment (5 mM) which is prevented by siRNA of Drp1 (80 nM). Glutamate treatment was as effective as the positive damage-control CCCP which causes a fast breakdown of the mitochondrial membrane potential. ***p<0.001 compared to glutamate-treated controls (ANOVA, Scheffé's-test). The experiments were repeated three times and the results presented as mean ± S.D.

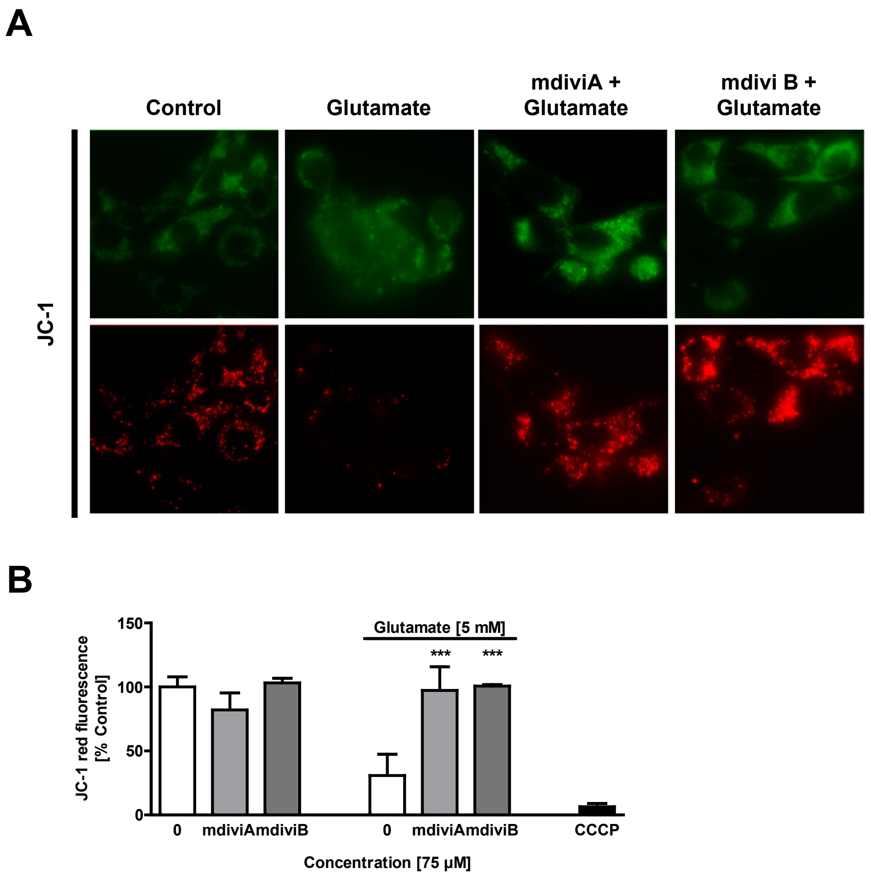

Figure 27 Inhibition of Drp1 prevents glutamate-induced mitochondrial depolarization

A, Mitochondrial membrane potential was analyzed by JC-1 fluorescence: upper panels showed epifluorescence photomicrographs indicating equal cellular uptake of JC-1 by green fluorescence; lower panels depicted intact mitochondria exposing red fluorescence. Glutamate treated (5 mM, 12 h) HT-22 cells show significantly reduced red fluorescence compared to controls whereas mdiviA and B (75 µM) prevented the breakdown of the mitochondrial membrane potential as indicated by preservation of the red JC-1 fluorescence. **B**, FACS analyses of n=3 per group revealed a decrease of the red JC-1 fluorescence to 30 % of control levels 12 h after glutamate-treatment (5 mM) which is prevented by mdiviA and B. Glutamate treatment was as effective as the positive damage-control CCCP which causes a fast breakdown of the mitochondrial membrane potential. ***$p<0.001$ compared to glutamate-treated controls (ANOVA, Scheffé's-test). The experiments were repeated three times and the results presented as mean ± S.D.

Drp1-dependent mitochondrial fission is essential for the maintenance of mitochondrial integrity in neurons. Any impairment in the Drp1-mediated fission process in healthy cells can promote changes in mitochondrial morphology with loss of neuronal viability. To observe the effect of totally blocking Drp1 activity in healthy HT-22 neurons, mdiviA was added in increased concentrations of 75 - 500 µM.

The approach of high concentrations of Drp1 inhibitor mdiviA showed a massive decrease of cell viability as evaluated by the MTT assay (Figure 28A). In the HT-22 cells system, application of increasing concentration of Drp1 inhibitor mdiviA enhanced the fission of mitochondria and drastically reduced mitochondria with tubulin-structure and enhanced the amount of rounded, fragmented mitochondria (category 3) (Figure 28B). This has been shown impressively in fluorescence photomicrographs of mGFP-transfected HT-22 cells treated with increased concentrations of mdiviA (Figure 28C). Chemical or genetic interference with the mitochondrial fission machinery is reported to inhibit apoptotic mitochondrial fragmentation and delays cell death, which has to been considered beneficial for diseases, where mitochondrial fusion proteins are mutated and mitochondrial fission is enhanced.

The findings of this experiment clearly indicate that a deregulation by inhibition of Drp1 leads to a significant shift of the balance of fusion/fission protein activities towards fission. This deregulation of outbalanced fusion and fission mechanism has deleterious effects on mitochondrial homeostasis and consequently on neuronal survival. Thus, the regulation of mitochondrial dynamics must be tightly regulated in neurons, which suggests that Drp1 function is important for mitochondrial integrity and cellular homeostasis which cannot be sustained when Drp1 is totally blocked.

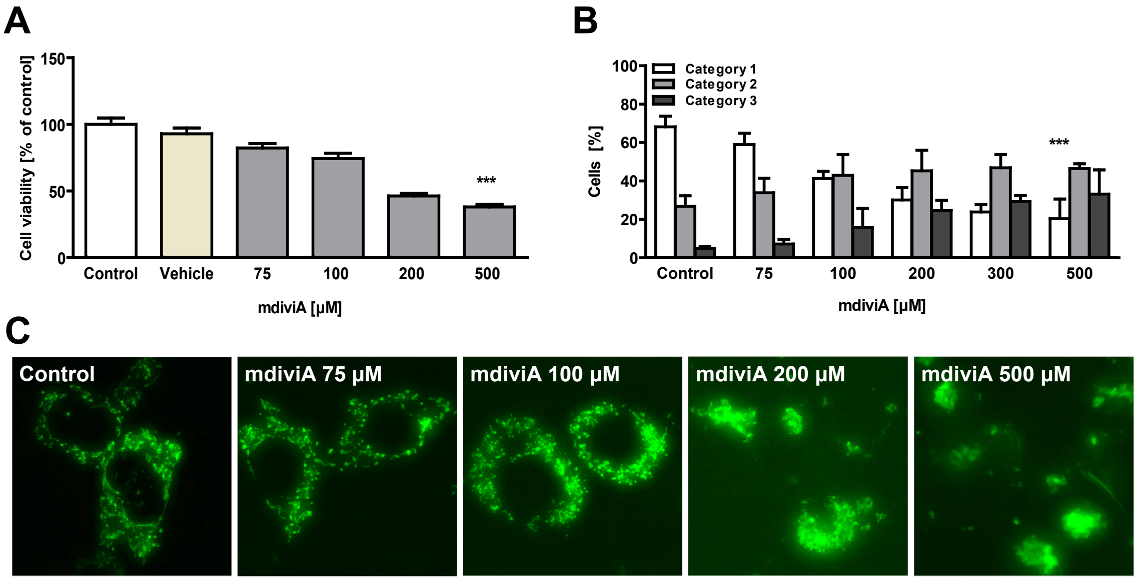

Figure 28 Higher concentrations of Drp1 inhibitor mdiviA leads to enhanced mitochondrial fragmentation and neuronal cell death

A, HT-22 cells were cultured in 96-well plates with 7,000 cells per well and MTT assay was used to determine the cell viability 18 h after treatment with Drp1 inhibitor mdiviA (75 - 500 µM) (n=8). ***p<0.001 compared to control cells (ANOVA, Scheffé's-test). **B**, Quantification of mitochondrial morphology of five hundred cells per condition. Category 1: elongated tubulin-like, category 2: intermediate, category 3: fragmented. **C**, Fluorescence photomicrographs (63x objective) of mGFP-transfected HT-22 cells showed that Drp1 inhibitor mdiviA (75 - 500 µM) enhanced mitochondrial fission in concentration-dependent manner after 18 h. HT-22 cells. ***p<0.001 compared control cells (ANOVA, Bonferroni-test). The experiments were repeated three times and the results presented as mean ± S.D.

3.5.4 Mdivi compounds mdiviC and E show protective effects on mitochondrial fragmentation in HT-22 cells

Further mdivi-1 derivates, named mdiviC and E, were used in this model of glutamate-induced oxytosis in HT-22 cells and showed similar effects on restoration of mitochondrial morphology and cell viability as detected before with mdiviA and B (Figure 29). MdiviC structure is modified by an additional chloride and mdiviE is modified by an additional trifluoromethyl group to the mdiviA structure (Figure 5).

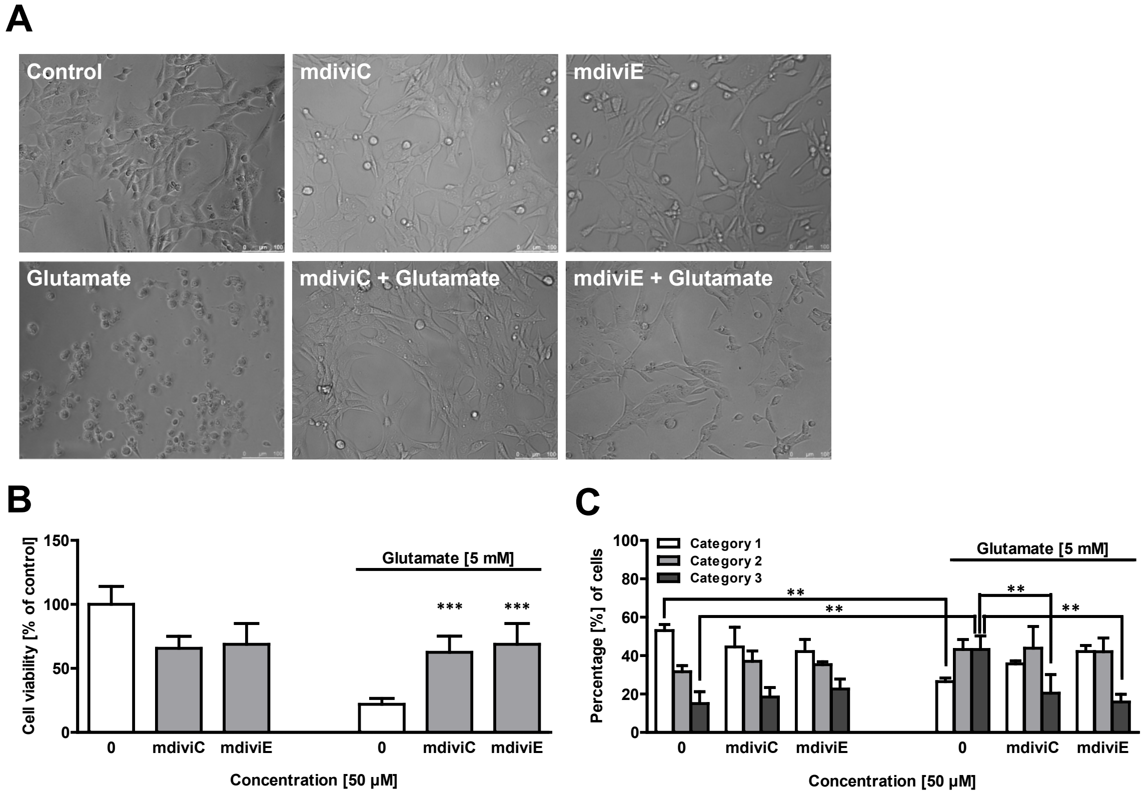

Figure 29 Further mdivi compounds, mdiviC and E show similar protective effect on mitochondrial fragmentation in HT-22 cells

A, Photomicrographs (10x objective) showed after glutamate treatment typically round HT-22 cell shape. Addition of Drp1 inhibitors mdiviC and E (50 µM, 18 h) showed spindle-like shapes as control. **B**, HT-22 cells were cultured in 96-well plates with 7,000 cells per well and MTT assay was used to determine the cell viability 18 h after glutamate treatment (5 mM). Drp1 inhibitor mdiviC and E (50 µM) attenuated glutamate-induced cell death (n=8). ***$p<0.001$ compared to glutamate (5 mM)-treated cells (ANOVA, Scheffé's-test). **C**, Quantification of mitochondrial morphology of five hundred cells per condtition. Mito-GFP-transfected HT-22 cells were cotreated with mdiviC and E (50 µM) and glutamate (5 mM) for 18 h. Category 1: tubulin-like, category 2: intermediate, category 3: fragmented. **$p<0.01$ compared to glutamate (5 mM)-treated cells (ANOVA, Bonferroni-test). The experiments were repeated three times and the results presented as mean ± S.D.

3.5.5 The negative isoform of Drp1 inhibitor mdiviG cannot prevent mitochondrial fission in HT-22 cells

In contrast, a closely related compound mdiviG (Figure 5), which previously was observed to have no efficacy in Drp1-dependent mitochondrial division, failed to inhibit glutamate-induced fragmentation and reverse glutamate-induced cell death, indicating that the effects of the active mdivi compounds are selective for Drp1 inhibition (Figure 30).

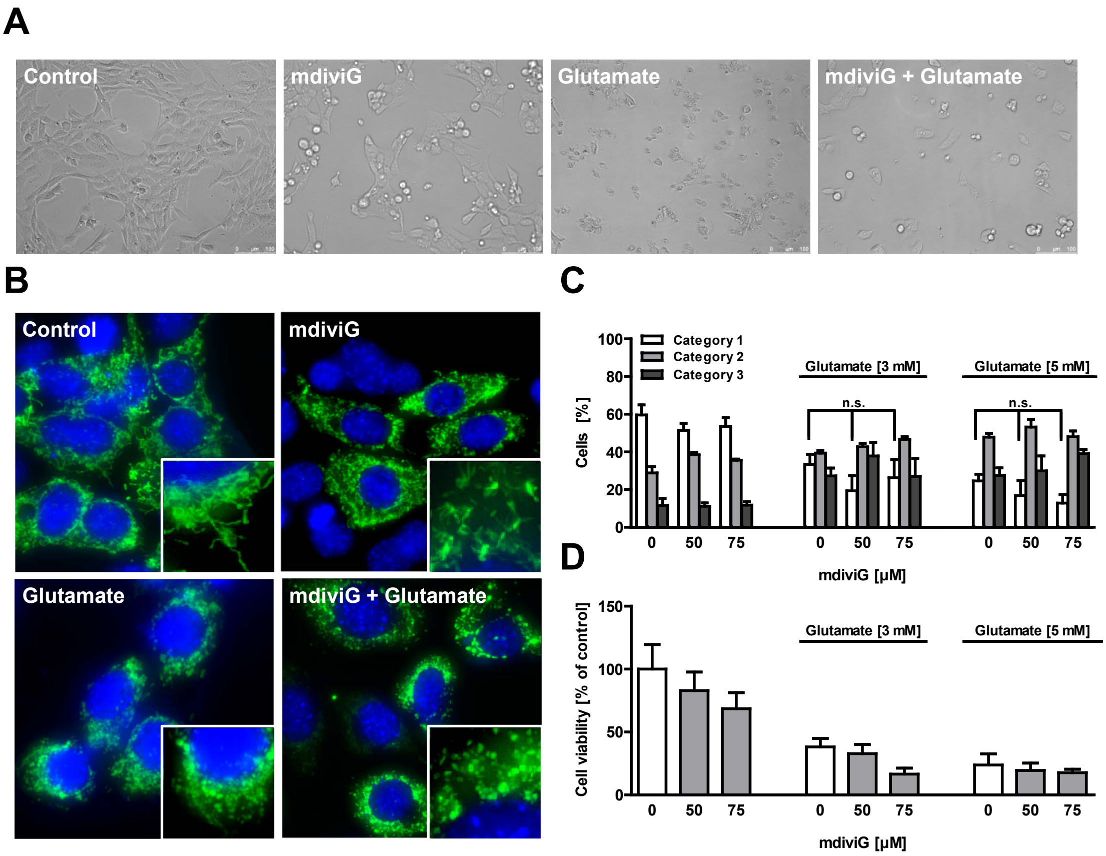

Figure 30 The negative isoform of Drp1 inhibitor mdiviG cannot prevent mitochondrial fission in HT-22 cells

A, Photomicrographs (10x objective) show no morphology differences after mdiviG (75 µM, 18 h) treatment compared to glutamte treatment. **B**, Fluorescence photomicrographs (63x objective) of mGFP-transfected and DAPI-stained HT-22 cells showed that negative isoform of Drp1 inhibitor mdiviG (50, 75 µM) could not prevent fission of mitochondria in glutamate-exposed (5 mM, 18 h) HT-22 cells. **C**, Quantification of mitochondrial morphology of five hundred cells per condition. Cells treated with mdiviG (50, 75 µM) + glutamate (3 and 5 mM) showed similar amount of fragmented mitochondria in counted cells compared to glutamate-treated cells. Category 1: elongated tubulin-like, category 2: intermediate, category 3: fragmented. N.s. non-significant (ANOVA, Bonferroni-test). **D**, HT-22 cells were cultured in 96-well plates with 7,000 cells per well and MTT assay was used to determine the cell viability 18 h after glutamate treatment (3 and 5 mM). Drp1 inhibitor mdiviG didn`t attenuate glutamate-induced cell death (n=8). N.s. non-significant (ANOVA, Scheffé's-test). The experiments were repeated three times and the results presented as mean ± S.D.

3.5.6 Inhibition of Drp1 prevents tBid-induced mitochondrial fragmentation and neuronal cell death

The recent data demonstrated a role for the proapoptotic BH3-only protein Bid in the regulation of enhanced mitochondrial fission and in the loss of MMP in the present model system of HT-22 oxytosis. Therefore, the present study examined the role of Drp1 in Bid-mediated neuronal cell death. HT-22 cells were transfected with the toxic tBid-expressing vector to induce tBid-toxicity accompanied by enhanced mitochondrial fragmentation. Notably, the cotreatment with mdiviA and B with tBid-vector prevented tBid-induced cell damage and morphologic shape changes (Figure 31A, B). Moreover, treatment with mdiviA or B restored the cell viability assessed by the MTT assay. Vector-induced expression of tBid reduced cell viability to 30 % of control levels, whereas cell viability was restored to control levels when the Drp1 inhibitors were applied to tBid expressing cells (Figure 31B).

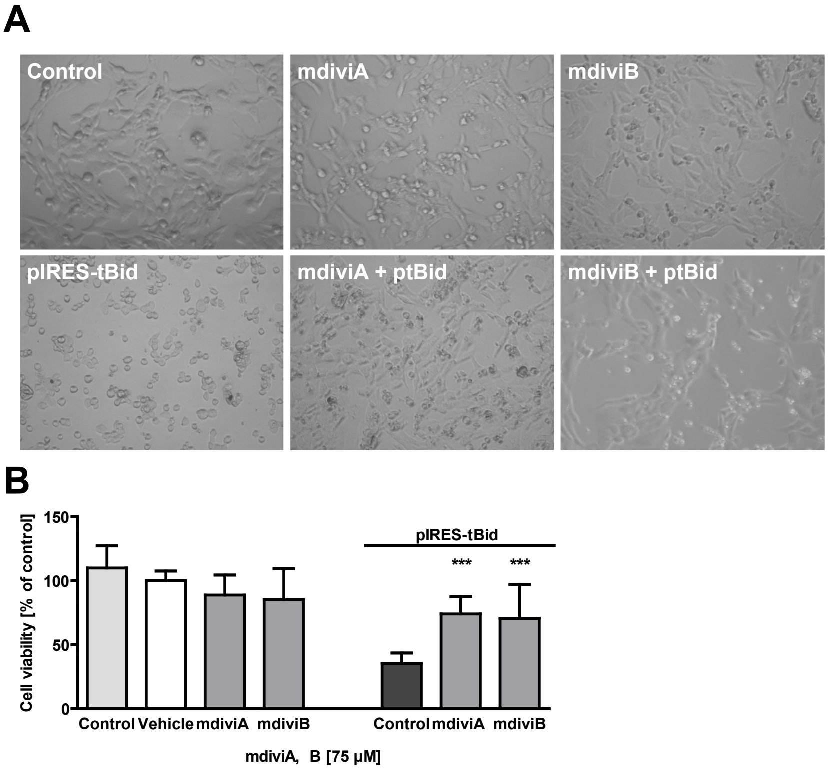

Figure 31 Inhibition of Drp1 prevents tBid-induced neuronal cell death

A, Photomicrographs (10x objective) of tBid-transfected and mdiviA and B treated HT-22 cells showed protective effect of cellular shape with mdiviA and B (75 µM, 12 h) treatment compared to tBid-induced toxicity. **B**, MTT assay was used to determine the cell viability 12 h after tBid toxicity. Drp1 inhibitors mdiviA and B (75 µM) attenuated tBid toxicity (n=8). ***$p<0.001$ compared to tBid toxicity (ANOVA, Scheffé's-test). The experiments were repeated three times and the results presented as mean ± S.D.

Specifically, mitochondrial fragmentation associated with tBid-toxicity was significantly attenuated by Drp1 inhibitors mdiviA and B (Figure 32A). Quantification of mitochondrial morphology confirmed that mdiviA and B (75 µM) reduced fragmented, shorter mitochondria of category 3 in tBid-transfected HT-22 cells compared to tBid transfection alone (Figure 32A, B). This protective effect of mdiviA and B against tBid-induced cell death was confirmed by FACS analysis of apoptotic cells after FITC-Annexin-V-staining (Figure 32C), where inhibition of Drp1 by mdiviA and B resulted in a complete protection of this tBid-induced cell death.

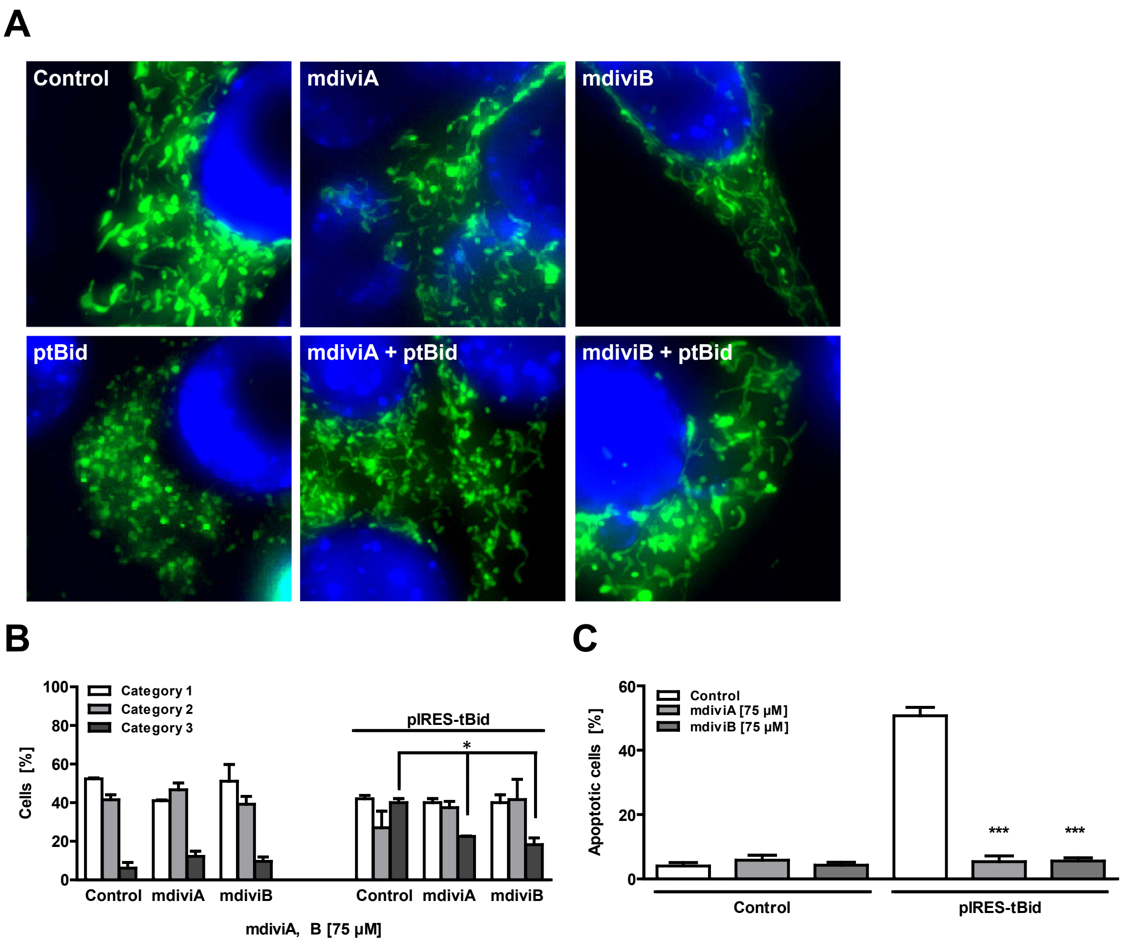
A
Control
mdiviA
mdiviB
ptBid
mdiviA + ptBid
mdiviB + ptBid
B
Category 1
Category 2
Category 3
Cells [%]
100
80
60
40
20
0
pIRES-tBid
*
Control
mdiviA
mdiviB
Control
mdiviA
mdiviB
mdiviA, B [75 µM]
C
Control
mdiviA [75 µM]
mdiviB [75 µM]
Apoptotic cells [%]
60
40
20
0
***
***
Control
pIRES-tBid

Figure 32 Inhibition of Drp1 prevents tBid-induced mitochondrial fragmentation and neuronal cell death

A, Fluorescence photomicrographs (63x objective) showed that the Drp1 inhibitors mdiviA and mdiviB (75 µM) prevented fission of mitochondria in tBid-induced toxicity after 12 h in HT-22 cells. **B**, Quantification of mitochondrial morphology of five hundred cells per condition. Category 1: elongated tubulin-like, category 2: intermediate, category 3: fragmented. $^*p<0.05$ compared to glutamate (5 mM)-treated cells (ANOVA, Bonferroni-test). **C**, FACS analysis of HT-22 cells after FITC-Annexin-V labeling to detect apoptotic cells. Transfection of pIRES-tBid resulted in enhanced Annexin-V binding of apoptotic HT-22 cells compared to controls. MdiviA and B (75 µM) significantly reduced tBid-induced cell death (n=3). $^{***}p<0.001$ compared to tBid-toxicity (ANOVA, Scheffé's-test). The experiments were repeated three times and the results presented as mean ± S.D.

In summery, these data demonstrate that Bid/tBid-mediated mitochondrial fragmentation and MOMP is dependent on Drp1 activity, since the Drp1 inhibition prevented tBid-induced fission and preserved cell viability. These findings were confimed by immunocytochemistry analysis of Drp1 translocation which is inhibited by the Bid inhibitor BI-6c9 (Figure 17). This sustain the detrimential interaction of Bid and Drp1 that occured upstream of mitochondrial pathways that involved mitochondrial fission.

3.6 The Role of Drp1 in primary neurons *in vitro* and *in vivo*

3.6.1 Mdivi compounds protect primary neurons against glutamate-induced excitotoxicity

So far, the protective effects of Drp1 inhibition have been shown in immortalized HT-22 hippocampal neurons, which die because of glutathione depletion after glutamate-induced inhibition of the glutamate-cystine antiporter (40). HT-22 cells lack NMDA and AMPA/kainate receptors, and consequently, the HT-22 model of oxytosis only partly reflects the mechanisms of neuronal death after acute brain injury, which involves glutamate-induced immediate increase in the intracellular Ca^{2+}-concentration through activation of the ion channel coupled glutamate receptors. Nevertheless, formation of ROS is also a major feature involved in glutamate toxicity in primary neurons downstream of initial calcium overload of the cells. Therefore, the study revealed the effects of the mdivi compounds in a model of glutamate-induced excitotoxicity in primary cortical neurons, which express NMDA and AMPA/kainate receptors. Primary rat cortical cultures were treated on day 9 after the preparation. At this time point the neurons express ionotropic glutamate receptors and are highly sensitive to glutamate-induced excitotoxicity. MdiviA and B (25 µM) were added together with glutamate at concentrations of 30 µM. Cell viability was evaluated 18 h after glutamate treatment by DAPI staining of the nuclei and subsequent quantification of pyknotic nuclei. Similar to the results obtained in HT-22 cells, treatment of primary neurons with mdiviA or B significantly attenuated glutamate neurotoxicity (Figure 33).

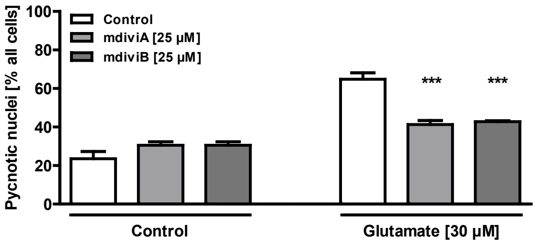

Figure 33 Mdivi compounds protect primary neurons against glutamate-induced excitotoxicity

Quantification of pyknotic nuclei in % of four independent experiments. Primary rat cortical neurons were treated on day 9 for 18 h with glutamate 30 µM and mdiviA and B (25 µM). After 18 h, cells were fixed in 4 % PFA. After fixation cells were stained with DAPI and approximately five hundred nuclei were counted per treatment condition. MdiviA and B significantly reduced glutamate-induced cell death (n=5). ***p<0.001 compared to glutamate-treated control cells (ANOVA, Scheffé's-test). The experiments were repeated four times and the results presented as mean ± S.D.

3.6.2 Mdivi compounds protect primary neurons against oxygen glucose deprivation (OGD) *in vitro*

Cerebral ischemia causes severe and persistent brain damage is accompanied with a high mortality rate. To date, tissue plasminogen activator (tPa) is the only available therapy in patients suffering from ischemic stroke. However the number of stroke patients eligible for tPA treatment is very limited for safety reasons and, thus, the vast majority of patients do not receive any therapy targeting the cause of ischemia or mechanisms of the following delayed infarct development (140).

Here, oxygen glucose deprivation (OGD) was used as an *in vitro* model for cerebral ischemia to investigate the protective effect and the role of Drp1 in delayed neuronal cell death. Similar protective effects of the mdivi compounds were also detected in primary neurons exposed to OGD (Figure 34A, B).

Primary rat cortical neurons were treated with mdiviA and B (25 µM) one hour prior to OGD and were exposed to OGD for four hours. After 18 h of reoxygenation the cell viability was analyzed by DAPI staining and quantification of pyknotic nuclei. In this *in vitro* model system of ischemic conditions in a culture dish, control neurons displayed condensed, pyknotic nuclei 18 h after OGD with 75 %, whereas the neurons receiving the mdivi compounds A and B maintained healthy nuclear morphology to control levels (Figure 34A). Quantification of four independent experiments revealed that mdivi compounds A or B reduced OGD-induced cell death by approximately 55 % (Figure 34B).

These results indicate that Drp1 activity is involved in ischemic neuronal cell death induced by OGD.

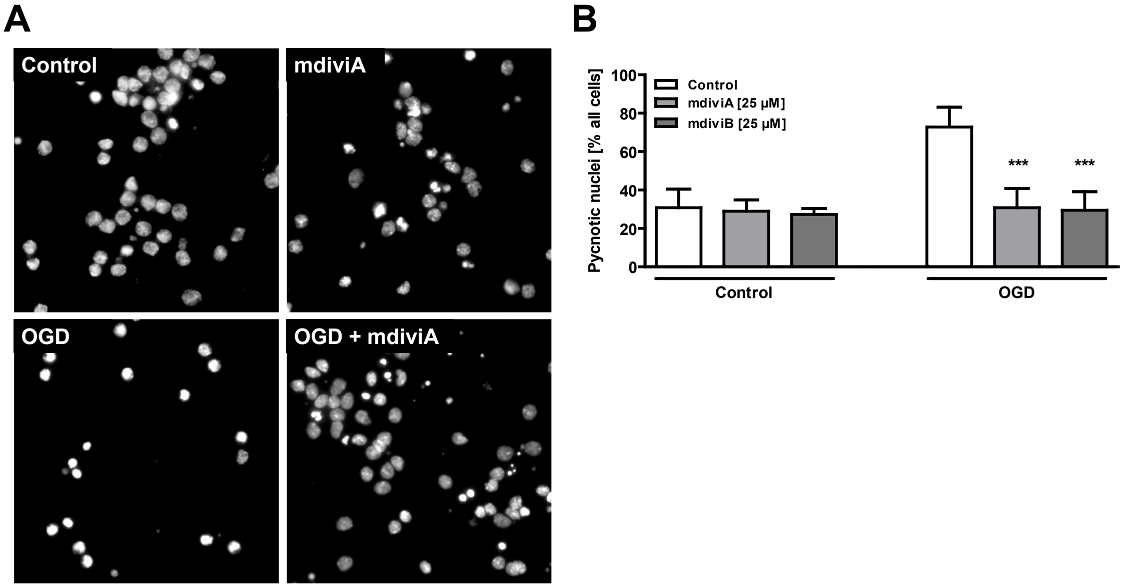

Figure 34 Mdivi compounds protect primary neurons against OGD *in vitro*

Primary rat cortical neurons (day 9) were exposed 4 h to OGD. **A**, Fluorescence microscope images (40x objective) of DAPI-stained embryonic cortical neurons were obtained after 18 h of exposure to OGD. **B**, Counting of DAPI-stained neurons displaying pyknotic nuclei after 4 h of OGD revealed that 25 µM Drp1 inhibitor mdiviA and B significantly protect neurons from hypoxic-hypoglycemic cell death (n=5). ***p<0.001 vs. untreated neurons subjected to OGD (ANOVA, Scheffé's-test). Cultures treated with 25 µM mdiviA or B contained >60 % healthy nuclei, whereas all other OGD-treated groups showed 75 % pyknotic and/or fragmented nuclei, indicating apoptotic damage (OGD, right white column). The respective control cultures with 1x EBSS medium + glucose contained only very few apoptotic nuclei (Control, left white column). The experiments were repeated three times and the results presented as mean ± S.D.

3.6.3 Mdivi compounds attenuate ischemic brain damage *in vivo*

The findings on the efficacy of mdivi compounds in the *in vitro* models encouraged to expand the work for further investigations of their protective potential *in vivo*, in a model of ischemic stroke (Figure 35). The model of transient middle artery occlusion (MCAo) was performed by Uta Mamrak at the Ludwig-Maximilians-University in Munich, Germany.

The C57BL/6 mice obtained intraperitoneal injections of two different doses of mdiviA (3 mg/kg) and mdiviB (1 and 3 mg/kg) one hour before the induction of MCAo. Transient focal ischemia was induced for 45 min. by a silicon-coated nylon filament that was introduced into the internal carotid artery to occlude the middle cerebral artery (MCA). The infarct volume was analyzed 24 h after reperfusion. Pretreatment of mdiviA (3 mg/kg) and mdiviB (1 and 3 mg/kg) significantly reduced the mean infarct volume by 34 % and 30 % compared to vehicle (DMSO) controls, respectively, suggesting that Drp1 is a mediator of acute brain damage after MCAo (Figure 35A, B). In addition the neuroscore was evaluated in the mice at 1 and 24 hours after reperfusion. The neuroscore is used to judge the motor activity of the animals. In contrast to the protective effects determined by histology, functional analysis by the neuroscore showed no difference between control and treated mice after one hour. Mice pretreated with mdiviA and B slightly improved the neuroscore at 24 h after reperfusion (Figure 35C, D).

These results indicate that Drp1 participate in ischemic brain damage, whereas further analyses are required to evaluate the potential functional recovery that may be associated with the observed protection of brain tissue.

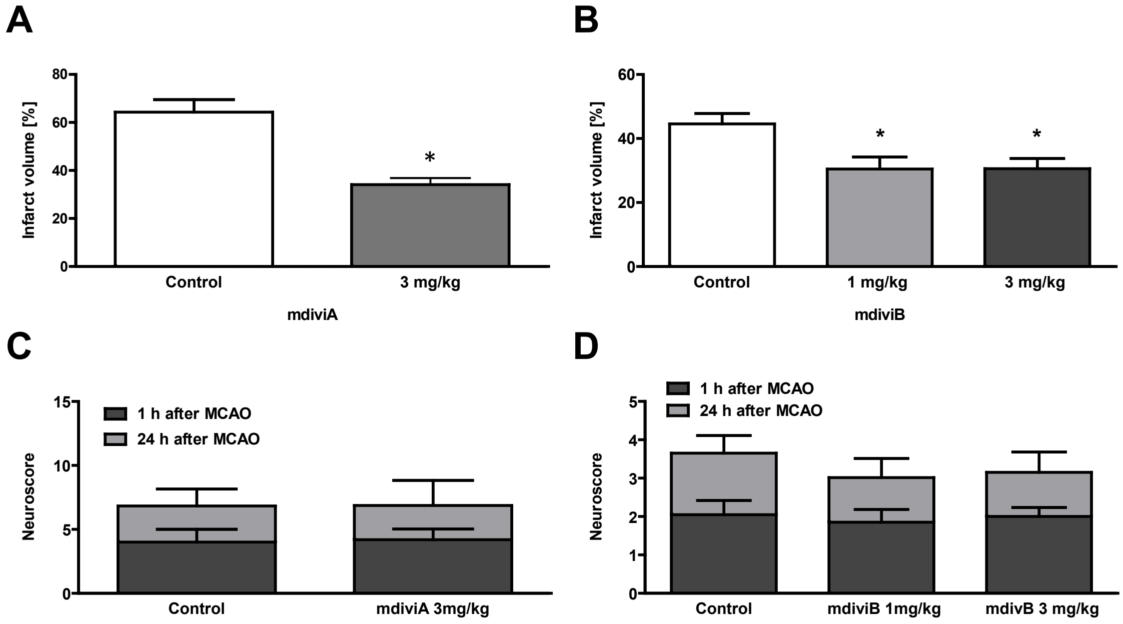

Figure 35 Mdivi compounds attenuate ischemic brain damage *in vivo*

A and **B**, Transient focal ischemia was induced for 45 min. by a silicon-coated nylon filament that was introduced into the internal carotid artery to occlude the middle cerebral artery (MCA). Surgery was performed in deep isoflurane/N_2O anesthesia with controlled ventilation, and ischemia and reperfusion were verified by laser Doppler fluxmetry. The infarct volume was calculated on the basis of the histomorphometric data from twelve-fifteen consecutive sections (every 500 µM) obtained 24 h after onset of ischemia. MdiviA (3 mg/kg) and mdiviB (1 and 3 mg/kg) reduced the mean infarct volume by 34 % and 30 % compared to vehicle (DMSO) controls, respectively. **C** and **D**, The neuroscore was determined at 1 and 24 hours after reperfusion in order to analyze the motor activitiy of the animals. Data in this figure are represented as mean +/- SEM. n=5 for mdiviA and n=10 for mdiviB (Mann-Whitney-U-test).

3.7 Mitochondrial distribution and mobility

3.7.1 Tubulin structures are destroyed after glutamate toxicity in HT-22 cells

It is known that tubulin filaments are involved in the transport of mitochondria in neurons and interact with dyneins and kinesins for mitochondrial transport into dendrites and axons to the places of high energy demand. It is commonly observed that mitochondria are often located around the nucleus after oxidative stress (92;93). To examine the reason for perinuclear location of mitochondria, the current thesis further investigated tubulin structures and their conformational changes associated with glutamate-induced cell death.

In immunocytochemistry analysis of HT-22 cells, tubulin was stained by antibody in green and mitochondria by Mitotracker DeepRed in red. In control cells, tubulin displayed as long filaments and mitochondrial structures showed a tubular network, distributed in the whole cytosol. In contrast, glutamate-treated HT-22 cells displayed destroyed, punctuated tubulin structures after 14 h of the onset of glutamate exposure. This observation was highly consistent with the previous findings that mitochondria appeared in punctuated, fragmented organelles and accumulating around the nucleus with very similar kinetics as the tubulin destruction after the glutamate challenge (Figure 36A). Treatment with mdiviA or B (75 µM) and even BI-6c9 (10 µM) prevented this fragmentation of tubulin structures as well as mitochondrial fission, respectively. Quantification of percentages of cells with fragmented tubulin structures confirmed the observation that mdiviA or B, and even BI-6c9 acted as an upstream regulator to prevent tubulin destruction (Figure 36B). Measurements of the cytosolic area covered by mitochondria in HT-22 cells revealed that mitochondria move in the vicinity of the nucleus and the cytosolic area size remained more or less stable. Glutamate led to mitochondrial movement, where mitochondria covered an area from only 48 % of the cell. Small molecule inhibitors, like mdiviA and BI-6c9 could significantly avoid this movement of mitochondria to the nucleus and recovered the distribution of mitochondria to nearly control levels (Figure 36C).

These findings strongly suggest the influence of Drp1 and Bid on tubulin structures and mitochondrial location around the nucleus in a so far unknown manner and kinetic.

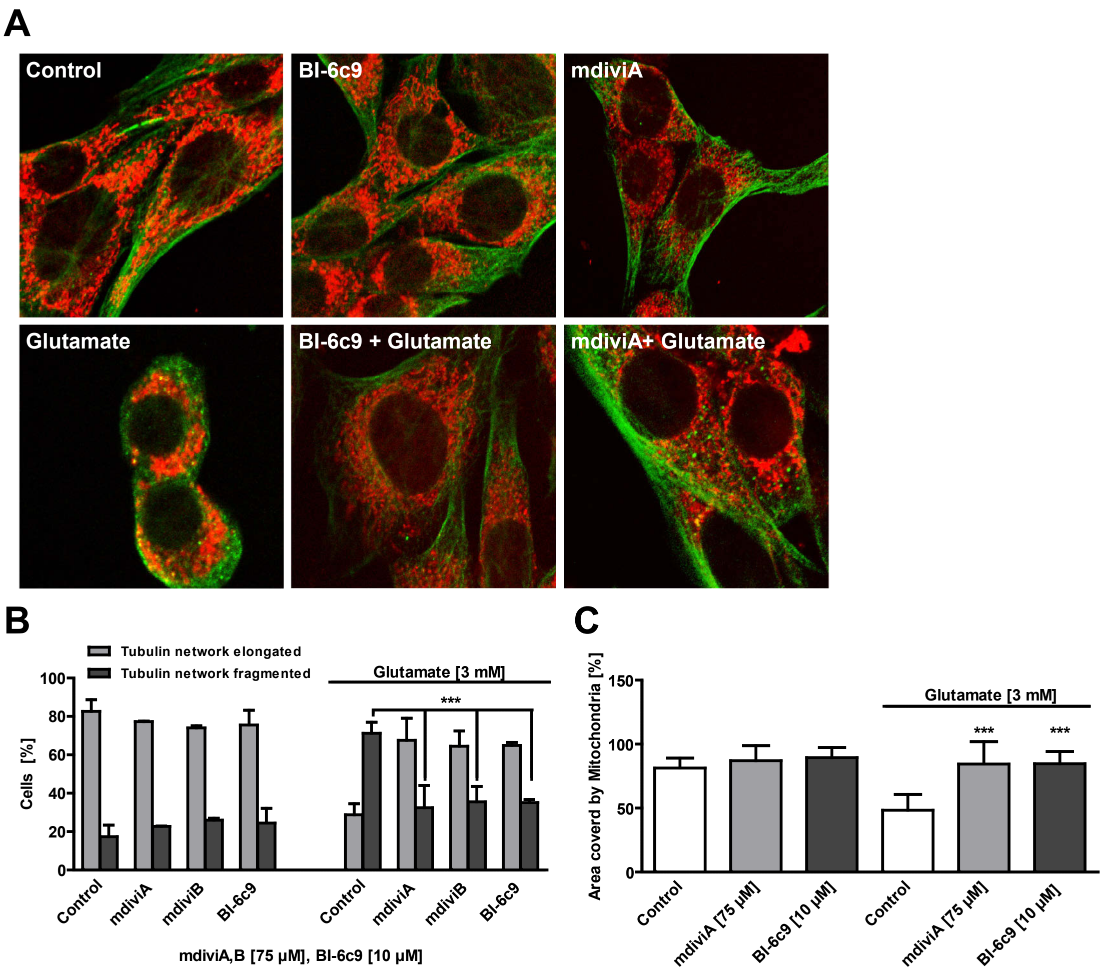
A
Control
BI-6c9
mdiviA
Glutamate
BI-6c9 + Glutamate
mdiviA+ Glutamate
B
Tubulin network elongated
Tubulin network fragmented
Glutamate [3 mM]
***
Cells [%]
0
20
40
60
80
100
Control
mdiviA
mdiviB
BI-6c9
Control
mdiviA
mdiviB
BI-6c9
mdiviA,B [75 µM], BI-6c9 [10 µM]
C
Area coverd by Mitochondria [%]
0
50
100
150
Glutamate [3 mM]
***
***
Control
mdiviA [75 µM]
BI-6c9 [10 µM]
Control
mdiviA [75 µM]
BI-6c9 [10 µM]

Figure 36 Tubulin structures are destroyed after glutamate toxicity in HT-22 cells

MdiviA, B and BI-6c9 interact with tubulin and influence the mitochondrial movement and distribution in HT-22 cells. **A**, HT-22 cells were cultured for 24 h in 8-well-ibidi plates and treated with 3 mM glutamate and mdiviA and B (75 µM) and BI-6c9 (10 µM) for 14 h. Immunocytochemistry analysis revealed that tubulin structures (green) were destroyed, mitochondria (red) fragmented and moved into the vicinity of the nucleus after glutamate (3 mM) stimulus. MdiviA and BI-6c9 inhibited the destruction of tubulin filaments and prevented mitochondiral fission. **B**, Quantification of tubulin morphology of five hundred cells per condition in at least four independent experiments. ***$p<0.001$ compared to glutamate (3 mM)-treated cells (ANOVA, Scheffé's-test). **C**, Determination of mitochondrial localisation in the HT-22 cells. HT-22 cells were stained with Mitotracker DeepRed and treated with mdiviA, B (75 µM) and glutamate (3 mM) for 16 h. The area of cytosol and the area of mitochondria were quantified with LASAF sofware (Leica, Wetzlar, Germany). The quotient: area covered by mitochondria/area cytosol in percantage represented in low values fragmented, perinuclear located mitochondria, which are less distributed in the cytosol. Control cells or mdiviA or BI-6c9 treated cells represented a high value of the quotient, mitochondria are distributed in the whole cytosol. ***$p<0.001$ compared to glutamate (3 mM)-treated cells (n=20, ANOVA, Scheffé's-test). The experiments were repeated three times and the results presented as mean ± S.D

3.7.2 Cyclosporine A prevents mitochondrial fragmentation after glutamate-toxicity in HT-22 cells

Mitochondrial membrane permeabilization (MMP) can derive from two distinct, but partially overlapping, molecular mechanisms. On the one hand, large channels formed by “multi-domain” proapoptotic proteins of the Bcl-2 family (Bax and Bak) might selectively promote mitochondrial outer membrane permeabilization (MOMP). On the other hand, cell death inducers such as Ca^{2+} or oxidative stress can trigger MMP at the inner mitochondrial membrane (IMM), by favoring the opening of the permeability transition pore complex (PTPC) for the release of proapoptotic proteins, such as Cytc and AIF (38). Further is known, that Ca^{2+}-dependent phosphatase calcineurin regulates the subcellular localization of Drp1 by dephosphorylation. Dephosphorylation of Drp1 by calcineurin promotes translocation of Drp1 to the mitochondria causing their fission in apoptotic cell death (113).

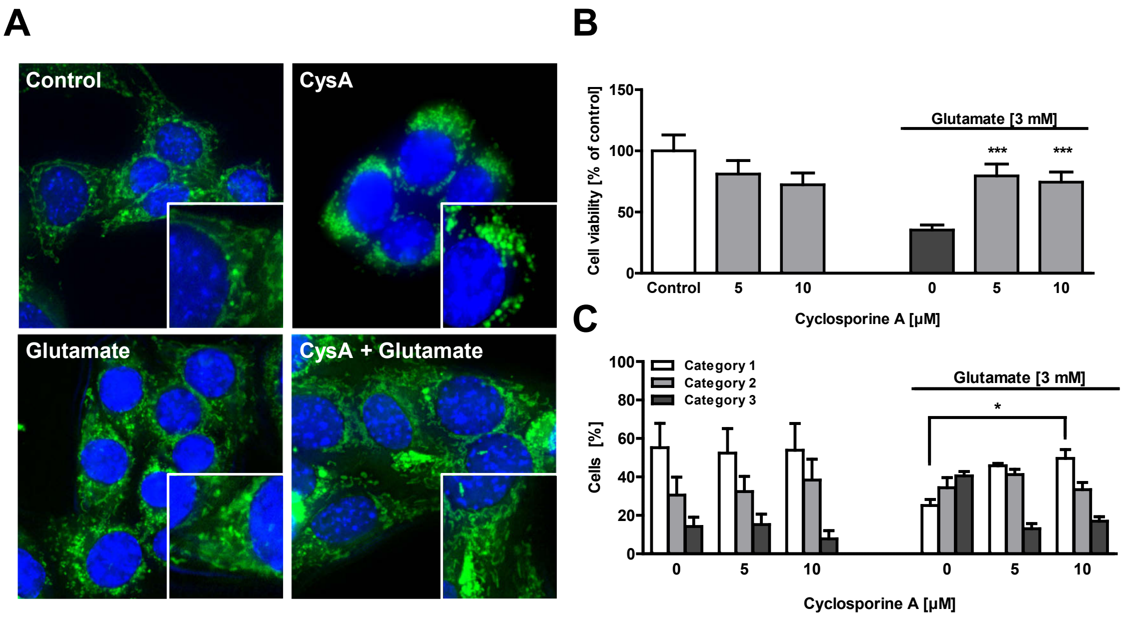

Figure 37 Cyclosporine A prevents mitochondrial fragmentation after glutamate toxicity in HT-22 cells

A, Fluorescence photomicrographs (63x objective) showed mGFP-transfected and DAPI-stained HT-22 cells. The pore blocker cyclosporine A (CysA 5 and 10 µM, 18 h) prevented fission of mitochondria after glutamate (3 mM, 18 h). **B**, HT-22 cells were cultured in 96-well plates with 7,000 cells per well and MTT assay was used to determine the cell viability 18 h after glutamate toxicity (3 mM). Cyclosporine A (5, 10 µM) showed significantly protective effects compared to glutamate-treated cells (n=8). ***$p<0.001$ compared to glutamate-treated cells (ANOVA, Scheffé’s-test). **C**, Quantification of mitochondrial morphology of five hundred cells per condition. Category 1: tubulin-like, category 2: intermediate, category 3: fragmented. Cyclosporine A (10 µM, 18 h) significantly prevented mitochondrial fragmentation after glutamate treatment (3 mM, 18 h) (n=3). *$p<0.05$ compared to glutamate (3 mM)-treated cells (ANOVA, Bonferroni-test). The experiments were repeated three times and the results presented as mean ± S.D.

To address the question, if glutamate-induced Ca^{2+}-increase induces the activity of calcineurin thereby influencing Drp1 localization, cyclosporine A (CysA), as a specific inhibitor of calcineurin was used. It is interesting to note, that CysA binds additionally to cyclophilin D (CypD), one part in the PTPC and thereby inhibiting PTPC opening, respectively (141).

CysA prevented cell death in the glutamate toxicity model in HT-22 cells as evaluated by MTT assay (Figure 37B). In addition glutamate-induced mitochondrial fragmentation was also prevented by CysA 18 h after the onset of glutamate treatment (Figure 37A, C). The significant protective effect of CysA is due the inhibition of the activity of Ca^{2+}-dependent calcineurin, which dephosphorylated Drp1 and thereby induced the increased translocation of Drp1 to the mitochondria and subsequently mitochondrial fragmention after glutamate toxicity. In addition, CysA inhibited the opening of MPT pores after glutamate challange. Both events seemed to be active in this model system of oxidative stress and were prevented by CysA (5, 10 µM) (Figure 37A, B).

Based on the fact that the HT-22 model of oxytosis only partly reflects the mechanisms of neuronal death, cyclosporine A was also tested in a model of glutamate-induced excitotoxicity in primary cortical neurons. Similar to the previous findings in HT-22 cells, treatment with CysA (5, 10 µM) of primary rat cortical neurons significantly attenuated glutamate-toxicity as quantified by the MTT assay (Figure 38).

The mitochondrial transition pore and the role of Ca^{2+}-dependent calcineurin in the regulation of Drp1 activity presented further mechanisms in the complex regulation of mitochondrial fission in glutamate-induced cell death. Both mechanisms can be specifically blocked by CysA.

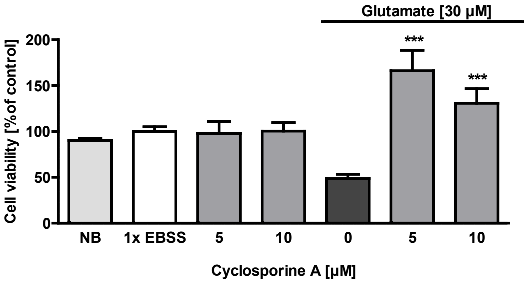

Figure 38 Cyclosporine A prevents mitochondrial fragmentation after glutamate toxicity in primary cortical neurons

MTT assay was used to determine the cell viability 18 h after glutamate toxicity. Primary rat cortical neurons were treated on day 9 for 18 h with glutamate (30 µM) and mdiviA and B (25 µM). Cyclosporine A (5, 10 µM) showed significantly protective effects compared to glutamate-treated cells (n=8). ***p<0.001 compared to glutamate-treated cells (ANOVA, Scheffé's-test). The experiments were repeated three times and the results presented as mean ± S.D.

These experiments assumed that calcineurin could be activated by glutamate and cause dephosphorylation of Drp1, followed by Drp1 translocation to the mitochondria. Furthermore, these experiments give evidences that the opening of the PTPC occur in parallel to mitochondrial fission in glutamate-induced cell death. However, further studies are necessary to clarify, if the opening of the transition pore is a consequence or epiphenomena during mitochondrial fission in these model systems of glutamate neurotoxicity in HT-22 cells and primary cortical neurons. Further, the regulation of Drp1 by calcineurin could provide a target to manipulate apoptotic mitochondrial fission and a helpful tool to clarify the mechanism of Drp1-dependent mitochondrial fragmentation in neuronal cell death. Therefore, future studies have to elucidate, which exact role calcineurin has in the glutamate toxicity model in HT-22 cells.

3.7.3 Protein interacting partners of Drp1 in HT-22 cells after glutamate-toxicity

Mitochondrial fission is a complex process, which is mainly regulated by the Drp1 protein. It has been suggested that the mitochondrial outer membrane protein Fis-1 and the proapoptotic Bcl-2 family proteins Bax and Bcl-xl (100;110) operate directly as positive regulators of Drp1 to promote mitochondrial fission in apoptosis (46;103;105;111;112). The potential interacting partners of Drp1 in the glutamate oxytosis model are unknown, yet. Thus, protein lysates were analyzed by immunoprecipitation of Drp1 to identify potential protein interaction partners and further regulator proteins of mitochondrial fission in HT-22 cells. HT-22 cells were treated with glutamate (3 mM) and cells were harvested at defined times, ranging from 8 h to 12 h after the onset of glutamate exposure. The following immunoprecipitation experiment revealed two Bcl-2 family proteins which interacted with Drp1. Enhanced binding of Bcl-xl and Bax was detected 10 - 12 h after the onset of the glutamate treatment (Figure 39).

These findings fit well to recently published data, indicating that Drp1 and Bax interacted to enhance mitochondrial dysfunction by opening the membrane pore and inducing fragmentation of this organelle (112). No interaction of Drp1 was detected with BH3-only protein Bid. This suggest that Bid and Drp1 do not interact directly to induce mitochondrial fragmentation and further studies are required to find the exact mechanism, on which both proteins regulate mitochondrial fission and dysfunction in glutamate-induced cell death. Further, the experiment in HT-22 cells reveals that Bax could be a key regulator and the link between Drp1 and Bid in the regulation of MOMP and fission in HT-22 cells after glutamate-toxicity. This theory is confirmed by current literature, where is describing that both proteins are able to interact directly with Bax.

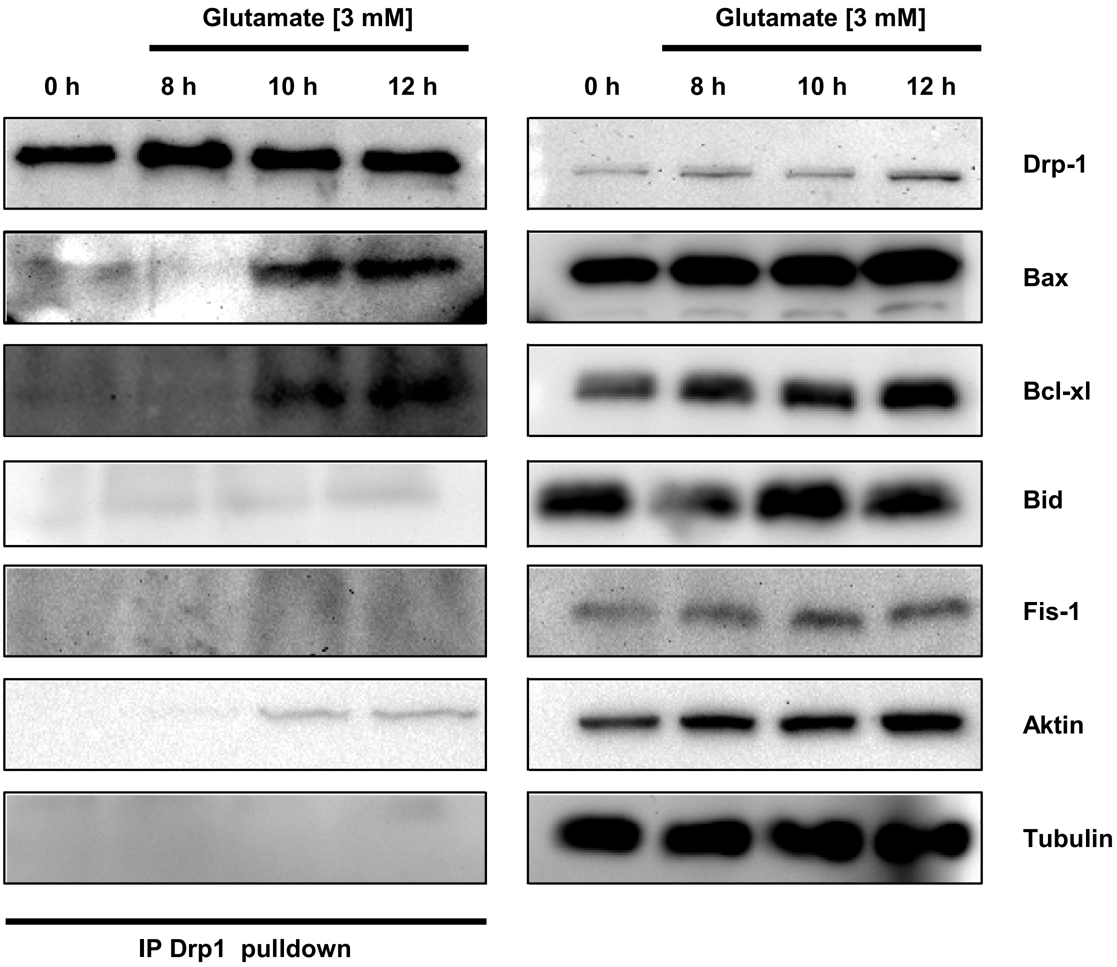
Glutamate [3 mM]
Glutamate [3 mM]
0 h
8 h
10 h
12 h
0 h
8 h
10 h
12 h
Drp-1
Bax
Bcl-xl
Bid
Fis-1
Aktin
Tubulin
IP Drp1 pulldown

Figure 39 Western blot analysis of Drp1 and interacting partners in HT-22 cells after glutamate-toxicity in HT-22 cells

Immunoprecipitation analysis of Drp1 protein was prepared from 2.5 mg total protein lysat of HT-22 cells which are treated with 3 mM glutamate for 8, 10 and 12 hours. Western blot analysis showed on the left side the pulldown of Drp1 and on the right side total protein lysat with 30 µg. 10 hours after glutamate treatment in HT-22, Drp1 interacts with Bcl-2 family proteins Bax and Bcl-xl. No interaction was detectable with BH3-only protein Bid.

3.8 The Role of Drp1 and Bid in different models of oxidative stress

The previous results suggested that Drp1 and also Bid are key mediators of glutamate-induced mitochondrial fission and cell death in HT-22 cells as well as in primary neurons. In order to elucidate, whether Drp1 activation or Bid activation is also involved in neuronal cell death induced by different oxidative stress stimuli, several prominent models of oxidative stress were analyzed in HT-22 cells, to address the involvement of Drp1 and Bid. To this end, HT-22 neurons were exposed to radical donors such as glucose oxidase (GO) and H_2O_2, 4-HNE (4-Hydroxynonenal) as well as to nitrogen monoxide (NO)-donors, such as DEANONOate and sodium nitropusside (SNP).

3.8.1 Bid inhibition does not prevent neuronal cell death by radical donors

The radical donors glucose oxidase and H_2O_2 induced cell death in HT-22 cells in a concentration- and time-dependent manner (Figure 40A, B). Both model substances are common radical donors and were applied in several studies on mechanisms of neurodegenerative diseases (142;143). It is important to note, that treatment with H_2O_2 leads to rapid production of high ROS levels, whereas glucose oxidase serves as a more continuous source for the release of H_2O_2.

To determine the potent role of the BH3-only protein Bid in GO- and H_2O_2-induced cell death, HT-22 cells were pretreated with BI-6c9 (10 µM) for one hour before incubation with H_2O_2 (600 - 700 µM) and GO (10 - 20 mU/ml). Cell viability was evaluated by MTT assay at 16 h. Inhibition of Bid could not prevent cell death induced by radical donors (Figure 40C, D). In contrast, studies with radical scavenger, like NAC showed protective effects HT-22 cells against H_2O_2-induced cell death (144).

In conclusion these data show that cell damage induced by radical donors is not comparable with glutamate-induced cell death and the associated oxytosis. Bid apparently plays no role in cell death in HT-22 cells exposed to radical donors.

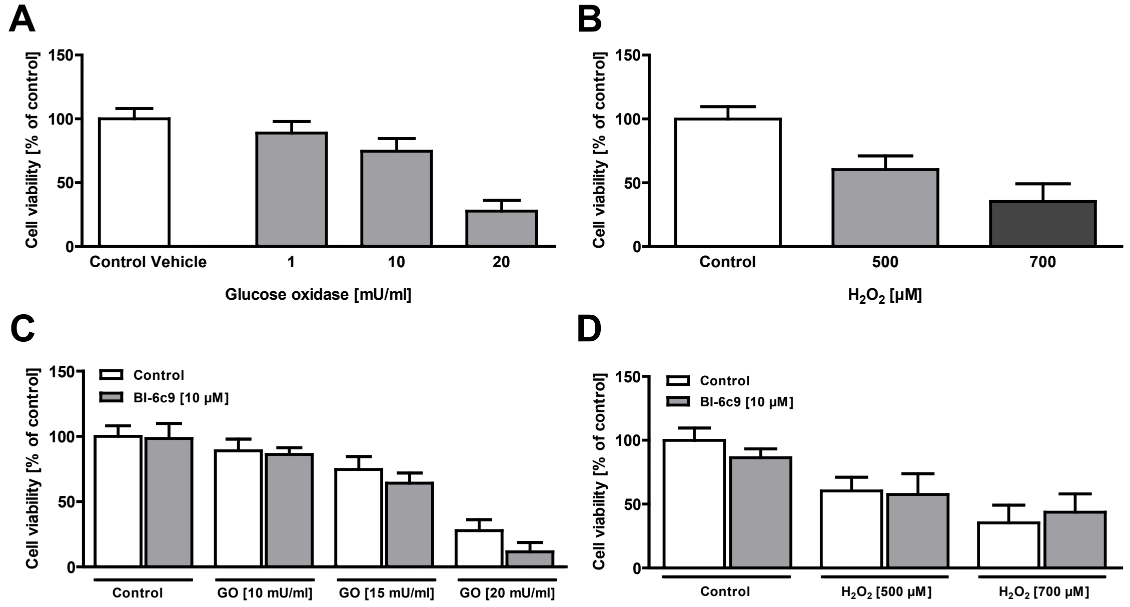

Figure 40 Bid inhibitor BI-6c9 does not prevent radical donor induced cell death

HT-22 cells were cultured in 96-well plates with 7,000 cells per well and treated with **A**, glucose oxidase (GO) (1 - 20 mU/ml) and **B**, H_2O_2 (500 - 700 µM). Cell death was evaluated by MTT assay 14 - 16 h after the onset of the treatment (n=8). Cells died in a concetration- and time-dependent manner. HT-22 cells were treated with **C**, glucose oxidase (GO) (10 - 20 mU/ml) and **D**, H_2O_2 (500 - 700 µM). H_2O_2 and glucose oxidase were added 1 h after pretreatment with BI-6c9 (10 µM). After 16 h cell death was evaluated using the MTT assay (n=8). The experiments were repeated three times and the results presented as mean ± S.D.

3.8.2 4-HNE-induced cell death is not prevented by BI-6c9

Peroxidation of cellular membrane lipids or circulating lipoprotein molecules generates highly reactive aldehydes. Among these, the most important reactive aldehyde is the toxic second messenger of free radical formation, 4-Hydroxynonenal (4-HNE), which is often detected in brain tissues of patients suffering from neurodegenerative diseases, e.g. in the brain of AD patients. Application of 4-HNE in neuronal cultures is a widely used model system *in vitro* to investigate mechanisms of neurodegeneration (145-147). To elucidate the question, if Bid is activated in 4-HNE-induced neuronal cell death, BI-6c9 (10 µM) was added one hour before treatment with 4-HNE. 4-HNE induced concentration- and time-dependent cell death in HT-22 neurons (Figure 41A), which could not be prevented by the Bid inhibitor BI-6c9 (10 µM) 16 h after the exposure to 4-HNE as quantified by the MTT assay (Figure 41B). These data suggest that Bid was not involved in the death signaling pathway of 4-HNE induced cell death in HT-22 neurons. Further, these data indicated that glutamate toxicity does not involve formation of large amounts of 4-HNE and 4-HNE triggers different apoptotic pathways in HT-22 cells than glutamate.

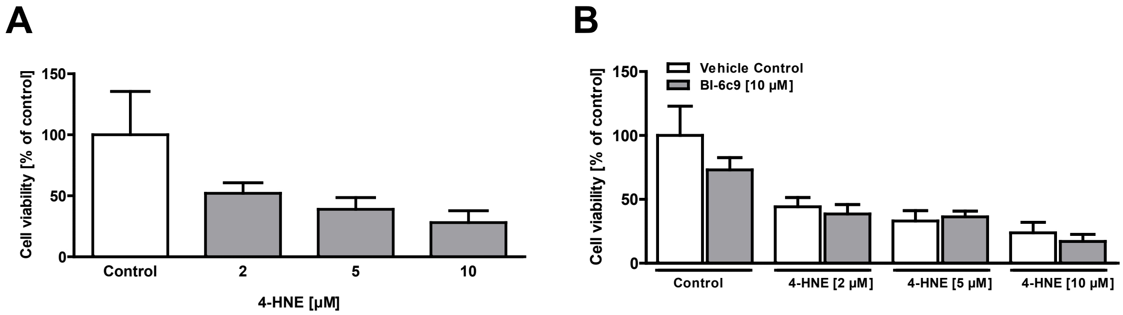

Figure 41 4-Hydroxynonenal (4-HNE) causes cell death independent on Bid activation in HT-22 cells

HT-22 cells were cultured in 96-well plates with 7,000 cells per well. **A**, HT-22 cells are treated with 4-HNE (2 - 10 µM) for 16 h. Time- and concentration-dependent cell death was induced by 4-HNE and evaluated by MTT assay (n=8). **B**, The inhibition of Bid by one hour preincubation with the Bid inhibitor BI-6c9 (10 µM) failed to prevent 4-HNE-induced damage atfer 16 h. Cell viability was detected using the MTT assay (n=8). The experiments were repeated three times and the results presented as mean ± S.D.

3.8.3 NO toxicity and subsequent nitrosylation of Drp1 does not occur in glutamate-treated HT-22 cells

In recent studies it has been shown, that NO-mediated neuronal cell death occur amongst others by nitrosylation of proteins, like Drp1 (116;120;148-150) after induction of oxidative stress or disruption of the calcium homeostasis (32;116;151). To address the question, whether Drp1 was regulated in the NO-induced cell death in HT-22 cells and if NO-mediated post-translationally modification of Drp1 played a role in this kind of cell death, the NO-donor DEANONOate was applied. DEANONOate was added at final concentrations of 2 - 10 mM to induce cellular toxicity by a fast release of NO. DEANONOate is a very unstable chemical substance, which induced high NO-levels immediately after the onset of the treatment.

In HT-22 cells, DEANONOate (2 - 10 mM) induced a concentration-dependent damage which was evaluated by MTT assay (Figure 42A) after 14 - 16 h after the onset of the treatment. Application of Drp1 inhibitor mdiviA (75 µM) and Bid inhibitor BI-6c9 (10 µM) one hour prior to DEANONOate (2 mM) failed to prevent NO-mediated neuronal cell death in HT-22 cells (Figure 42B, C). These results suggest that Bid and Drp1 activation is not involved in the NO-induced cell death in HT-22 cells.

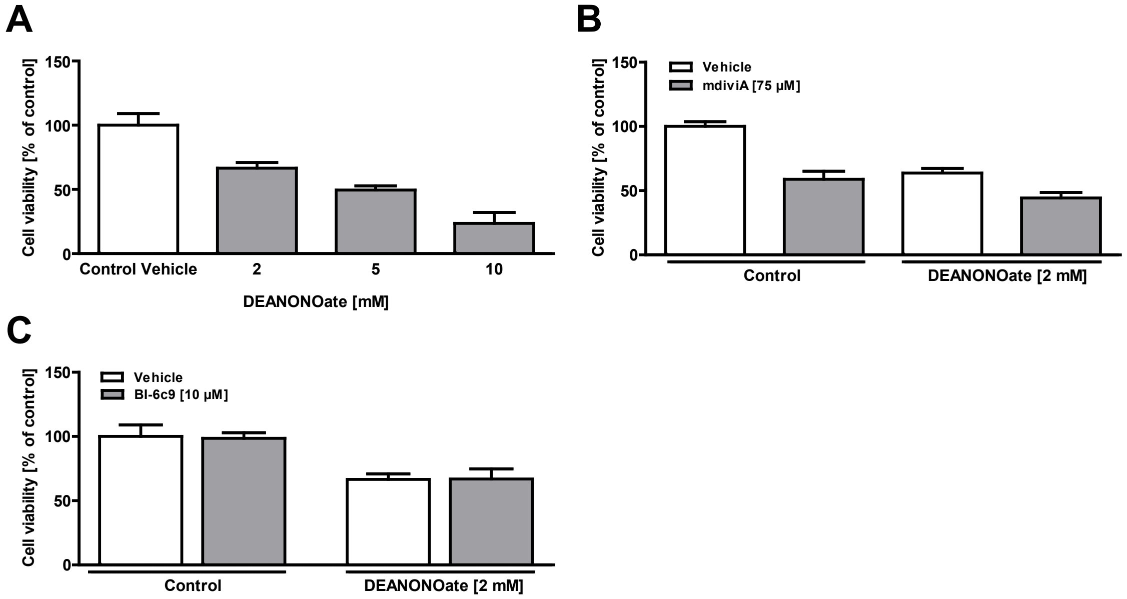

Figure 42 NO toxicity does not involve Drp1 and Bid activity

HT-22 cells were seeded out in 96-well plates with 7,000 cells per well. 24 h after seeding of the cells treatments starts with the pretreatment of the inhibitors. **A**, NO donor DEANONOate (2 - 10 mM) reduced cell viability in HT-22 cells in a concentration-dependent manner. **B** and **C**, mdiviA (75 µM) was added 1 h prior to DEANONOate (2 mM) and Drp1 and Bid inhibition did not prevent DEANONOate-induced cell death. Cell viability was analyzed by MTT assay 14 - 16 h after the onset of the treatment (n=8). The experiments were repeated three times and the results presented as mean ± S.D.

In order to examine the role of potential NO-release in detail, the HT-22 cells were also treated with sodium nitropusside (SNP, 20 µM - 20 mM) to induce the formation of NO, CN^- and Fe^{2+}. It is important to note, that SNP leads to a continuous release of Fe^{2+} and CN^- and persistent low levels of NO overtime in the cell, in contrast to the application of DEANONOate, where toxic NO levels are immediately achieved. SNP reduced the cell viability in the HT-22 cells in a concentration- and time-dependent manner after 16 hours of exposure (Figure 43A). Adding the Bid inhibitor BI-6c9 (10 µM) one hour prior to SNP significantly reduced cell death as detected by the MTT assay after 16 h (Figure 43B). In contrast, the Drp1 inhibitor mdiviA (75 µM) added one hour prior the SNP treatment failed to prevent SNP toxicity (Figure 43B). Real time measurements of cell viability by the xCELLigence System showed that inhibition of Bid by BI-6c9 clearly prevented the SNP-induced neuronal cell death which is confirmed by the MTT assay (Figure 43C). In summary, neuronal cell death induced by different NO-donors, such as DEANONOate or SNP activate different apoptotic pathways compared to glutamate. Apparently, Drp1 was not involved in this NO-mediated cell death in neuronal HT-22 cells. In contrast, Bid seems somehow to be involved in the SNP-induced neuronal cell death in HT-22 cells, which has to be studied in greater detail in the future.

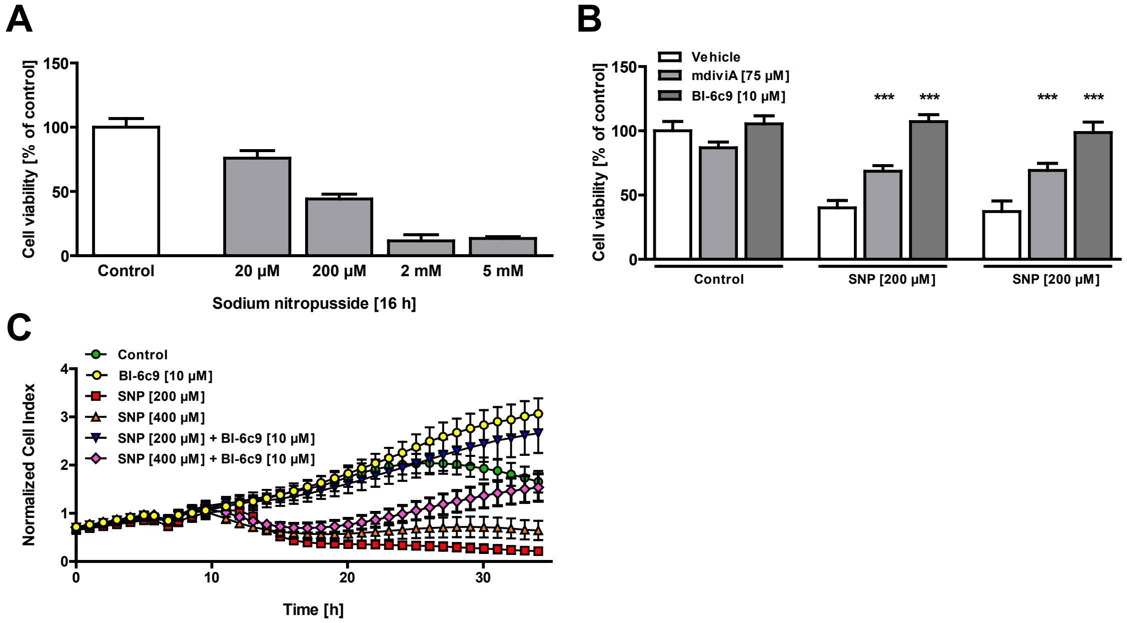

Figure 43 Bid inhibtion prevents SNP-induced neuronal cell death, but not Drp1-inhibiton

HT-22 cells were seeded in 96-well plates with 7,000 cells per well. Twenty-four after seeding of the cells treatment started with the pretreatment of the inhibitors BI-6c9 (10 µM) and mdiviA (75 µM). **A**, The SNP (20 µM - 5 mM) reduces cell viability in HT-22 cells in a concentration-dependent manner. **B** and **C**, mdiviA (75 µM) and BI-6c9 (10 µM) were added 1 h prior to SNP (200 and 400 µM) and Bid inhibition prevents SNP-induced cell death in HT-22 cells. Cell viability was analyzed by MTT assay 14 - 16 h after the onset of the treatment (n=8). ***p<0.001 compared to SNP (200 and 400 µM)-treated cells (Anova, Scheffé's-test). **C**, HT-22 cells were cultured for 48 h in 96-well E-plates and treated with 200 and 400 µM SNP and BI-6c9 (10 µM) for 18 h. Real time detection of cellular impedance was performed with xCELLigence System (n=8) (Roche, Penzberg, Germany). The experiments were repeated three times and the results presented as mean ± S.D.

In order to examine the mechanism of SNP toxicity in further detail and with regard to post-translational modification by nitrosylation of Drp1 in this model system of oxidative stress, total protein lysates of HT-22 cells were analyzed by western blotting to evaluate the tyrosine nitrosylation after exposure to SNP. The NO-donor DEANONOate was used as a positive control to confirm the function of the antibody. Tyrosine nitrosylation was not detectable in cells exposed to SNP suggesting that the formation of NO and subsequent tyrosine nitrosylation was not the dominant trigger in neuronal cell death and did not modify the Drp1 protein in HT-22 cells (Figure 44).

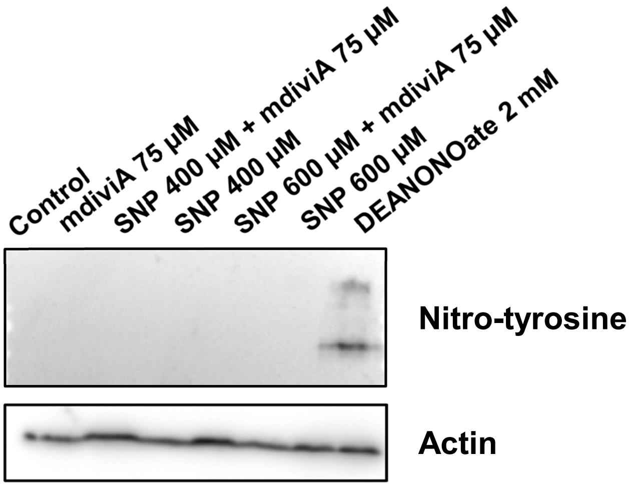
Control
mdiviA 75 µM
SNP 400 µM + mdiviA 75 µM
SNP 400 µM
SNP 600 µM + mdiviA 75 µM
SNP 600 µM
DEANONOate 2 mM
Nitro-tyrosine
Actin

Figure 44 SNP does not induce detectable tyrosine nitrosylation

Total protein lysate was obtained from damaged HT-22 cells after 16 h exposure to SNP (400 and 600 µM) ± mdiviA (75 µM) and DEANONOate (2 mM) and analyzed by western blotting. Nitrosylation of tyrosine residues were detected using an anti-nitro-tyrosine antibody (New England Biolabs-Cell Signaling, Heidelberg, Germany). DEANONOate, but not SNP induced tyrosine nitrosylation

4 Discussion

The major aim of this thesis was to analyze the mitochondrial dynamics and their regulation by the proteins Drp1 and Bid in models of glutamate-induced neuronal cell death. The involvement of Bid and Drp1 was mainly characterized in immortalized mouse hippocampal HT-22 neurons and in primary neuronal cultures exposed to toxic glutamate concentrations. In addition, the roles of Bid and Drp1 in other models of oxidative stress induced by H_2O_2, 4-HNE and NO-donors like SNP and DEANONOate were addressed.

The first part of this study revealed the critical involvement of enhanced mitochondrial fission in glutamate-induced cell death. The results showed that glutamate-induced apoptosis was associated with enhanced mitochondrial fission, loss of mitochondrial membrane potential and relocation of fragmented mitochondria to the nucleus. Further, the results obtained here provided evidence for an essential role of the BH3-only protein Bid in mitochondrial fragmentation of neuronal apoptosis caused by oxidative stress. The mitochondrial fragmentation, the associated loss of the mitochondrial membrane potential and cell death were prevented by BI-6c9, a highly specific Bid inhibitor, indicating a major role of Bid in death signaling upstream of mitochondrial fission, and the altered cellular distribution and integrity of these organelles in neuronal cells.

The second part of this study explored whether Drp1 played a major role in neuronal cell death after glutamate-toxicity in HT-22 cells and primary cortical neurons. To investigate the role of Drp1, highly specific small molecule inhibitors of Drp1 and siRNA approach were used for the first time in this model system of oxidative stress in neuronal cells. The data demonstrated a significant neuroprotective effect through inhibition of Drp1, suggesting that this regulator of mitochondrial fission is involved in delayed neuronal cell death. This conclusion is based on findings showing that down-regulation of Drp1 by siRNA or by small molecule inhibitors significantly preserved mitochondrial morphology and mitochondrial membrane potential, and reduced glutamate toxicity in neuronal cells. In addition, the Drp1 inhibitors protected primary cortical neurons against oxygen glucose deprivation *in vitro*, and preserved brain tissue after cerebral ischemia *in vivo*. These results exposed Drp1 as a key factor in ischemic and glutamate-induced neuronal cell death and identified Drp1-dependent mitochondrial fission as a potential therapeutic target in acute cerebrovascular diseases.

Overall, data obtained from the present study demonstrated for the first time that Bid and Drp1 are key regulators of mitochondrial cell death pathways associated with glutamate toxicity and enhanced oxidative stress in neurons. Bid-mediated neuronal cell death involved Drp1-dependent mitochondrial fission, mitochondrial relocation to the nucleus, mitochondrial membrane permeabilization, and release of mitochondrial cell death regulators such as AIF. Therefore, the presented data exposed the inhibition of Bid and inhibition of Drp1 as a promising therapeutic strategy to prevent mitochondrial fragmentation and dysfunction, hallmarks of neuronal cell death in many acute and chronic neurodegenerative diseases.

4.1 Enhanced mitochondrial fission induced by glutamate in HT-22 cells

Mitochondria routinely divide and fuse through the actions of conserved large GTPases. Under physiological conditions the rate of such mitochondrial dynamics is balanced by the rate of fusion and fission events. Especially in neurons, mitochondrial dynamics appear to play an even more critical role because of complex energy requirements for maintaining and restoring neuronal membrane potential and particular synaptic functions, such as neurotransmitter synthesis and release. Dysregulation of mitochondrial dynamic proteins enhance fragmentation, loss of mitochondria in dendritic spines and increase synapse formation and dysfunction. In the present study, the mitochondria network in neuronal cells underwent dramatic rearrangement after the apoptotic damage induced by glutamate, resulting in fragmented mitochondrial phenotype associated with enhanced mitochondrial fission, loss of mitochondrial potential and relocation of fragmented mitochondria to the vicinity of the nucleus.

Exposure of HT-22 cells to glutamate resulted in enhanced, ROS formation in a time-dependent manner and this ROS formation was associated with a significant change in mitochondrial morphology. Mitochondria were organized as a tubular network under control conditions, however, after exposure to glutamate the network broke up in short tubules and round fragments. In HT-22 cells, mitochondrial fragmentation and the organelle`s relocation to the nucleus started 3 - 4 hours after exposure to glutamate and was associated with the increased ROS formation, lipid peroxidation and the decreased cell viability. It is interesting to note that the recruitment of the mitochondria was detectable by the accumulation and agglomeration of the highly fragmented mitochondria in the vicinity of the nucleus, suggesting that in dying neurons enhanced mitochondrial fission was permissive for an enhanced transport of these organelles towards the nucleus. This was further confirmed by the measurements showing that the cytososolic area covered by mitochondria in the cell after glutamate was significantly reduced and a breakdown of the tubulin network at later time points. These kinetics of mitochondrial changes fitted well with the kinetics of cell death execution that has been established in the applied model of glutamate-induced oxidative cell death. In particular, multiple lines of evidence proposed a prelude of several hours for the glutamate-induced glutathione depletion and Bid-mediated disruption of mitochondrial function. Previous studies defined a therapeutic time window of 8 - 10 h after the onset of the glutamate challenge that allowed delayed application of antioxidants or e.g. the Bid inhibitor to rescue mitochondrial function and to prevent neuronal cell death (39).

The impedance measurements correlated very well with established measurements of cell viability by the standard MTT assay and clearly demonstrated that oxidative cell death occurred not before 8 – 10 h after onset of the glutamate challenge. In this time frame, enhanced mitochondrial fission and peri-nuclear accumulation of the organelles precede the final execution of cell death that is featured by mitochondrial membrane permeabilization and release of mitochondrial AIF to the nucleus. Further, the observed agglomeration of fragmented mitochondria in close vicinity to the nucleus further explains the relatively fast kinetics of the following death execution that occurs within 1 - 3 h after the preluding events and involves rapid translocation of AIF to the nucleus as shown by video-microscopy in earlier work (39). The high number of fragmented and permeabilized mitochondria is likely to be a prerequisite for the observed rapid transfer of the deadly mitochondrial protein over the short distance to the nuclei of lethally stressed cells.

In conclusion, enhanced mitochondrial fission is a key feature for programmed cell death execution, since fragmented mitochondria can easily accumulate around the nucleus where they release their deadly message after reaching the “point of no return” marked by mitochondrial membrane permeabilization.

4.2 The Bcl-2 family proteins modulate mitochondrial dynamics

4.2.1 The Bcl-2 family proteins control mitochondrial dynamics in nonapoptotic cells

Accumulating evidence suggests that members of the Bcl-2 family influence mitochondrial network-dynamics in healthy neuronal cells. The proapoptotic proteins Bax and Bak were the first Bcl-2 family members discovered to play a role in mitochondrial dynamics in nonapoptotic cells by interacting with components of the machinery regulating mitochondrial dynamics. It has been reported that Bax and Bak, can directly interact with mitofusins. Both proteins promote mitochondrial fragmentation by regulating the localisation of Mfn-1, its mobility in the outer mitochondrial membrane (OMM) as well as its ability to oligomerize (152;153). Further, antiapoptotic Bcl-xl has been shown to interact with Drp1 in neurons and Bcl-xl may regulate mitochondrial fusion and fission in a Drp1-dependent manner with impact on synapse formation and -activity, biomass and mitochondrial localization in the synapses (110).

4.2.2 The Bcl-2 proteins control mitochondrial dynamics in apoptotic cells

The control of mitochondrial dynamics in apoptotic cells is a matter of intense ongoing research. Apoptosis-associated mitochondrial outer membrane permeabilization (MOMP) leads to increased ROS formation, reduced ATP levels and the release of proapoptotic proteins such as AIF, Cytc, EndoG and among others. In apoptotic cells, mitochondrial MOMP, is tightly regulated by Bcl-2 family proteins (48;154), and is functionally associated with mitochondrial fission and fusion proteins. For example, during apoptosis, Bax and Bak promote Drp1-dependent mitochondrial fragmentation by colocalization of Bax with Drp1 and Mfn-2 at sites of the mitochondria outer membrane which then become fission sites. These protein interactions stabilize the association of Drp1 with the mitochondrial membrane and are prerequisite to inducing fragmentation of the organelles (153). In turn, Drp1 stimulates Bax oligomerization by triggering hemifusion of the mitochondrial membrane (112). Such Drp1 facilitated Bax oligomerization is likely an essential step towards enhanced membrane permeability, and the Bax-dependent release of proapoptotic factors from the mitochondria into the cytosol. Such Bax translocation to the mitochondria correlates with a reduction of mitochondria fusion (155). Furthermore, Bak regulates mitochondrial dynamics by interaction with mitofusins to decrease mitochondrial fusion (112;156;157).

Interestingly, overexpression of Bcl-xl inhibited Bax-induced Cytc release, but not Bax-induced fragmentation (93;158). Bcl-xl increases the rates of both, fusion and fission in a Drp1-dependent manner. Bcl-xl appear to maintain proper dendritic spine and synaptic structures in neurons via regulation of Drp1-dependent mitochondrial morphology and biomass (84;110;159). The present thesis now revealed an impact of Bid in the regulation of mitochondrial dynamics during apoptosis. Hence, Bcl-2 family proteins cause mitochondrial fragmentation by activation of fission and/or blocking fusion.

4.2.3 Bid is a key regulator of mitochondrial fission in glutamate-induced cell death in HT-22 cells

The present study provides evidence for a key role of the BH3-only protein Bid in mitochondrial pathways of neuronal apoptosis caused by oxidative stress. The data suggested that glutamate significantly disturbed the delicate balance between mitochondrial fission and fusion in neuronal cells and that fission of mitochondria-accompanied cell death. In the currently used model system, glutamate induced oxidative cell death through glutathione depletion and accelerated formation of reactive oxygen species (ROS), which was associated with enhanced mitochondrial fission, the depolarization of the mitochondrial outer membrane, relocation of fragmented mitochondria to the nucleus, and the release of mitochondrial AIF to the nucleus (39;92;160-162). All the latter mitochondrial features of apoptosis were prevented by Bid siRNA and the Bid inhibitor BI-6c9.

These data demonstrated that depolarization of the mitochondrial outer membrane and mitochondrial fragmentation are both important key events of mitochondrial apoptosis induced by oxidative stress, and both events were apparently Bid-dependent. The conclusion of the pivotal role for Bid upstream of such mitochondrial dysfunction is substantiated by experiments demonstrating pronounced neuroprotective effects of the Bid inhibitor BI-6c9 in models of glutamate-induced excitotoxicity and oxygen glucose deprivation in primary cultured neurons, and similar studies in HT-22 neurons using Bid siRNA (39;160;163). Further, genetic deletion of Bid attenuated neuronal death in a model of oxygen glucose deprivation *in vitro* and reduced brain damage in models of cerebral ischemia and brain trauma *in vivo* (60;62). These findings supported the conclusion, that Bid activation and subsequent mitochondrial translocation are early key events recruiting mitochondria to the death machinery in neurodegenerative pathologies associated with glutamate toxicity and oxidative stress. The precise mechanism of Bid/tBid-dependent mitochondrial fragmentation, loss of mitochondrial membrane potential and release of proapoptotic mitochondrial proteins is the subject of current studies. However, data obtained from this thesis demonstrated an essential interaction of Bid with Drp1, the main regulator of mitochondrial fission. The process of Bid/tBid-dependent mitochondrial fission may involve interactions of Bid with other Bcl-2 family proteins, like Bax and Bak, which also be regulated by factors of the fission and fusion machinery, like Drp1.

Previous studies showed, that tBid and full-length Bid exert similar effects on mitochondria and AIF-dependent cell death in neurons (39;164). Further studies confirmed that full-length Bid was sufficient to induce mitochondrial dysfunction in neurons (164). One study identified two separate apoptotic pathways where Bid translocation to the mitochondria played a significant role. On the one hand, activated tBid is capable of inducing mitochondrial demise in caspase-dependent death receptor mediated pathways, and, on the other hand, full-length Bid mediated glutamate-induced caspase-independent cell death pathways in different time frames/kinetics; while tBid induced rapid mitochondrial damage, detrimental effects of activated full-length Bid occurred much slower (70).

Glutamate-induced apoptosis in cerebellar granule and hippocampal neurons in a caspase-independent manner, involving the translocation of full-length Bid to the mitochondria 6 h after glutamate challenge. Further, translocation of full-length Bid and a collapse of the mitochondrial outer membrane permeabilization accompanied with a rapid increase of cytosolic Ca^{2+} occured prior to a cleavage of the Bid protein, indicated that Bid cleavage was a secondary event to translocation and mitochondrial depolarization in this model system. This suggested the potential for activation of calpains to cleave full-length Bid following the translocation and the collapse of the mitochondrial depolarization within these neurons (70). Addtionally, alterations in phospholipids have been shown to be a hallmark of excitotoxic, Ca^{2+}-dependent cell death. It has been presented that change in the cellular phospholipid content such as increased phosphatidic acid and phosphatidylglycerol levels enhanced the ability of full-length Bid to translocate and to permeabilize mitochondria (165). Further, it has been demonstrated that full-length Bid is able to oligomerize and trigger the insertion of Bax in isolated mitochondria (58). These data indicate that Bid can mediate mitochondrial damage and cell death as a full-length protein, which fits to the observation that tBid was hardly detectable in cytosolic or mitochondrial extracts from HT-22 cells or primary neurons after the glutamate challenge. This suggested that either full-length Bid was activated and then able to translocate to the mitochondria or only a small part of Bid was cleaved to tBid (39;162).

These findings are in contrast to reported findings in non-neuronal MCF-7 cells, where TRAIL-death receptor-mediated Bid cleavage, tBid translocation and mitochondrial deplorization occured in less than 2 min. time frame suggesting that very little Bid translocation/cleavage was sufficient to trigger mitochondrial outer membrane permeabilization during death receptor-induced apoptosis (70).

In this study, transfection with a toxic tBid-vector was used to induce tBid-mediated mitochondrial toxicity in HT-22 cells. The fast kinetics of tBid-induced cell death within 12 h in HT-22 cells showed that tBid was able to mediate mitochondrial dysfunction. It is important to note, that the Bid inhibitor BI-6c9 prevented the translocation of both, full-length Bid and tBid to the mitochondria and the detrimental effects on mitochondria, suggesting that the effects of both forms of activated Bid are comparable and may occur concomittantly in HT-22 neurons.

Currently, there are several hypotheses which propose to explain why tBid specifically translocates to mitochondria during apoptosis. One of the hypothesis, suggests that tBid acts as a ligand for other proteins of the Bcl-2 family such as Bax and Bak to induce mitochondrial outer membrane pore formation (7;56;166). Another hypothesis postulates, that tBid is post-transcriptionally myristinylated, which enhances targeting of tBid to the mitochondria (167). A third hypothesis proposed that tBid is able to remodel the intermembrane cristae which led to a release of Cytc to promote apoptosis independent of Bax/Bak activities (13;168). A fourth hypothesis postulated that tBid binds to cardiolipin at mitochondrial contact sites. In this context, it has been suggested, that full-length Bid and caspase-8 docked at the OMM via cardiolipin and formed an activating platform that enhanced the production of tBid (169;170). The latter finding is in line with reports that suggest that full-length Bid translocates to the mitochondria where it oligomerized directly with Bax or full-length Bid occurs prior to the interaction with the mitochondria cleaved to tBid to activate mitochondrial death pathways (171).

Overall, mitochondrial transactivation of full-length Bid or tBid may mark the execution phase of apoptotic death signaling. Therefore, activated Bid is regarded as a key mediator of mitochondrial neuronal cell death pathways associated with enhanced oxidative stress. The current study demonstrated for the first time, that Bid is a key regulator of mitochondrial fission, mitochondrial relocation to the nucleus, and mitochondrial integrity in neuronal cells exposed to oxidative stress. Therefore, Bid is a promising therapeutic target to prevent mitochondrial fragmentation and dysfunction which are hallmarks of neuronal cell death in most neurodegenerative diseases.

4.3 The role of Drp1 in the oxidative stress model of HT-22 cells

4.3.1 Mitochondrial fission is Drp1-dependent after glutamate

The present study demonstrated a significant neuroprotective effect by inhibition of Drp1, suggesting that this regulator of mitochondrial fission plays a major role in delayed neuronal cell death. This conclusion is based on findings showing that down-regulation of Drp1 by siRNA or by new small molecule inhibitors significantly preserved mitochondrial morphology and mitochondrial membrane potential and reduced glutamate toxicity in neuronal cells. These results showed that glutamate-induced mitochondrial fission was associated with depolarization of the mitochondrial membrane, and both events were Drp1 dependent. These data let suppose the theory that mitochondrial fission could happen in parallel to mitochondrial membrane permeabilization. In fact, pharmacological inhibition of Drp1 and Drp1 siRNA prevented mitochondrial membrane depolarization, and the rescue of mitochondrial membrane integrity was associated with preserved mitochondrial morphology and neuronal survival. These data clearly put Drp1 upstream of the detrimental loss of mitochondrial integrity, indicating that mitochondrial fragmentation is not only associated with features of mitochondrial cell death pathways and involved regulators of mitochondrial fission play a central role in these processes.

4.3.2 Drp1 and Bcl-2 family proteins control mitochondrial fission in HT-22 cells

The presented data demonstrated a role for the proapoptotic BH3-only protein Bid in Drp1-mediated mitochondrial fragmentation (39;92). As reported before, Bid was involved in the loss of MOMP and release of mitochondrial AIF in apoptotic neurons and played a key role in mechanisms of delayed neuronal death after cerebral ischemia (60;133;160). The present thesis now demonstrated that tBid-induced loss of MOMP and mitochondrial fragmentation depends on Drp1 activity since Drp1 inhibition prevented tBid-induced mitochondrial fission and preserved cell viability. In addition, the Bid inhibitor BI-6c9 prevented Drp1 translocation to the mitochondria. These data indicated a detrimental interplay between Bid and Drp1 that occurs upstream of mitochondrial death pathways that involve mitochondrial fission, MOMP and AIF release to the nucleus. Further, Drp1-dependent mitochondrial fission is closely linked to death signaling pathways triggered by proapoptotic Bcl-2 proteins. Consistent with the current literature (153), the present study was able to show, that Bax and Bcl-xl colocalized with Drp1 after glutamate toxicity what substantiated that Bax could be the connection of Bid- and Drp1-dependent mitochondrial fission. In addition, recent data suggested a role for tBid in enhancing Drp1-induced polymerization of Bax at mitochondrial fission sites, which further supporting the important role of Bid in these pathways of mitochondrial cell death (112).

In damaged neurons, inhibition of Drp1 may serve to shift the observed mitochondrial fission back to an outbalanced ratio of fusion and fission thereby preventing neuronal dysfunction and death. Alternatively, the role of Drp1 in neuronal cell death may be independent of its role in mitochondrial fission. Recently, Martinou and co-workers suggested Drp1 recruitment to cardiolipin-rich membrane sites as a prerequisite for membrane hemifusion and Bax oligomerization at mitochondria (112). Bax oligomerization, subsequent MMP, and release of proapoptotic factors to the cytosol were significantly delayed with Drp1 mutants lacking membrane recruitment and hemifusion activity. This observation is in line with these present findings of Drp1 recruitment to mitochondria prior to the demise of these organelles. Notably, Drp1-induced Bax oligomerization also required the presence of tBid which further supports the conclusion that both, Drp1 and Bid interact at the mitochondrial membrane for execution of mitochondrial death pathways in neurons. These findings suggest that Bid and oligomerized Bax accumulate at Drp1 recruiting sites which then become mitochondrial fission sites. Further, Drp1 activation is critical for mitochondrial fragmentation in apoptotic cell death. Thus, in dying neurons mitochondrial fission may be regarded as a morphological hallmark indicating the process of mitochondrial membrane permeabilization and mitochondrial death pathways. In the underlying mechanisms contrast the physiological fission of mitochondria, where fragmentation of these organelles permanently occurs without fatal damage to the organelles. Whether physiological fission in neurons also requires Bid and Bax has not been elucidated. However, earlier studies indicated that mitochondrial fusion dominated over fission in neurons exposed to pharmacological inhibitors of Bid and after siRNA-mediated Bid silencing (92). Further studies are required, to define the mechanisms that link oxidative stress, detrimental Bid activation and Drp1 activities at the sites of mitochondria in neurons.

A recent study showed that tBid can directly trigger christae remodeling by disassembly of Opa1 oligomeres in the inner mitochondiral membrane. This leads to a loss of christae structure with the release of Cytc and mitochondrial fission (168). To identifiy the regulating mechanisms of Bid/tBid it would be necessary to investigate if this tBid-induced christae remodeling happened during glutamate-induced cell death. Further, several reports showed that post-translational modifications like phosphorylation, sumoylation or ubiquitination on specific protein sites of Drp1 influenced its activity and localization in the cell. In line with previous studies, this thesis confirmed indirectly, that phosphorylation influenced the Drp1 activity in glutamate-induced apoptosis. Glutamate enhanced Ca^{2+} levels thereby stimulating the dephosphorylation of Drp1 by calcineurin, which, in turn, caused the translocation of Drp1 to the mitochondria and subsequent mitochondrial fragmentation. This was prevented by using the calcineurin inhibitor CspA, which revealed that dephosphorylation of Drp1, is an important post-translational modification to regulate Drp activity in glutamate-induced cell death. In addition, as shown in this thesis, NO and therefore nitrosylation of Drp1 did not play a significant role in glutamate-induced cell death. However, based on the finding that phosphorylation influenced the Drp1 activity, further investigations are warranted to define the potential roles of protein kinase A or Ca^{2+}/calmodulin-dependent protein kinase I alpha mediated mechanisms of Drp-1 activation and their relevance in the glutamate-induced cell death. The importance of post-translational modifications of Drp1 is underlined by recent findings indicating that phosphorylation and S-nitrosylation may significantly influence the Drp1 activity towards the direction of enhanced fission (116-118;141).

4.4 Two major structural changes in mitochondria correlate with glutamate-induced apoptosis

4.4.1 Mitochondrial fission and mitochondrial membrane permeabilization

Two major classes of structural changes in mitochondria are correlated with apoptosis: the opening of the mitochondrial outer membrane permeabilization (MOMP) and mitochondrial fission and fusion. These events have been studied independently in the past. Mitochondrial outer membrane permeabilization is defined as the “point of no return”, which promotes apoptosis by permitting proapoptotic proteins such as Cytc and AIF to promote downstream events of apoptosis. However, the mechanism underlying MOMP is still elusive. Recently, mitochondrial fission has been proposed to be closely related with MOMP in the execution of cell death. This hypothesis is based on the observations that apoptosis-associated mitochondrial fragmentation via Bax/Bak occured concomitantly with the Cytc-release (172). MOMP is believed to result from Bcl-2 protein conformation changes, protein-protein and protein-membrane-interactions. In particular, Bax seems to play a pivotal role to connect these two processes, because Bax is involved in the formation of the membrane permeabilization pore together with Bak and interacts with fusion and fission proteins like Drp1, and Mfn-1 and -2. This thesis demonstrated that Bid is additionally one pivotal regulator of MOMP and Drp1-dependent fission in glutamate-induced apoptosis.

However, several independent observations suggested that these events are merely coincident and can be functionally uncoupled. Different scenarios have been proposed on how mitochondrial dynamics are involved in the execution of apoptosis (99;173):

1. Both Bax and Drp1-dependent mitochondrial fission are responsible for apoptosis but these two regulation machineries work independently, in parallel. Apoptotic stimuli induce Bax translocation, oligomerization and Bax/Bak interactions on the OMM resulting in MOMP and Drp1-dependent fission of the mitochondria (85;106;174).
2. Drp1-dependent mitochondrial fission is promoted by Bax translocation and responsible for MOMP (86;106;175).
3. Mitochondrial fission is an essential step before MOMP. Apoptotic signals induce the release of calcium from the Endoplasmatic reticulum (ER) at first. This triggers the Drp1 translocation to mitochondria and induction of fragmentation. Mitochondrial fission induces Bax translocation, which is followed by MOMP (96;106).
4. Mitochondrial fission lies downstream of MOMP but is not necessary for MOMP. Apoptotic stimuli trigger the translocation of Bax to the mitochondria. This results in the release of intermembrane space proteins like Cytc or Opa1, which could explain the inhibition of mitochondrial fusion occurring during apoptosis (96;106;175-177).
5. Uncoupling of Bax/Bak-associated fragmentation and MOMP is based on studies in which Bax and Bak were transiently expressed along with antiapoptotic members of the Bcl-2 family, such as Bcl-xl or Bcl-2. In these studies, Bcl-2 and Bcl-xl failed to suppress Bax-induced fission but clearly suppressed MOMP and downstream apoptosis signaling (93;158).

These scenarios suggest that mitochondrial fission may participate in apoptosis through different pathways depending on the cell type, and/or apoptotic signal characteristics. Which scenario is relevant for the execution of neuronal cell death in the present model system of oxidative stress was one of the major questions addressed by this thesis. The data strongly suggest that mitochondrial fission occurs in parallel to mitochondrial membrane permeabilization and thus imply that Drp1 possesses multiple functions in mammalian cells.

4.4.2 The role of Drp1 in MOMP

Further, the data of the present thesis suggest that Drp1 acts upstream of mitochondrial membrane permeabilization and together with Bcl-2 proteins to directly modulate MOMP. Earlier data revealed that Drp1 self-assembly during apoptosis is relevant to trigger Drp1 functions at mitochondria. Such Drp1 self-assembly is blocked by mdiviA and therefore critical in MOMP. Here in this thesis, Drp1 inhibition by mdiviA clearly prevented mitochondrial depolarization in HT-22 cells. One possible explanation is that Drp1 directly interacts and co-assembles with Bid-activated Bax/Bak, creating a complex that is more active for both MOMP and mitochondrial division (125). In addition, enhanced fission exhibited by Drp1 clusters on mitochondria is dramatically lost after Bax recruitment to mitochondria during apoptosis, indicating that the biochemical properties of Drp1 are altered in a Bax-dependent manner (122). Evidence for this explanation is now shown by results of this thesis, indicating that Bax and Drp1 interact 10 - 12 h after glutamate challenge. This fits well with the established kinetics of glutamate-induced cell death, where MOMP was detected 10 - 12 h after the glutamate challenge. Thus, Drp1 may have a positive regulatory role in MOMP that is independent of its role in mitochondrial division, further demonstrating that Drp1 possesses multiple roles in mammalian cells depending on physiological or pathological settings.

Another possible mechanism for Drp1 during apoptosis is that it exerts its effects on MOMP by regulating the mitochondrial fusion machinery (125). Recent studies have shown that in healthy cells, Bax and Bak are required to maintain normal levels of mitochondrial fusion activity and alter the behavior of the mitochondrial outer membrane fusion protein, Mfn-2 (26). This contrasts the role of Bak and Bax during apoptosis, where, activated Bax and Mfn-2, are co-localized in clusters on the outer membrane to attenuate mitochondrial fusion (153). Thus, it is possible that Drp1 recruitment to an activated Bax/Bak complex alters their activities, causing inhibition of Mfn-2-dependent fusion activity. This in turn, may facilitates MOMP, likely via the control of cristae structures (178). Indeed, it has been reported that RNAi depletion of Drp1 in HeLa cells does not affect the release of Smac/DIABLO from mitochondria during apoptosis, but attenuates cytochrome c release, which is sequestered in the mitochondrial cristae (100;177). That mdiviA has a general influence on MOMP and likely does not exert its effects through changes in cristae structure was also shown by experiments, where mdiviA blocked Bax/Bak-dependent release of Smac/DIABLO from mitochondria *in vitro* (125). In consideration of this theory it is relevant to elucidate the role of mitochondrial fusion regulators, like Mfn-2, in glutamate-induced cell death.

4.5 The role of Drp1 in primary neurons

So far, the proposed detrimental role of Drp1 in neurons is based in large parts on the presented findings in HT-22 cells and is now also extended to postmitotic neurons, since Drp1 inhibitors also prevented glutamate excitotoxicity and OGD-induced death in primary cultured neurons, and in a model of cerebral ischemia *in vivo*. In these model systems, it is well established that the underlying death program also includes Bid-mediated mitochondrial damage and AIF release to the nucleus (60;133;134). The Drp1 inhibitors mdiviA and mdiviB also significantly protected primary cultured neurons from glutamate- and OGD-induced cell death *in vitro*. Further, in a model of ischemic stroke in mice, the small molecule inhibitors of Drp1 resulted in a significant reduction of the mean infarct volume compared to vehicle-treated controls. These data exposed Drp1 as a key factor in ischemic and glutamate-induced neuronal cell death, and identified Drp1-dependent mitochondrial fission as a potential therapeutic target in acute cerebrovascular diseases.

Therefore, inhibition of Drp1 as presented here using the mdivi compound expose a novel therapeutic strategy for both acute and chronic neurological diseases. This is in line with successful approaches of Drp1 inhibitor mdiviA in other experimental models of ischemic tissue damage, induced by cardiac or renal ischemia and reperfusion, respectively. Further, inhibitors of Drp1 have a therapeutic potential for a wide array of chemotherapeutic drug-induced tissue damage (157;179).

Regulation of mitochondrial dynamics in healthy cells appears to play a particularly critical role in neurons, because neurons have long processes, particular electrical properties, complex energy requirements and synaptic functions, such as neurotransmitter release which all require continuous supply of energy through mitochondrial ATP synthesis. Therefore, Drp1 regulated fission is regarded as an essential mechanism to allow mitochondrial transport to remote axonal and dendritic locations and synapses in the neurons. Mitochondrial fusion is essential for mitochondrial maintainence through mtDNA and protein exchange and recovery in fused organelles.

Notably, in this thesis, studies elucidating the effect of Drp1 inhibition in healthy neurons demonstrated that high concentrations of the Drp1 inhibitor mdiviA resulted in enhanced fission and cell death and not the expected enhanced fusion of mitochondria. These toxic effects provoked by Drp1 inhibition are in line with applications of dominant-negative mutant of the fission protein Drp1, such as Drp1^{K38A}. Exogenously expressed, Drp1^{K38A} causes a loss of mitochondria from dendritic spines and a reduction in synapse number and size, whereas enhanced mitochondrial fission increases synapse formation (110;180). Similarly to this, mutations in mitochondrial fusion proteins also cause enhanced mitochondrial fission in a number of different human neuropathies (97;136;181;182). In contrast, depletion of endogenous Drp1 has been shown to prevent mitochondria from distributing to synapses thereby causing synaptic dysfunction as a result of increased mitochondrial length. Further, interference with Drp1-mediated fission promote increased mitochondrial fusion, and this may also interfere with mitochondrial transport and function in neurons (82;110;115;183;184). For example, inhibition of Drp1 leads to persistent mitochondrial fusion that neither allows mitochondrial regeneration nor transport within the neurons thereby causing accumulation of mitochondrial DNA and protein damage and ultimately resulting in mitochondrial dysfunction and cell death. This is consistent with a recently described human mutation in Drp1 associated with severe abnormal brain development (185). These examples indicate that mitochondrial dynamics are tightly regulated in neurons and the fine-tuned balance of mitochondrial fission and fusion is of major importance for neuronal viability and function. Thus, future investigations are warranted to address whether additional inhibition of other regulators of mitochondrial fission and fusion may provide similar effects as observed here with the applied Drp1 inhibitors and whether combinatory approaches are suitable to achieve neuroprotection in models of acute and chronic neurodegenerative disorders.

Regardless of the pivotal role of the outbalanced fusion and fission mechanisms in neurons, these data exposed Drp1 as a key factor regulating mitochondrial dysfunction in models of acute and chronic neurological disorders, respectively.

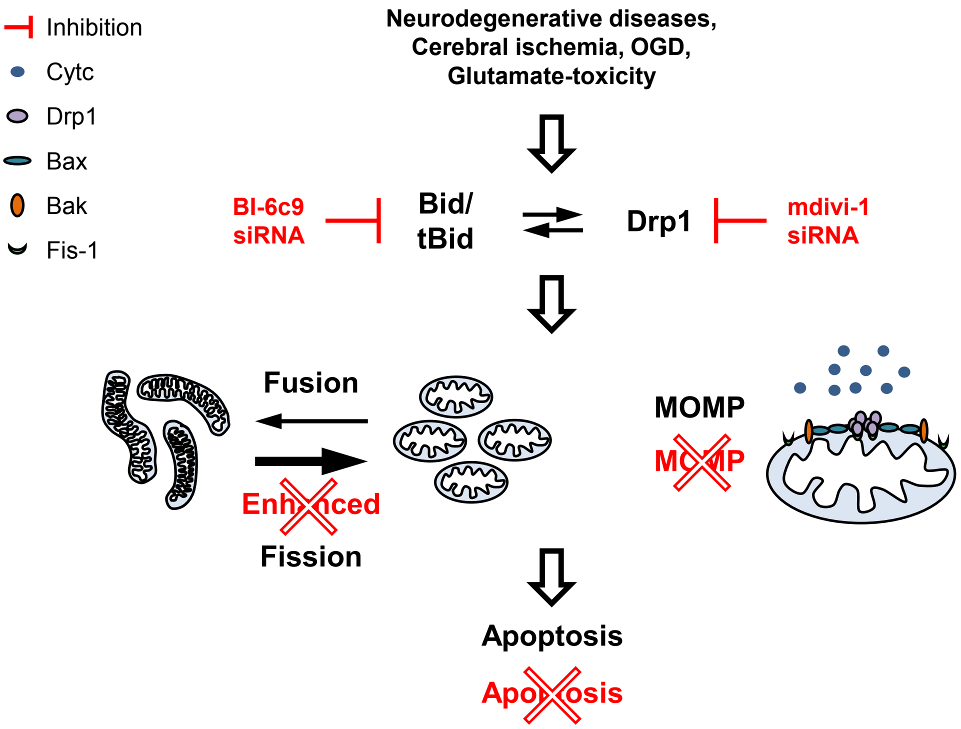
Inhibition
Cytc
Drp1
Bax
Bak
Fis-1
Neurodegenerative diseases,
Cerebral ischemia, OGD,
Glutamate-toxicity
BI-6c9
siRNA
Bid/
tBid
Drp1
mdivi-1
siRNA
Fusion
Enhanced
Fission
MOMP
MOMP
Apoptosis
Apoptosis

Figure 45 The pivotal role of BH3-only protein Bid and Drp1 in cell death induced by oxidative stress

Mitochondrial dynamics are mainly regulated by fusion (Mfn-1, -2, Opa1) and fission proteins (Drp1, Fis-1). Oxidative stress, induced by different neurodegenerative diseases, cerebral ischemia and others, leads to dysregulation of the balanced mitochondrial dynamics towards enhanced mitochondrial fission, depolarization of mitochondrial outer membrane (MOMP), relocation of fragmented mitochondria to the nucleus, and release of mitochondrial AIF and Cytc. Mitochondrial fission and MOMP occur in parallel dependent on an upstream detrimental interplay between full-length Bid, activated tBid and Drp1. Inhibition of either factor is sufficient to block the other's detrimental effect on mitochondria and execution of neuronal cell death. The Bid inhibitor BI-6c9 and siRNA prevented the translocation of both, full-length Bid and tBid, to the mitochondria. Down-regulation of Drp1 by siRNA or new small molecule inhibitor mdivi-1 significantly preserved mitochondrial morphology and mitochondrial membrane potential and reduced glutamate toxicity in neuronal cells. Therefore, inhibition of Bid or Drp1 is a promising therapeutic target to prevent mitochondrial fragmentation and dysfunction, which are hallmarks of neuronal cell death in acute and chronic neurodegenerative diseases, where glutamate toxicity and oxidative stress are prominent.

4.6 The role of Drp1 and Bid in other models of oxidative stress

4.6.1 The effects of Drp1 and Bid inhibition on neuronal damage by radical donors

In addition to the glutamate-induced oxidative cell death, several also well established and widely accepted models of oxidative stress were tested in HT-22 cells to elucidate whether Drp1 activation or Bid activation were involved in neuronal cell death induced by different oxidative stress stimuli. Radical donors such as glucose oxidase, H_2O_2 and 4-HNE were used previously in other studies of neurological disorders to increase formation of ROS and consequently cell death (142;143;186).

Inhibition of Bid by BI-6c9 failed to prevent cell death induced by radical donors, H_2O_2 or glucose oxidase, which showed that Bid was not involved in these models of oxidative cell death. Morever, these findings suggest that ROS production has a key role after glutamate challenge and demonstrated that the mechanism, occurring in HT-22 cells after glutamate challenge differ from those after treatment with radical donors. To this date, the applied model systems of radical donors are under debate concerning their suitability for research on mechanism in neurodegeneration, because treatment with H_2O_2 does not reflect the physiological H_2O_2 formation, but leads to rapid increases in ROS levels, whereas glucose oxidase may induce a more continuous production of H_2O_2.

Further, the widely accepted model of oxidative stress by adding the highly reactive 4-HNE was used to induce cellular damage in HT-22 cells. 4-HNE is a toxic second messenger of free radical formation after peroxidation of cellular lipids or circulating lipid proteins and is used as marker in several neurodegenerative diseases such as Alzheimer`s disease and arteriosclerosis (145;187). This thesis studied the effect of 4-HNE in HT-22 cells and analyzed the role of Bid after exposure to 4-HNE. The inhibition of Bid by BI-6c9 could not prevent 4-HNE-induced damage, indicating, that glutamate toxicity does not involve the formation of large amounts of highly reactive, toxic 4-HNE, and Bid is not primarily activated in the 4-HNE-mediated oxidative stress in HT-22 cells. Thus, these results suggest that 4-HNE induces different apoptotic pathway in HT-22 compared to the pathways of glutamate-induced oxytosis that were delineated in the present thesis.

4.6.2 The role of NO toxicity in HT-22 cells

NO is a gas which mediates physiological functions such as blood vessel dilation, neurotransmission and immune cell response, and contributes to various pathological actions through formation of reactive nitrogen species (RNS). Excess RNS may disturb protein function and induce mitochondrial fragmentation in numerous neurological diseases including Alzheimer`s disease, Parkinson`s disease, Huntington's disease and cerebral ischemia. NO mediates neuronal cell death by interacting with various reactive oxygen species, DNA, enzymes, NMDA receptors and through nitrosylation of proteins like caspases, metalloproteinases and proteins regulating mitochondrial integrity such as Drp1 (116;120;148-150). Thus, RNS may be a leading cause for oxidative stress in different neurodegenerative processes (32;116;151;188-191).

A recent study showed, that nitrosative stress triggers persistent mitochondrial fragmentation prior to neuronal cell death in isolated neurons *in vitro* and in an experimental model of ischemic stroke *in vivo*, where NO-induced ultrastructure changes of mitochondria, increased ROS and reduced intracellular ATP levels (95). The particular role of Drp1 S-nitrosylation by NO for the regulation of Drp1 activity and subsequent mitochondrial fragmentation in AD pathology, however, is a matter of controversy. The authors proposed an increase in GTPase activity upon S-nitrosylation and formation of dimers to play a significant role in neuronal cell death in AD brain tissue but not in PD. In contrast to these findings, Bossy et al. recently reported that S-nitrosylation has no significant impact on Drp1 oligomerization and is not required for Drp1 activation (192). Thus, the mechanisms and the importance of Drp1-nitrosylation for Drp1-mediated mitochondrial fission remain controversial.

To analyze the relevance of NO-toxicity for Drp1 regulation in the glutamate toxicity model, HT-22 cells were challanged by the NO-donors DEANONOate and sodium nitropusside. Both NO-donors induced NO release as well as the formation of $CN^{-,}$ and Fe^{2+}. Inhibition of Bid and Drp1 failed to protect HT-22 cells against NO-toxicity induced by DEANONOate. Further, DEANONOate led to a fast, but short term increase of NO-concentration while SNP induces a continuous, endogenous level of NO, CN^- and Fe^{2+}. The Bid inhibitor BI-6c9 significantly reduced cell death induced by SNP. Thus, Bid seems somehow to be involved in the SNP-induced neuronal cell death in HT-22 cells however this has to be revealed in further detail.

In addition, these results suggest that SNP and DEANONOate induced different mechanisms after fast and short NO production compared to the proposed continuous NO production during cell death in neurodegenerative diseases. Further in comparison with DEANONOate, cell death induced by SNP seems to be more complex regarding the involvment of NFkB activation and glutathione depletion, as well as the release activities of CN^- and Fe^{2+} (193). To examine the SNP-toxicity in further detail and with regard to post-translational modification of Drp1 by nitrosylation, total protein lysates of HT-22 cells were analyzed by western blotting to evaluate the tyrosine nitrosylation after exposure to SNP. The NO-donor DEANONOate was used as a positive control to confirm the function of the antibody. Tyrosine nitrosylation was not detectable in cells exposed to SNP, suggesting that the formation of NO and subsequent tyrosine nitrosylation is not the dominant trigger in neuronal cell death and does not modify the Drp1 protein and his activity in HT-22 cells exposed to glutamate and SNP.

The question if NO toxicity is relevant in glutamate-induced cell death can also be answered by recent work from Tobaben, 2011 (144). Experiments with neuronal (nNOS) and endothelial (eNOS) nitrite oxide synthase inhibitors failed to prevent neuronal HT-22 cell death after glutamate treatment. Analysis of total protein lysates of the tyrosine nitrosylation of proteins after glutamate was not detectable. The analyses confirmed the result that enhanced NO formation and the resulting nitrosylation of proteins appeared to be less important, since inhibitors of NO synthases, targeting iNOS and nNOS did not attenuate mitochondrial fission and cell death after exposure of HT-22 cells to glutamate. Further, nitrosylation of Drp1 could not be detected in this model system of glutamate-induced oxytosis.

In summary the results obtained from the different models of oxidative stress demonstrated, that glutamate-induced a very particular form of oxidative stress, that is not comparable to cell death induced by radical donors like GO or H_2O_2 or oxidative toxicity induced by 4-HNE. The activation and the key mediator role of Bid and Drp1 were linked specifically to glutamate-induced cell death and did not occur in the other applied models of oxidative stress. A further conclusion derived from these data was, that the HT-22 cells served as a suitable model system for oxidative stress to investigate neurodegenerative processes *in vitro*. Which further post-translational modifications of Drp1 are relevant in this model system of neuronal cell death have to be elucidated in further ongoing studies. As mentioned before, phosphorylation of Drp1, could be a potential modification by calcineurin and PKA, which are activated by increased Ca^{2+} levels.

4.7 Mdivi-1, the first inhibitor of mitochondrial dynamin-related protein 1

The identification of mdivi-1 as a potent small molecule inhibitor is remarkable, because of the following properties: mdivi-1 acts as an inhibitor to attenuate the early stages of mitochondiral division, mediated by dynamin-related proteins (Drps) by preventing the polymerization of higher order structures of Drp1. Mdivi-1 compounds (derivatives mdiviA, B, C and E) display a high degree of selectivity of targeting the unassembled pool of the mitochondrial division dynamin proteins and its binding creates and/or stabilizes an assembly-deficient conformation. The assembly of mitochondrial Drp1 is critical for its function. Further, in regard to the conservation of the dynamin-related protein super family members, mdivi-1 has no effect on other Drps, such as the endocytic dynamins or the mitochondrial fusion dynamins. This selectivity is promising for the division dynamin Drp1 as a therapeutic target (109;125).

The identification of mdiviA and other structurally related inhibitors of the mitochondrial division dynamin extend to the resolution of genetic, cytological and biochemical approaches by selective, rapid and reversible modulations in mitochondrial division or Drp1 activities. This modulation can be induced in a wild-type background without depletion of protein levels by complex techniques such as RNAi or the need for the generation of mutant or knockout cell lines. In addition, the effects of increased or decreased Drp1 activity can be monitored immediately in combination with biochemical assays to identify the biochemical activity and the role of Drp1 in cellular function (109).

As demonstrated in this study, mdiviA is a useful tool to identify the role of Drp1 in intrinsic apoptosis. Additionally, in earlier studies of cell-free MOMP assays where mitochondrial division does not occur it was shown that mdiviA blocked Cytc release (125). Thus, Drp1 played a significant regulatory role in MOMP that is independent of its role in mitochondrial division, demonstrating that Drp1 possesses multiple independent roles in mammalian cells beyond the control of mitochondrial dynamics (109). In addition, the approach of mdiviA in cultured mammalian cells to inhbit Drp1 activity has revealed a regulatory role for a hyperfused mitochondrial state in the regulation of cyclin E levels and consequently in cell cycle progression (194).

4.8 The therapeutic potential of small molecule inhibitors of Drp1

The high therapeutic potential of small molecule inhibitors of mitochondrial division is not only demonstrated in the results obtained from the present thesis, but was also obtained with dominant negative forms of Drp1 in cell culture models of Parkinson’s, Alzheimer’s and Huntington’s disease, where inhibition of Drp1 activity attenuated disease associated phenotypes of mitochondria (95;116;195;196). The role of Drp1 to facilitate apoptosis has also been exploited for its therapeutic potential. Small molecule inhibitors of Drp1 might protect impressively against apoptotic cell death in model systems of re-exposure of cells to oxygen after cerebral ischemia and reperfusion or after myocardial infarction induced apoptotic cell death, which led to severe tissue and organ damage. In fact, this approach appears highly promising since Drp1 inhibition through genetic approaches and mdiviA compound were also applied successfully in experimental models of cardiac and renal ischemia/reperfusion, respectively (157;179). In addition, it has been shown that mdiviA is efficacious in rodent models of cisplatin-induced renal damage (157), and thus, inhibitors of Drp1 might also have a therapeutic potential for a wider array of chemotherapeutic drug-induced tissue damage (109). Although not yet investigated, it seems likely that mdivi-1 compounds or other inhibitors of mitochondrial division would prove beneficial for mitochondrial fusion-linked neuropathies CMT2A and DOA, where the detrimental effects of ongoing division in the absence or attenuation of mitochondrial fusion are clearly evident (181;182). Interestingly, recent work had shown that partial restoration of mitochondrial fusion in mammalian cells can rescue the long term defects associated with loss of fusion proteins such as, for example, decreased respiratory capacity, reduction in mtDNA levels, and increased rates of mtDNA (197;198). Thus, small molecule inhibitors of mitochondrial division, which could serve to restore the connectivity of the mitochondrial network, might also rescue the defects associated with loss/attenuation of mitochondrial fusion (109).

Further, in cases of human diseases caused by heteroplasmic mtDNA mutations, inhibitors of Drp1 may also serve as potential therapeutics. Inhibition of mitochondrial division would increase connectivity of mitochondria and enhance access to products of wild type mtDNA genes to allow for complementation of respiratory chain or other dysfunctional mitochondrial proteins (109). It is important to note, however, that mitochondrial division is an essential event in cells for mitochondrial quality control and transport (185;199;200). In this context, mdivi-1 compounds may cause increasing mitochondrial connectivity, more frequently. On the other hand, although not yet validated in the according model systems, small molecule activators of Drp1 and inhibitors of mitochondrial fusion proteins might serve as anti-cancer therapies, because of their potential to stimulate apoptotic cell death at high doses or after prolonged inhibition of mitochondrial fragmentation (109).

5 Summary

The most prominent role for mitochondria is to supply the cell with metabolic energy in form of ATP. Furthermore, mitochondria are involved in many catabolic and anabolic reactions of different metabolites, e.g. phospholipids, the regulation of ROS metabolism and calcium homeostasis. In addition to their central role in various biochemical pathways, mitochondria are key regulators of neuronal apoptosis, in development and aging. Beside this, mitochondria are highly dynamic organelles which build, dependent on physiological conditions, large interconnected networks or appear as spherical, small rounded organelles. Impaired regulation of mitochondrial dynamics that shifts the balance towards fission is associated with neuronal death in delayed neuronal cell death after acute brain injury by ischemic stroke or brain trauma, and in age-related neurodegenerative diseases, such as Alzheimer’s disease or Parkinson’s disease. Emerging evidence suggests that oxidative stress disturbs mitochondrial morphology dynamics, resulting in detrimental mitochondrial fragmentation and dysfunction. In particular, such fatal mitochondrial fission has been detected in neurons exposed to oxidative stress, suggesting mitochondrial dysfunction is a key feature in the intrinsic death pathway.

Major parts of the study were performed in a model of glutamate toxicity in immortalized hippocampal HT-22 neurons, since glutamate selectively induced oxidative stress through glutathione depletion in these cells. To verify the relevance of the findings in HT-22 cells for post-mitotic neurons, further experiments included models of glutamate-induced excitotoxicity and oxygen glucose deprivation primary embryonic neurons *in vitro* and in a mouse model of cerebral ischemia *in vivo*.

The first part of this study investigated, whether enhanced mitochondrial fission accompanied by glutamate-induced neuronal cell death. The present study demonstrated that glutamate-induced apoptosis was associated with enhanced mitochondrial fission, loss of mitochondrial membrane potential and relocation of fragmented mitochondria to the nucleus. Further, the results obtained here provided evidence for a key role of the BH3-only protein Bid in mitochondrial fragmentation of neuronal apoptosis caused by oxidative stress. The mitochondrial fragmentation, the associated loss of the mitochondrial membrane potential, and consequent neuronal cell death were prevented by BI-6c9, a highly specific Bid inhibitor.

The second part of this study explored whether Drp1 played a major role in neuronal cell death after glutamate-toxicity in HT-22 cells and primary cortical neurons. To verify the role of Drp1 in glutamate-induced cell death, highly specific small molecule inhibitors of Drp1 and siRNA approaches in neurons were applied in this model-system of oxidative stress in neurons. Data obtained from the present study demonstrated a significant neuroprotective effect through inhibition of Drp1, suggesting that this regulator of mitochondrial fission played a major role in delayed neuronal cell death. This conclusion is based on findings showing that down-regulation of Drp1 by siRNA or by small molecule inhibitors significantly preserved mitochondrial morphology and mitochondrial membrane potential, and reduced glutamate toxicity in neuronal cells. In addition, the Drp1 inhibitors protected primary cortical neurons against oxygen glucose deprivation *in vitro*, and preserved brain tissue after cerebral ischemia *in vivo*. These data expose Drp1 as a key factor in ischemic and glutamate-induced neuronal cell death and identify Drp1-dependent mitochondrial fission as a potential therapeutic target in acute cerebrovascular diseases.

Finally, studies on the potential interaction between Bid and Drp1 revealed for the first time that both factors cooperate during neuronal apoptosis to mediate mitochondrial fragmentation, loss of mitochondrial membrane integrity and intrinsic apoptosis. Inhibition of either factor was sufficient to block the other’s detrimental effect on mitochondria and execution of neuronal cell death.

Overall, data obtained from the present study demonstrate for the first time Bid and Drp1 as the key regulators of mitochondrial neuronal cell death pathways associated with enhanced oxidative stress in HT-22 cells and primary neuronal cells as well as in the mouse model of cerebral ischemia, respectively. Bid-mediated neuronal cell death involves Drp1-dependent mitochondrial fission, mitochondrial relocation to the nucleus, mitochondrial membrane permeabilization, and release of mitochondrial cell death regulators such as AIF. Therefore, the presented data expose the inhibition of Bid by BI-6c9 and Drp1 using mdivi-1 compounds as a promising therapeutic target to prevent mitochondrial fragmentation and dysfunction which are hallmarks of neuronal cell death in acute and chronic neurodegenerative diseases, where glutamate toxicity and oxidative stress are prominent.

6 Zusammenfassung

Die bekannteste Rolle von Mitochondrien ist, die Zelle mit Energie in Form von ATP zu versorgen. Des Weiteren sind Mitochondrien an einer Vielzahl von anabolen und katabolen Reaktionen von verschiedenen Zwischenprodukten wie Phospholipiden, sowie an der Regulation des ROS-Metabolismus und der Calcium-Homöostase beteiligt. Zusätzlich zu ihrer zentralen Rolle in den verschiedenen biochemischen Signalwegen, sind Mitochondrien Schlüsselorganelle in Signalwegen der neuronalen Apoptose und in Entwicklungs- und Alterungsprozessen der Zelle. Mitochondrien sind hoch dynamische Organelle, welche sich abhängig der physiologischen Bedingungen als lange miteinander verbundene Netzwerke oder als kleine, runde Organelle darstellen. Unter pathologischen Bedingungen und im neuronalen Zelltod ist die Regulation der Mitochondrienmorphologie deutlich verändert, wobei das Gleichgewicht der mitochondrialen Dynamik in Richtung Fragmentierung verschoben wird. Entsprechende Veränderungen der Mitochondrien treten z. B. im verzögerten neuronalen Zelltod nach Schlaganfall oder Schädel-Hirn-Trauma auf und vermehrt fragmentierte Mitochondrien sind auch in geschädigtem Hirngewebe bei altersbedingten neurodegenerativen Erkrankungen, wie Morbus Alzheimer und Morbus Parkinson nachgewiesen worden.

Vorarbeiten zu dieser Studie und neuere Publikationen weisen darauf hin, dass oxidativer Stress die mitochondriale Struktur zerstört, was in einer nachträglicher mitochondrialen Fragmentierung und Dysfunktion resultiert. Im Besonderen ist solch fatale mitochondriale Fragmentierung in Neuronen unter oxidativem Stress nachgewiesen worden, die Schlussfolgerung nahe legt, dass mitochondriale Dysfunktion eine wichtige Eigenschaft des intrinsischen Apoptosewegs ist. Im Rahmen dieser Arbeit wurde vor allem eine neuronale hippokampale Zelllinie (HT-22 Zellen) verwendet, um die Regulation und die Bedeutung der vermehrten Mitochondrienfragmentierung im oxidativen neuronalen Zelltod zu untersuchen. In diesen Zellen führt eine Behandlung mit Glutamat zu einem kontinuierlichen Abfall der intrazellulären Glutathionspiegel und induziert somit oxidativen Stress. Zusätzlich wurden primäre neuronale Zellkulturen und ein *in vivo*-Modell der zerebralen Ischämie eingesetzt, um die in HT-22 Zellen erhaltenen Ergebnisse zu bestätigen und auszubauen.

Der erste Teil dieser Arbeit untersucht, ob verstärkte mitochondriale Fragmentierung den Glutamat-induzierten Zelltod begleitet. Die Ergebnisse zeigen eindeutig, dass Glutamat-induzierte Apoptose mit einer verstärkten Fragmentierung von Mitochondrien, dem Verlust von mitochondrialen Membranpotential und einer Umverteilung von fragmentierten Mitochondrien um den Zellkern verbunden ist. Weiter zeigen die hier dargestellten Ergebnisse eine Schlüsselrolle für das BH3-Protein Bid in der mitochondrialen Fragmentierung auf, die durch den oxidativen Stress ausgelöst wurde. Durch einen spezifischen Bid Inhibitor (BI-6c9) konnten die mitochondriale Fragmentierung und der Verlust des mitochondrialen Membranpotentials in HT-22 Zellen verhindert werden.

Der zweite Teil der Arbeit untersucht die Rolle des Dynamin Proteins Drp1 im neuronalen Zelltod nach Glutamat-Schädigung in HT-22 Zellen und in primären kortikalen Neuronen.Um die Rolle von Drp1 im Glutamat-induzierten Zelltod nachzuweisen, wurde in dem hier angewendeten Modellsystem des oxidativen Stress zum ersten Mal hoch spezifische Drp1 Inhibitoren und Drp1 siRNA angewendet. Die Ergebnisse dieser Untersuchungen zeigten einen signifikanten neuroprotektiven Effekt durch die Inhibition von Drp1, was darauf hinweist, dass Drp1 ein wichtiger Regulator der mitochondrialen Fragmentierung im verzögerten neuronalen Zelltod ist. Diese Schlussfolgerung basierte auf Befunden, die zeigten, dass die Deletion von Drp1 durch siRNA oder durch den Drp1 Inhibitor die mitochondriale Morphologie, das mitochondriale Membranpotential und die Glutamat-induzierte Schädigung sowohl in HT-22, als auch in primären Neuronen verhindert werden. Der Drp1 Inhibitor blockierte zudem den neuronalen Zelltod nach Sauerstoff-Glukose-Entzug in primären Neuronen und verringerte auch signifikant das Infarktvolumen in einem Schlaganfallmodell in Mäusen. Diese Daten heben Drp1 als einen Schlüsselfaktor bei ischämisch- und Glutamat-induziertem neuronalen Zelltod hervor und identifizierten Drp1-abhängige mitochondriale Fragmentierung als eine mögliche therapeutischen Zielstruktur für die Therapie von akuten zerebrovaskulären Erkrankungen. Weitere Untersuchungen zu einer möglichen Wechselwirkung zwischen Bid und Drp1 im neuronalen Zelltod zeigten zudem erstmalig, dass offenbar beide Proteine nach oxidativem Stress zusammen an der Mitochondrienmembran agieren, um intrinsische Signalkaskaden der Apoptose zu induzieren. Die Hemmung eines der Proteine war ausreichend, um die mitochondriale Translokation bzw. die toxischen Effekte des Partners an den Mitochondrien zu hemmen und so den neuronalen Zelltod zu verhindern.

Insgesamt konnte in dieser Arbeit zum ersten Mal gezeigt werden, dass Bid und Drp1 zusammen als Schlüsselregulatoren des mitochondrialen neuronalen Zelltodes in HT-22 Zellen agieren und das die Hemmung von Drp1 auch in primären Neuronen, und auch in einem Schlaganfallmodell in Mäusen eine protektive Wirkung vermittelt. Der Bid-vermittelte neuronale Zelltod umfasst Drp1-abhängige mitochondriale Fragmentierung, mitochondriale Umverteilung um den Zellkern, mitochondriale

Membranschädigung und die Freisetzung von mitochondrialen Apoptose-Mediatoren wie AIF. Aus diesem Grund sind Bid und Drp1 vielversprechende therapeutische Zielstrukturen, die durch neuartige Inhibitor-Moleküle blockiert werden können, um mitochondriale Fragmentierung und Dysfunktion, als Kennzeichen des neuronalen Zelltodes bei akuten und chronischen neurodegenerativen Erkrankungen zu verhindern, in denen Glutamatschädigung bzw. oxidativer Stress zu den wesentlichen auslösenden Faktoren für die Nervenschädigung führen.

7 Abbreviations

Abbreviation	Full text
°C	Grad Celcius
µ	Micro
µM	Micromolar
AD	Alzheimer`s disease
AIF	Apotosis inducing factor
ALS	Amyotrophic lateral sclerosis
AMPA	2-amin-3-(3-hydroxy-5-methylisoxazol-4-yl)propionate
AMR	ATP monitoring reagent
ANOVA	Analysis of variance
Apaf-1	Apoptosis protease activating factor
ATP	Adenosinetriphosphate
Bad	Bcl-2 antagonist of cell death
Bak	Bcl-2 antagonist/killer 1
Bax	Bcl-2 associated protein X
BCA	Bicinchoninic acid
Bcl-2	B-cell lymphoma- 2
Bcl-xl	Bcl-2 related long isoform
BH	Bcl-2 homology
Bid	Bcl-2 interacting domain death antagonist
Bim	Bcl-2 interacting mediator of cell death
Bodipy	4,4-diflouro-5-(4-phenyl1,3-butadienyl)-4-bora-3a,4a-diaza-s-indacene-3-undecanoic acid
Bp	Base pairs
Ca^{2+}	Calcium
CAD	Caspase-activated deoxyribonuclease
CARD	Caspase recruitment domain
CCCP	Carbonylcyanide-3-chlorophenylhydrazone

Abbreviation	Full text
CMT2A	Charcot Marie Tooth 2A
CNS	Central nervous system
CO2	Carbon dioxide
COX	Cylooxygenase
Cu^{1+}	Copper
CypD	Cyclophilin D
CysA	Cyclosporine A
Cytc	Cytochrome c
DAPI	4`, 6-diamidino-2-phenylindole dihydrochloride
DCF	Dichloro-dihydroflouresceine-diacetate
DD	Death domain
DEANONOate	DEA/NO, 2-(N,N-Diethylamino)-diazenolate-2-oxide diaethylammonium salt
DED	Death effector domain
DMEM	Dulbecco`s modified eagle medium
DMSO	Dimethylsulfoxide
DNA	Deoxyribonucleic acid
DOA	Dominant optic atrophy
Drp	Dynamin-related protein
Drp1	Dynamin-related protein 1
DTT	DL-Dithiotreitol
EBSS	Earl`s balanced salt solution
EBSS w/o glucose	Earls balanced salt solution without glucose
EDTA	Ethylenediaminetetraacetic acid
EGTA	Ethylene glycol-bis(2-aminoethylether)-N,N,N`,N´-tetraacetic acid
EndoG	Endonuclease G
FACS	Flourescence activated cell sorting
FCS	Fetal calf seum
FRET	Förster resonance energy transfer

Abbreviation	Full text
GAPDH	Glyceraldehyde-3-phosphate-dehydrogenase
GDAP	Ganglioside-induced differentiation associated protein 1
GDNF	Glial cell line derived neurotrophic factor
GFP	Green flourescence protein
GO	Glucose oxidase
GSH	Gluthatione
h	Hour
H_2O_2	Hydrogen peroxide
HBSS	Hank`s balanced medium
HCl	Hydrochloric acid
HEPES	4-(2-Hydroxyethyl)piperazine-1-ethanesulfonic acid
HNE	4-Hydroxynonenal-dimethylacetat
HRP	Horse reddish peroxidase
IAP	Inhibitors of apoptosis
ICAD	Inactive caspase-activated deoxyribonuclease
IMM	Inner mitochondrial membrane
JC-1	5,5´,6,6´-tetrachloro-1,1´,3,3´-tetraethyl-benzimidazolylcarbocyanine iodide
JNK	c-Jun N-terminal kinases
kDa	Kilo Dalton
MCA	Middle carotid artery
MCAO	Middle carotid artery occlusion
Mcl-1	Myeloid cell leukemia 1
mdivi	Mitochondrial division inhibitor
MEM+	Eagle’s minimum essential medium
Mff	Miochondrial fission factor
Mfn-1, -2	Mitofusin-1, -2
Mg^{2+}	Magnesium
mGFP	Mitochondiral targeting green fluorescent protein

Abbreviation	Full text
mM	Millimolar
MMP	Mitochondrial membrane permeability
MOMP	Mitochondrial outer membrane permeabilization
MPT	Mitochondrial membrane transition
mtDNA	Mitochondrial DNA
MTT	3-(4,5-Dimethylthiazol-2-yl)-2,5-diphenyltetrazolium bromide
mU	Milli unit
N_2	Nitrogen
NaHCO3	Sodium hydrogen carbonate
NaOH	Sodium hydroxide
nM	Nanomolar
NMDA	N-methyl-D-aspartic acid
NNR	Nucleotide releasing reagent
NO	Nitrogen monoxide
NOS	Nitrogen monoxide synthase
OG	Glucose oxidase
OGD	Oxygen glucose deprivation
OMM	Outer mitochondrial membrane
Opa1	Optic atrophy 1
PBS	Phosphate bufferd saline
PCD	Programmed cell death
PD	Parkinson`s disease
PEI	Polyethylenimine
PFA	Paraformaldeyde
pH	Potentia hydrogenii
PI	Propidium iodide
PLL	Poly-L -ornithine
PTP	Permeability transition pore
PTPC	Permeability transition pore complex

Abbreviation	Full text
PVDF	Polyvinylidenfluorid
RNS	Reactive nitrogen species
ROS	Reactive oxygen species
RT	Room temperature
SD	Standard deviation
SDS	Sodium dodecyl sulfate
SDS-PAGE	Sodium dodecyl sulfate polyacrylamide gel electrophoresis
SEM	Standard deviation of the mean
SNP	Sodium nitropusside
tBid	Truncated Bid
TBS	Tris-bufferd solution
TBST	Tris-bufferd solution with Tween 20
TE	Trypsin-EDTA
TEMED	Tetramethylenethylendiamin
TNF	Tumor necrosis factor
tPa	Tissue plasminogen activator
TRAIL	Tumor necrosis factor related apoptosis inducing ligand
wt	Wild type
XIAP	X-chromosomal linked inhibitor of apoptosis

8 References

1. Culmsee,C., and Landshamer,S. 2006. Molecular insights into mechanisms of the cell death program: role in the progression of neurodegenerative disorders. *Curr Alzheimer Res* **3**:269-283.
2. Loo,D.T., Copani,A., Pike,C.J., Whittemore,E.R., Walencewicz,A.J., and Cotman,C.W. 1993. Apoptosis is induced by beta-amyloid in cultured central nervous system neurons. *Proc. Natl. Acad. Sci. U. S. A* **90**:7951-7955.
3. Mattson,M.P. 2000. Apoptosis in neurodegenerative disorders. *Nat. Rev. Mol. Cell Biol.* **1**:120-129.
4. Rathmell,J.C., and Thompson,C.B. 1999. The central effectors of cell death in the immune system. *Annu. Rev. Immunol.* **17**:781-828.
5. Dive,C., Gregory,C.D., Phipps,D.J., Evans,D.L., Milner,A.E., and Wyllie,A.H. 1992. Analysis and discrimination of necrosis and apoptosis (programmed cell death) by multiparameter flow cytometry. *Biochim. Biophys. Acta* **1133**:275-285.
6. Majno,G., and Joris,I. 1995. Apoptosis, oncosis, and necrosis. An overview of cell death. *Am. J. Pathol.* **146**:3-15.
7. Korsmeyer,S.J., Wei,M.C., Saito,M., Weiler,S., Oh,K.J., and Schlesinger,P.H. 2000. Pro-apoptotic cascade activates BID, which oligomerizes BAK or BAX into pores that result in the release of cytochrome c. *Cell Death Differ* **7**:1166-1173.
8. Oppenheim,R.W. 1991. Cell death during development of the nervous system. *Annu. Rev. Neurosci.* **14**:453-501.
9. Kerr,J.F., Wyllie,A.H., and Currie,A.R. 1972. Apoptosis: a basic biological phenomenon with wide-ranging implications in tissue kinetics. *Br. J. Cancer* **26**:239-257.
10. Vandenabeele,P., Galluzzi,L., Vanden,B.T., and Kroemer,G. 2010. Molecular mechanisms of necroptosis: an ordered cellular explosion. *Nat. Rev. Mol. Cell Biol.* **11**:700-714.
11. Graham,S.H., and Chen,J. 2001. Programmed cell death in cerebral ischemia. *J Cereb Blood Flow Metab* **21**:99-109.
12. Green,D.R. 2005. Apoptotic pathways: ten minutes to dead. *Cell* **121**:671-674.

13. Karbowski,M., and Youle,R.J. 2003. Dynamics of mitochondrial morphology in healthy cells and during apoptosis. *Cell Death Differ* **10**:870-880.

14. Kroemer,G., Petit,P., Zamzami,N., Vayssiere,J.L., and Mignotte,B. 1995. The biochemistry of programmed cell death. *Faseb J* **9**:1277-1287.

15. Mattson,M.P., Culmsee,C., and Yu,Z.F. 2000. Apoptotic and antiapoptotic mechanisms in stroke. *Cell Tissue Res* **301**:173-187.

16. Mattson,M.P., Duan,W., Pedersen,W.A., and Culmsee,C. 2001. Neurodegenerative disorders and ischemic brain diseases. *Apoptosis* **6**:69-81.

17. Stefanis,L. 2005. Caspase-dependent and -independent neuronal death: two distinct pathways to neuronal injury. *Neuroscientist.* **11**:50-62.

18. Oliver,L., and Vallette,F.M. 2005. The role of caspases in cell death and differentiation. *Drug Resist. Updat.* **8**:163-170.

19. Kroemer,G., and Martin,S.J. 2005. Caspase-independent cell death. *Nat. Med.* **11**:725-730.

20. Kitazumi,I., and Tsukahara,M. 2011. Regulation of DNA fragmentation: the role of caspases and phosphorylation. *FEBS J.* **278**:427-441.

21. Enari,M., Sakahira,H., Yokoyama,H., Okawa,K., Iwamatsu,A., and Nagata,S. 1998. A caspase-activated DNase that degrades DNA during apoptosis, and its inhibitor ICAD. *Nature* **391**:43-50.

22. Cheung,E.C., McBride,H.M., and Slack,R.S. 2007. Mitochondrial dynamics in the regulation of neuronal cell death. *Apoptosis.* **12**:979-992.

23. Mattson,M.P., Gleichmann,M., and Cheng,A. 2008. Mitochondria in neuroplasticity and neurological disorders. *Neuron* **60**:748-766.

24. Mehta,S.L., Manhas,N., and Raghubir,R. 2007. Molecular targets in cerebral ischemia for developing novel therapeutics. *Brain Res. Rev.* **54**:34-66.

25. Chipuk,J.E., Fisher,J.C., Dillon,C.P., Kriwacki,R.W., Kuwana,T., and Green,D.R. 2008. Mechanism of apoptosis induction by inhibition of the anti-apoptotic BCL-2 proteins. *Proc Natl Acad Sci U S A* **105**:20327-20332.

26. Karbowski,M., Norris,K.L., Cleland,M.M., Jeong,S.Y., and Youle,R.J. 2006. Role of Bax and Bak in mitochondrial morphogenesis. *Nature* **443**:658-662.

27. Joza,N., Pospisilik,J.A., Hangen,E., Hanada,T., Modjtahedi,N., Penninger,J.M., and Kroemer,G. 2009. AIF: not just an apoptosis-inducing factor. *Ann. N. Y. Acad. Sci.* **1171**:2-11.

28. Lindsten,T., Zong,W.X., and Thompson,C.B. 2005. Defining the role of the Bcl-2 family of proteins in the nervous system. *Neuroscientist.* **11**:10-15.

29. Dirnagl,U., Iadecola,C., and Moskowitz,M.A. 1999. Pathobiology of ischaemic stroke: an integrated view. *Trends Neurosci.* **22**:391-397.

30. Arundine,M., and Tymianski,M. 2003. Molecular mechanisms of calcium-dependent neurodegeneration in excitotoxicity. *Cell Calcium* **34**:325-337.

31. Beckman,J.S., and Crow,J.P. 1993. Pathological implications of nitric oxide, superoxide and peroxynitrite formation. *Biochem. Soc. Trans.* **21**:330-334.

32. Dawson,V.L., Dawson,T.M., London,E.D., Bredt,D.S., and Snyder,S.H. 1991. Nitric oxide mediates glutamate neurotoxicity in primary cortical cultures. *Proc. Natl. Acad. Sci. U. S. A* **88**:6368-6371.

33. Sattler,R., and Tymianski,M. 2001. Molecular mechanisms of glutamate receptor-mediated excitotoxic neuronal cell death. *Mol. Neurobiol.* **24**:107-129.

34. Culmsee,C., and Krieglstein,J. 2007. Ischaemic brain damage after stroke: new insights into efficient therapeutic strategies. International Symposium on Neurodegeneration and Neuroprotection. *EMBO Rep* **8**:129-133.

35. Lin,M.T., and Beal,M.F. 2006. Mitochondrial dysfunction and oxidative stress in neurodegenerative diseases. *Nature* **443**:787-795.

36. Phillis,J.W., Horrocks,L.A., and Farooqui,A.A. 2006. Cyclooxygenases, lipoxygenases, and epoxygenases in CNS: their role and involvement in neurological disorders. *Brain Res. Rev.* **52**:201-243.

37. Bolanos,J.P., Moro,M.A., Lizasoain,I., and Almeida,A. 2009. Mitochondria and reactive oxygen and nitrogen species in neurological disorders and stroke: Therapeutic implications. *Adv. Drug Deliv. Rev.* **61**:1299-1315.

38. Galluzzi,L., Blomgren,K., and Kroemer,G. 2009. Mitochondrial membrane permeabilization in neuronal injury. *Nat. Rev. Neurosci.* **10**:481-494.

39. Landshamer,S., Hoehn,M., Barth,N., Duvezin-Caubet,S., Schwake,G., Tobaben,S., Kazhdan,I., Becattini,B., Zahler,S., Vollmar,A., Pellecchia,M., Reichert,A., Plesnila,N., Wagner,E., and Culmsee,C. 2008. Bid-induced release of AIF from mitochondria causes immediate neuronal cell death. *Cell Death Differ* **15**:1553-1563.

40. Schubert,D., and Piasecki,D. 2001. Oxidative glutamate toxicity can be a component of the excitotoxicity cascade. *J Neurosci* **21**:7455-7462.

41. Bannai,S. 1984. Transport of cystine and cysteine in mammalian cells. *Biochim. Biophys. Acta* **779**:289-306.

42. Davis,J.B., and Maher,P. 1994. Protein kinase C activation inhibits glutamate-induced cytotoxicity in a neuronal cell line. *Brain Res.* **652**:169-173.

43. Sagara,Y., Dargusch,R., Chambers,D., Davis,J., Schubert,D., and Maher,P. 1998. Cellular mechanisms of resistance to chronic oxidative stress. *Free Radic. Biol. Med.* **24**:1375-1389.

44. Burdo,J., Dargusch,R., and Schubert,D. 2006. Distribution of the cystine/glutamate antiporter system xc- in the brain, kidney, and duodenum. *J. Histochem. Cytochem.* **54**:549-557.

45. Tan,S., Sagara,Y., Liu,Y., Maher,P., and Schubert,D. 1998. The regulation of reactive oxygen species production during programmed cell death. *J. Cell Biol.* **141**:1423-1432.

46. Cheung,E.C., McBride,H.M., and Slack,R.S. 2007. Mitochondrial dynamics in the regulation of neuronal cell death. *Apoptosis* **12**:979-992.

47. Kroemer,G. 1999. Mitochondrial control of apoptosis: an overview. *Biochem Soc Symp* **66**:1-15.

48. Youle,R.J., and Strasser,A. 2008. The BCL-2 protein family: opposing activities that mediate cell death. *Nat Rev Mol Cell Biol* **9**:47-59.

49. Giam,M., Huang,D.C., and Bouillet,P. 2008. BH3-only proteins and their roles in programmed cell death. *Oncogene* **27 Suppl 1**:S128-S136.

50. Kim,R. 2005. Unknotting the roles of Bcl-2 and Bcl-xL in cell death. *Biochem. Biophys. Res. Commun.* **333**:336-343.

51. Autret,A., and Martin,S.J. 2009. Emerging role for members of the Bcl-2 family in mitochondrial morphogenesis. *Mol. Cell* **36**:355-363.

52. Kang,M.H., and Reynolds,C.P. 2009. Bcl-2 inhibitors: targeting mitochondrial apoptotic pathways in cancer therapy. *Clin. Cancer Res.* **15**:1126-1132.

53. Willis,S.N., Fletcher,J.I., Kaufmann,T., van Delft,M.F., Chen,L., Czabotar,P.E., Ierino,H., Lee,E.F., Fairlie,W.D., Bouillet,P., Strasser,A., Kluck,R.M., Adams,J.M., and Huang,D.C. 2007. Apoptosis initiated when BH3 ligands engage multiple Bcl-2 homologs, not Bax or Bak. *Science* **315**:856-859.

54. Kuwana,T., Bouchier-Hayes,L., Chipuk,J.E., Bonzon,C., Sullivan,B.A., Green,D.R., and Newmeyer,D.D. 2005. BH3 domains of BH3-only proteins differentially regulate Bax-mediated mitochondrial membrane permeabilization both directly and indirectly. *Mol. Cell* **17**:525-535.

55. Chipuk,J.E., Moldoveanu,T., Llambi,F., Parsons,M.J., and Green,D.R. 2010. The BCL-2 family reunion. *Mol. Cell* **37**:299-310.

56. Lovell,J.F., Billen,L.P., Bindner,S., Shamas-Din,A., Fradin,C., Leber,B., and Andrews,D.W. 2008. Membrane binding by tBid initiates an ordered series of events culminating in membrane permeabilization by Bax. *Cell* **135**:1074-1084.

57. Desagher,S., and Martinou,J.C. 2000. Mitochondria as the central control point of apoptosis. *Trends Cell Biol* **10**:369-377.

58. Eskes,R., Desagher,S., Antonsson,B., and Martinou,J.C. 2000. Bid induces the oligomerization and insertion of Bax into the outer mitochondrial membrane. *Mol Cell Biol* **20**:929-935.

59. Martin-Villalba,A., Herr,I., Jeremias,I., Hahne,M., Brandt,R., Vogel,J., Schenkel,J., Herdegen,T., and Debatin,K.M. 1999. CD95 ligand (Fas-L/APO-1L) and tumor necrosis factor-related apoptosis-inducing ligand mediate ischemia-induced apoptosis in neurons. *J. Neurosci.* **19**:3809-3817.

60. Plesnila,N., Zinkel,S., Le,D.A., min-Hanjani,S., Wu,Y., Qiu,J., Chiarugi,A., Thomas,S.S., Kohane,D.S., Korsmeyer,S.J., and Moskowitz,M.A. 2001. BID mediates neuronal cell death after oxygen/ glucose deprivation and focal cerebral ischemia. *Proc Natl Acad Sci U S A* **98**:15318-15323.

61. Letai,A., Bassik,M.C., Walensky,L.D., Sorcinelli,M.D., Weiler,S., and Korsmeyer,S.J. 2002. Distinct BH3 domains either sensitize or activate mitochondrial apoptosis, serving as prototype cancer therapeutics. *Cancer Cell* **2**:183-192.

62. Bermpohl,D., You,Z., Korsmeyer,S.J., Moskowitz,M.A., and Whalen,M.J. 2006. Traumatic brain injury in mice deficient in Bid: effects on histopathology and functional outcome. *J. Cereb. Blood Flow Metab* **26**:625-633.

63. Yin,X.M., Luo,Y., Cao,G., Bai,L., Pei,W., Kuharsky,D.K., and Chen,J. 2002. Bid-mediated mitochondrial pathway is critical to ischemic neuronal apoptosis and focal cerebral ischemia. *J. Biol. Chem.* **277**:42074-42081.

64. Chan,S.L., and Mattson,M.P. 1999. Caspase and calpain substrates: roles in synaptic plasticity and cell death. *J. Neurosci. Res.* **58**:167-190.

65. Goll,D.E., Thompson,V.F., Li,H., Wei,W., and Cong,J. 2003. The calpain system. *Physiol Rev.* **83**:731-801.

66. Polster,B.M., and Fiskum,G. 2004. Mitochondrial mechanisms of neural cell apoptosis. *J. Neurochem.* **90**:1281-1289.

67. Polster,B.M., Basanez,G., Etxebarria,A., Hardwick,J.M., and Nicholls,D.G. 2005. Calpain I induces cleavage and release of apoptosis-inducing factor from isolated mitochondria. *J. Biol. Chem.* **280**:6447-6454.

68. Jeong,S.Y., and Seol,D.W. 2008. The role of mitochondria in apoptosis. *BMB. Rep* **41**:11-22.

69. Billen,L.P., Shamas-Din,A., and Andrews,D.W. 2008. Bid: a Bax-like BH3 protein. *Oncogene* **27 Suppl 1**:S93-104.

70. Ward,M.W., Rehm,M., Duessmann,H., Kacmar,S., Concannon,C.G., and Prehn,J.H. 2006. Real time single cell analysis of Bid cleavage and Bid translocation during caspase-dependent and neuronal caspase-independent apoptosis. *J. Biol. Chem.* **281**:5837-5844.

71. Wallace,D.C. 2005. A mitochondrial paradigm of metabolic and degenerative diseases, aging, and cancer: a dawn for evolutionary medicine. *Annu. Rev. Genet.* **39**:359-407.

72. Giacomello,M., Drago,I., Pizzo,P., and Pozzan,T. 2007. Mitochondrial Ca2+ as a key regulator of cell life and death. *Cell Death. Differ.* **14**:1267-1274.

73. Nicholls,D.G., Vesce,S., Kirk,L., and Chalmers,S. 2003. Interactions between mitochondrial bioenergetics and cytoplasmic calcium in cultured cerebellar granule cells. *Cell Calcium* **34**:407-424.

74. Chan,D.C. 2006. Mitochondria: dynamic organelles in disease, aging, and development. *Cell* **125**:1241-1252.

75. Bereiter-Hahn,J., and Voth,M. 1994. Dynamics of mitochondria in living cells: shape changes, dislocations, fusion, and fission of mitochondria. *Microsc. Res Tech.* **27**:198-219.

76. Chen,H., and Chan,D.C. 2005. Emerging functions of mammalian mitochondrial fusion and fission. *Hum Mol Genet* **14 Spec No. 2**:R283-R289.

77. Liu,X., Weaver,D., Shirihai,O., and Hajnoczky,G. 2009. Mitochondrial 'kiss-and-run': interplay between mitochondrial motility and fusion-fission dynamics. *EMBO J.* **28**:3074-3089.

78. Twig,G., Graf,S.A., Wikstrom,J.D., Mohamed,H., Haigh,S.E., Elorza,A., Deutsch,M., Zurgil,N., Reynolds,N., and Shirihai,O.S. 2006. Tagging and tracking individual networks within a complex mitochondrial web with photoactivatable GFP. *Am. J. Physiol Cell Physiol* **291**:C176-C184.

79. Jendrach,M., Pohl,S., Voth,M., Kowald,A., Hammerstein,P., and Bereiter-Hahn,J. 2005. Morpho-dynamic changes of mitochondria during ageing of human endothelial cells. *Mech. Ageing Dev.* **126**:813-821.

80. Twig,G., Hyde,B., and Shirihai,O.S. 2008. Mitochondrial fusion, fission and autophagy as a quality control axis: the bioenergetic view. *Biochim. Biophys. Acta* **1777**:1092-1097.

81. McBride,H.M., Neuspiel,M., and Wasiak,S. 2006. Mitochondria: more than just a powerhouse. *Curr Biol* **16**:R551-R560.

82. Uo,T., Dworzak,J., Kinoshita,C., Inman,D.M., Kinoshita,Y., Horner,P.J., and Morrison,R.S. 2009. Drp1 levels constitutively regulate mitochondrial dynamics and cell survival in cortical neurons. *Exp Neurol* **218**:274-285.

83. Hoppins,S., Horner,J., Song,C., McCaffery,J.M., and Nunnari,J. 2009. Mitochondrial outer and inner membrane fusion requires a modified carrier protein. *J Cell Biol* **184**:569-581.

84. Berman,S.B., Pineda,F.J., and Hardwick,J.M. 2008. Mitochondrial fission and fusion dynamics: the long and short of it. *Cell Death. Differ.* **15**:1147-1152.

85. Frank,S., Gaume,B., Bergmann-Leitner,E.S., Leitner,W.W., Robert,E.G., Catez,F., Smith,C.L., and Youle,R.J. 2001. The role of dynamin-related protein 1, a mediator of mitochondrial fission, in apoptosis. *Dev Cell* **1**:515-525.

86. Youle,R.J., and Karbowski,M. 2005. Mitochondrial fission in apoptosis. *Nat. Rev. Mol. Cell Biol.* **6**:657-663.

87. Chan,P.H. 2004. Mitochondria and neuronal death/survival signaling pathways in cerebral ischemia. *Neurochem Res* **29**:1943-1949.

88. Chen,H., Detmer,S.A., Ewald,A.J., Griffin,E.E., Fraser,S.E., and Chan,D.C. 2003. Mitofusins Mfn1 and Mfn2 coordinately regulate mitochondrial fusion and are essential for embryonic development. *J Cell Biol* **160**:189-200.

89. Frezza,C., Cipolat,S., Martins de,B.O., Micaroni,M., Beznoussenko,G.V., Rudka,T., Bartoli,D., Polishuck,R.S., Danial,N.N., De,S.B., and Scorrano,L. 2006. OPA1 controls apoptotic cristae remodeling independently from mitochondrial fusion. *Cell* **126**:177-189.

90. Ishihara,N., Eura,Y., and Mihara,K. 2004. Mitofusin 1 and 2 play distinct roles in mitochondrial fusion reactions via GTPase activity. *J Cell Sci* **117**:6535-6546.

91. Bossy-Wetzel,E., and Lipton,S.A. 2003. Nitric oxide signaling regulates mitochondrial number and function. *Cell Death Differ* **10**:757-760.

92. Grohm,J., Plesnila,N., and Culmsee,C. 2009. Bid mediates fission, membrane permeabilization and peri-nuclear accumulation of mitochondria as a prerequisite for oxidative neuronal cell death. *Brain Behav. Immun.* **24**:831-838.

93. Sheridan,C., Delivani,P., Cullen,S.P., and Martin,S.J. 2008. Bax- or Bak-induced mitochondrial fission can be uncoupled from cytochrome C release. *Mol. Cell* **31**:570-585.

94. Szabadkai,G., Simoni,A.M., Chami,M., Wieckowski,M.R., Youle,R.J., and Rizzuto,R. 2004. Drp-1-dependent division of the mitochondrial network blocks intraorganellar Ca2+ waves and protects against Ca2+-mediated apoptosis. *Mol. Cell* **16**:59-68.

95. Barsoum,M.J., Yuan,H., Gerencser,A.A., Liot,G., Kushnareva,Y., Graber,S., Kovacs,I., Lee,W.D., Waggoner,J., Cui,J., White,A.D., Bossy,B., Martinou,J.C., Youle,R.J., Lipton,S.A., Ellisman,M.H., Perkins,G.A., and Bossy-Wetzel,E. 2006. Nitric oxide-induced mitochondrial fission is regulated by dynamin-related GTPases in neurons. *Embo J* **25**:3900-3911.

96. Yuan,H., Gerencser,A.A., Liot,G., Lipton,S.A., Ellisman,M., Perkins,G.A., and Bossy-Wetzel,E. 2007. Mitochondrial fission is an upstream and required event for bax foci formation in response to nitric oxide in cortical neurons. *Cell Death Differ* **14**:462-471.

97. Chen,H., McCaffery,J.M., and Chan,D.C. 2007. Mitochondrial fusion protects against neurodegeneration in the cerebellum. *Cell* **130**:548-562.

98. Arnoult,D., Grodet,A., Lee,Y.J., Estaquier,J., and Blackstone,C. 2005. Release of OPA1 during apoptosis participates in the rapid and complete release of cytochrome c and subsequent mitochondrial fragmentation. *J. Biol. Chem.* **280**:35742-35750.

99. Arnoult,D. 2007. Mitochondrial fragmentation in apoptosis. *Trends Cell Biol* **17**:6-12.

100. Arnoult,D., Rismanchi,N., Grodet,A., Roberts,R.G., Seeburg,D.P., Estaquier,J., Sheng,M., and Blackstone,C. 2005. Bax/Bak-dependent release of DDP/TIMM8a promotes Drp1-mediated mitochondrial fission and mitoptosis during programmed cell death. *Curr. Biol.* **15**:2112-2118.

101. Cipolat,S., Martins de,B.O., Dal,Z.B., and Scorrano,L. 2004. OPA1 requires mitofusin 1 to promote mitochondrial fusion. *Proc Natl Acad Sci U S A* **101**:15927-15932.

102. Koshiba,T., Detmer,S.A., Kaiser,J.T., Chen,H., McCaffery,J.M., and Chan,D.C. 2004. Structural basis of mitochondrial tethering by mitofusin complexes. *Science* **305**:858-862.

103. James,D.I., Parone,P.A., Mattenberger,Y., and Martinou,J.C. 2003. hFis1, a novel component of the mammalian mitochondrial fission machinery. *J Biol Chem* **278**:36373-36379.

104. Smirnova,E., Griparic,L., Shurland,D.L., and van der Bliek,A.M. 2001. Dynamin-related protein Drp1 is required for mitochondrial division in mammalian cells. *Mol Biol Cell* **12**:2245-2256.

105. Yoon,Y., Krueger,E.W., Oswald,B.J., and McNiven,M.A. 2003. The mitochondrial protein hFis1 regulates mitochondrial fission in mammalian cells through an interaction with the dynamin-like protein DLP1. *Mol Cell Biol* **23**:5409-5420.

106. Karbowski,M., Jeong,S.Y., and Youle,R.J. 2004. Endophilin B1 is required for the maintenance of mitochondrial morphology. *J Cell Biol* **166**:1027-1039.

107. Ingerman,E., Meeusen,S., Devay,R., and Nunnari,J. 2007. In vitro assays for mitochondrial fusion and division. *Methods Cell Biol* **80**:707-720.

108. Okamoto,K., and Shaw,J.M. 2005. Mitochondrial morphology and dynamics in yeast and multicellular eukaryotes. *Annu Rev Genet* **39**:503-536.

109. Lackner,L.L., and Nunnari,J. 2010. Small molecule inhibitors of mitochondrial division: tools that translate basic biological research into medicine. *Chem. Biol.* **17**:578-583.

110. Li,H., Chen,Y., Jones,A.F., Sanger,R.H., Collis,L.P., Flannery,R., McNay,E.C., Yu,T., Schwarzenbacher,R., Bossy,B., Bossy-Wetzel,E., Bennett,M.V., Pypaert,M., Hickman,J.A., Smith,P.J., Hardwick,J.M., and Jonas,E.A. 2008. Bcl-xL induces Drp1-dependent synapse formation in cultured hippocampal neurons. *Proc Natl Acad Sci U S A* **105**:2169-2174.

111. Hoppins,S., Lackner,L., and Nunnari,J. 2007. The machines that divide and fuse mitochondria. *Annu Rev Biochem* **76**:751-780.

112. Montessuit,S., Somasekharan,S.P., Terrones,O., Lucken-Ardjomande,S., Herzig,S., Schwarzenbacher,R., Manstein,D.J., Bossy-Wetzel,E., Basanez,G., Meda,P., and Martinou,J.C. 2010. Membrane remodeling induced by the dynamin-related protein Drp1 stimulates Bax oligomerization. *Cell* **142**:889-901.

113. Cereghetti,G.M., Stangherlin,A., Martins de,B.O., Chang,C.R., Blackstone,C., Bernardi,P., and Scorrano,L. 2008. Dephosphorylation by calcineurin regulates translocation of Drp1 to mitochondria. *Proc. Natl. Acad. Sci. U. S. A* **105**:15803-15808.

114. Chang,C.R., and Blackstone,C. 2007. Cyclic AMP-dependent protein kinase phosphorylation of Drp1 regulates its GTPase activity and mitochondrial morphology. *J. Biol. Chem.* **282**:21583-21587.

115. Chang,C.R., and Blackstone,C. 2007. Drp1 phosphorylation and mitochondrial regulation. *EMBO Rep.* **8**:1088-1089.

116. Cho,D.H., Nakamura,T., Fang,J., Cieplak,P., Godzik,A., Gu,Z., and Lipton,S.A. 2009. S-nitrosylation of Drp1 mediates beta-amyloid-related mitochondrial fission and neuronal injury. *Science* **324**:102-105.

117. Cribbs,J.T., and Strack,S. 2007. Reversible phosphorylation of Drp1 by cyclic AMP-dependent protein kinase and calcineurin regulates mitochondrial fission and cell death. *EMBO Rep.* **8**:939-944.

118. Han,X.J., Lu,Y.F., Li,S.A., Kaitsuka,T., Sato,Y., Tomizawa,K., Nairn,A.C., Takei,K., Matsui,H., and Matsushita,M. 2008. CaM kinase I alpha-induced phosphorylation of Drp1 regulates mitochondrial morphology. *J. Cell Biol.* **182**:573-585.

119. Harder,Z., Zunino,R., and McBride,H. 2004. Sumo1 conjugates mitochondrial substrates and participates in mitochondrial fission. *Curr Biol* **14**:340-345.

120. Nakamura,T., Cieplak,P., Cho,D.H., Godzik,A., and Lipton,S.A. 2010. S-nitrosylation of Drp1 links excessive mitochondrial fission to neuronal injury in neurodegeneration. *Mitochondrion.* **10**:573-578.

121. Taguchi,N., Ishihara,N., Jofuku,A., Oka,T., and Mihara,K. 2007. Mitotic phosphorylation of dynamin-related GTPase Drp1 participates in mitochondrial fission. *J. Biol. Chem.* **282**:11521-11529.

122. Wasiak,S., Zunino,R., and McBride,H.M. 2007. Bax/Bak promote sumoylation of DRP1 and its stable association with mitochondria during apoptotic cell death. *J Cell Biol* **177**:439-450.

123. Zunino,R., Schauss,A., Rippstein,P., ndrade-Navarro,M., and McBride,H.M. 2007. The SUMO protease SENP5 is required to maintain mitochondrial morphology and function. *J. Cell Sci.* **120**:1178-1188.

124. Reddy,P.H., Reddy,T.P., Manczak,M., Calkins,M.J., Shirendeb,U., and Mao,P. 2010. Dynamin-related protein 1 and mitochondrial fragmentation in neurodegenerative diseases. *Brain Res. Rev.*

125. Cassidy-Stone,A., Chipuk,J.E., Ingerman,E., Song,C., Yoo,C., Kuwana,T., Kurth,M.J., Shaw,J.T., Hinshaw,J.E., Green,D.R., and Nunnari,J. 2008. Chemical inhibition of the mitochondrial division dynamin reveals its role in Bax/Bak-dependent mitochondrial outer membrane permeabilization. *Dev Cell* **14**:193-204.

126. Kazhdan,I., Long,L., Montellano,R., Cavazos,D.A., and Marciniak,R.A. 2006. Targeted gene therapy for breast cancer with truncated Bid. *Cancer Gene Ther* **13**:141-149.

127. Morimoto,B.H., and Koshland,D.E., Jr. 1990. Excitatory amino acid uptake and N-methyl-D-aspartate-mediated secretion in a neural cell line. *Proc. Natl. Acad. Sci. U. S. A* **87**:3518-3521.

128. Lei,Z., Ruan,Y., Yang,A.N., and Xu,Z.C. 2006. NMDA receptor mediated dendritic plasticity in cortical cultures after oxygen-glucose deprivation. *Neurosci. Lett.* **407**:224-229.

129. Diemert,S., Grohm,J., Tobaben,S., Dolga,A., and Culmsee,C. 2010. Real-Time Detection of neuronal Cell Death by Impedance-Based Analysis using the xCELLigence System. *Application Note*.

130. van Engeland M., Nieland,L.J., Ramaekers,F.C., Schutte,B., and Reutelingsperger,C.P. 1998. Annexin V-affinity assay: a review on an apoptosis detection system based on phosphatidylserine exposure. *Cytometry* **31**:1-9.

131. Walker,J.M. 1994. The bicinchoninic acid (BCA) assay for protein quantitation. *Methods Mol. Biol.* **32**:5-8.

132. Laemmli,U.K. 1970. Cleavage of structural proteins during the assembly of the head of bacteriophage T4. *Nature* **227**:680-685.

133. Plesnila,N., Zhu,C., Culmsee,C., Groger,M., Moskowitz,M.A., and Blomgren,K. 2004. Nuclear translocation of apoptosis-inducing factor after focal cerebral ischemia. *J Cereb Blood Flow Metab* **24**:458-466.

134. Culmsee,C., and Plesnila,N. 2006. Targeting Bid to prevent programmed cell death in neurons. *Biochem Soc Trans* **34**:1334-1340.

135. Danial,N.N., and Korsmeyer,S.J. 2004. Cell death: critical control points. *Cell* **116**:205-219.

136. Frank,S. 2006. Dysregulation of mitochondrial fusion and fission: an emerging concept in neurodegeneration. *Acta Neuropathol.* **111**:93-100.

137. Knott,A.B., Perkins,G., Schwarzenbacher,R., and Bossy-Wetzel,E. 2008. Mitochondrial fragmentation in neurodegeneration. *Nat Rev Neurosci* **9**:505-518.

138. Lackner,L.L., and Nunnari,J.M. 2008. The molecular mechanism and cellular functions of mitochondrial division. *Biochim Biophys Acta*.

139. Zhang,Y., and Chan,D.C. 2007. Structural basis for recruitment of mitochondrial fission complexes by Fis1. *Proc. Natl. Acad. Sci. U. S. A* **104**:18526-18530.

140. Yepes,M., Roussel,B.D., Ali,C., and Vivien,D. 2009. Tissue-type plasminogen activator in the ischemic brain: more than a thrombolytic. *Trends Neurosci.* **32**:48-55.

141. Cereghetti,G.M., Costa,V., and Scorrano,L. 2010. Inhibition of Drp1-dependent mitochondrial fragmentation and apoptosis by a polypeptide antagonist of calcineurin. *Cell Death. Differ.* **17**:1785-1794.

142. Cente,M., Filipcik,P., Pevalova,M., and Novak,M. 2006. Expression of a truncated tau protein induces oxidative stress in a rodent model of tauopathy. *Eur. J. Neurosci.* **24**:1085-1090.

143. Lu,W.C., Chen,C.J., Hsu,H.C., Hsu,H.L., and Chen,L. 2010. The adaptor protein SH2B1beta reduces hydrogen peroxide-induced cell death in PC12 cells and hippocampal neurons. *J. Mol. Signal.* **5**:17.

144. Tobaben,S. 2011. The role of 12/15-lipoxygenases in ROS-mediated cell death. *Dissertation*.

145. Butterfield,D.A., Bader Lange,M.L., and Sultana,R. 2010. Involvements of the lipid peroxidation product, HNE, in the pathogenesis and progression of Alzheimer's disease. *Biochim. Biophys. Acta* **1801**:924-929.

146. Farooqui,A.A., and Horrocks,L.A. 2006. Phospholipase A2-generated lipid mediators in the brain: the good, the bad, and the ugly. *Neuroscientist.* **12**:245-260.

147. Zarkovic,K. 2003. 4-hydroxynonenal and neurodegenerative diseases. *Mol. Aspects Med.* **24**:293-303.

148. Nakamura,T., and Lipton,S.A. 2008. Emerging roles of S-nitrosylation in protein misfolding and neurodegenerative diseases. *Antioxid. Redox. Signal.* **10**:87-101.

149. Nakamura,T., and Lipton,S.A. 2010. S-Nitrosylation of Critical Protein Thiols Mediates Protein Misfolding and Mitochondrial Dysfunction in Neurodegenerative Diseases. *Antioxid. Redox. Signal.*

150. Nelson,E.J., Connolly,J., and McArthur,P. 2003. Nitric oxide and S-nitrosylation: excitotoxic and cell signaling mechanism. *Biol. Cell* **95**:3-8.

151. Lipton,S.A. 1999. Neuronal protection and destruction by NO. *Cell Death. Differ.* **6**:943-951.

152. Brooks,C., Wei,Q., Feng,L., Dong,G., Tao,Y., Mei,L., Xie,Z.J., and Dong,Z. 2007. Bak regulates mitochondrial morphology and pathology during apoptosis by interacting with mitofusins. *Proc Natl Acad Sci U S A* **104**:11649-11654.

153. Karbowski,M., Lee,Y.J., Gaume,B., Jeong,S.Y., Frank,S., Nechushtan,A., Santel,A., Fuller,M., Smith,C.L., and Youle,R.J. 2002. Spatial and temporal association of Bax with mitochondrial fission sites, Drp1, and Mfn2 during apoptosis. *J. Cell Biol.* **159**:931-938.

154. Kroemer,G., Galluzzi,L., and Brenner,C. 2007. Mitochondrial membrane permeabilization in cell death. *Physiol Rev* **87**:99-163.

155. Karbowski,M., Arnoult,D., Chen,H., Chan,D.C., Smith,C.L., and Youle,R.J. 2004. Quantitation of mitochondrial dynamics by photolabeling of individual organelles shows that mitochondrial fusion is blocked during the Bax activation phase of apoptosis. *J Cell Biol* **164**:493-499.

156. Billen,L.P., Kokoski,C.L., Lovell,J.F., Leber,B., and Andrews,D.W. 2008. Bcl-XL inhibits membrane permeabilization by competing with Bax. *PLoS Biol* **6**:e147.

157. Brooks,C., and Dong,Z. 2007. Regulation of mitochondrial morphological dynamics during apoptosis by Bcl-2 family proteins: a key in Bak? *Cell Cycle* **6**:3043-3047.

158. Delivani,P., Adrain,C., Taylor,R.C., Duriez,P.J., and Martin,S.J. 2006. Role for CED-9 and Egl-1 as regulators of mitochondrial fission and fusion dynamics. *Mol. Cell* **21**:761-773.

159. Berman,S.B., Chen,Y.B., Qi,B., McCaffery,J.M., Rucker,E.B., III, Goebbels,S., Nave,K.A., Arnold,B.A., Jonas,E.A., Pineda,F.J., and Hardwick,J.M. 2009. Bcl-x L increases mitochondrial fission, fusion, and biomass in neurons. *J Cell Biol* **184**:707-719.

160. Culmsee,C., Zhu,C., Landshamer,S., Becattini,B., Wagner,E., Pellecchia,M., Blomgren,K., and Plesnila,N. 2005. Apoptosis-inducing factor triggered by poly(ADP-ribose) polymerase and Bid mediates neuronal cell death after oxygen-glucose deprivation and focal cerebral ischemia. *J Neurosci* **25**:10262-10272.

161. Seiler,A., Schneider,M., Forster,H., Roth,S., Wirth,E.K., Culmsee,C., Plesnila,N., Kremmer,E., Radmark,O., Wurst,W., Bornkamm,G.W., Schweizer,U., and Conrad,M. 2008. Glutathione peroxidase 4 senses and translates oxidative stress into 12/15-lipoxygenase dependent- and AIF-mediated cell death. *Cell Metab* **8**:237-248.

162. Tobaben,S., Grohm,J., Seiler,A., Conrad,M., Plesnila,N., and Culmsee,C. 2011. Bid-mediated mitochondrial damage is a key mechanism in glutamate-induced oxidative stress and AIF-dependent cell death in immortalized HT-22 hippocampal neurons. *Cell Death. Differ.* **18**:282-292.

163. Becattini,B., Culmsee,C., Leone,M., Zhai,D.Y., Zhang,X.Y., Crowell,K.J., Rega,M.F., Landshamer,S., Reed,J.C., Plesnila,N., and Pellecchia,M. 2006. Structure-activity relationships by interligand NOE-based design and synthesis of antiapoptotic compounds targeting Bid. *Proceedings of the National Academy of Sciences of the United States of America* **103**:12602-12606.

164. Konig,H.G., Rehm,M., Gudorf,D., Krajewski,S., Gross,A., Ward,M.W., and Prehn,J.H. 2007. Full length Bid is sufficient to induce apoptosis of cultured rat hippocampal neurons. *BMC. Cell Biol.* **8**:7.

165. Esposti,M.D., Erler,J.T., Hickman,J.A., and Dive,C. 2001. Bid, a widely expressed proapoptotic protein of the Bcl-2 family, displays lipid transfer activity. *Mol. Cell Biol.* **21**:7268-7276.

166. Wei,M.C., Zong,W.X., Cheng,E.H., Lindsten,T., Panoutsakopoulou,V., Ross,A.J., Roth,K.A., MacGregor,G.R., Thompson,C.B., and Korsmeyer,S.J. 2001. Proapoptotic BAX and BAK: a requisite gateway to mitochondrial dysfunction and death. *Science* **292**:727-730.

167. Zha,J., Weiler,S., Oh,K.J., Wei,M.C., and Korsmeyer,S.J. 2000. Posttranslational N-myristoylation of BID as a molecular switch for targeting mitochondria and apoptosis. *Science* **290**:1761-1765.

168. Perkins,G., Bossy-Wetzel,E., and Ellisman,M.H. 2009. New insights into mitochondrial structure during cell death. *Exp. Neurol.* **218**:183-192.

169. Lutter,M., Fang,M., Luo,X., Nishijima,M., Xie,X., and Wang,X. 2000. Cardiolipin provides specificity for targeting of tBid to mitochondria. *Nat. Cell Biol.* **2**:754-761.

170. Lutter,M., Perkins,G.A., and Wang,X. 2001. The pro-apoptotic Bcl-2 family member tBid localizes to mitochondrial contact sites. *BMC. Cell Biol.* **2**:22.

171. Almeida,A., and Bolanos,J.P. 2001. A transient inhibition of mitochondrial ATP synthesis by nitric oxide synthase activation triggered apoptosis in primary cortical neurons. *J. Neurochem.* **77**:676-690.

172. Suen,D.F., Norris,K.L., and Youle,R.J. 2008. Mitochondrial dynamics and apoptosis. *Genes Dev.* **22**:1577-1590.

173. Perfettini,J.L., Roumier,T., and Kroemer,G. 2005. Mitochondrial fusion and fission in the control of apoptosis. *Trends Cell Biol* **15**:179-183.

174. Breckenridge,D.G., Stojanovic,M., Marcellus,R.C., and Shore,G.C. 2003. Caspase cleavage product of BAP31 induces mitochondrial fission through endoplasmic reticulum calcium signals, enhancing cytochrome c release to the cytosol. *J. Cell Biol.* **160**:1115-1127.

175. Lee,Y.J., Jeong,S.Y., Karbowski,M., Smith,C.L., and Youle,R.J. 2004. Roles of the mammalian mitochondrial fission and fusion mediators Fis1, Drp1, and Opa1 in apoptosis. *Mol Biol Cell* **15**:5001-5011.

176. Alirol,E., James,D., Huber,D., Marchetto,A., Vergani,L., Martinou,J.C., and Scorrano,L. 2006. The mitochondrial fission protein hFis1 requires the endoplasmic reticulum gateway to induce apoptosis. *Mol. Biol. Cell* **17**:4593-4605.

177. Parone,P.A., James,D.I., Da,C.S., Mattenberger,Y., Donze,O., Barja,F., and Martinou,J.C. 2006. Inhibiting the mitochondrial fission machinery does not prevent Bax/Bak-dependent apoptosis. *Mol. Cell Biol.* **26**:7397-7408.

178. Germain,M., Mathai,J.P., McBride,H.M., and Shore,G.C. 2005. Endoplasmic reticulum BIK initiates DRP1-regulated remodelling of mitochondrial cristae during apoptosis. *EMBO J.* **24**:1546-1556.

179. Ong,S.B., Subrayan,S., Lim,S.Y., Yellon,D.M., Davidson,S.M., and Hausenloy,D.J. 2010. Inhibiting mitochondrial fission protects the heart against ischemia/reperfusion injury. *Circulation* **121**:2012-2022.

180. Li,Z., Okamoto,K., Hayashi,Y., and Sheng,M. 2004. The importance of dendritic mitochondria in the morphogenesis and plasticity of spines and synapses. *Cell* **119**:873-887.

181. Alexander,C., Votruba,M., Pesch,U.E., Thiselton,D.L., Mayer,S., Moore,A., Rodriguez,M., Kellner,U., Leo-Kottler,B., Auburger,G., Bhattacharya,S.S., and Wissinger,B. 2000. OPA1, encoding a dynamin-related GTPase, is mutated in autosomal dominant optic atrophy linked to chromosome 3q28. *Nat. Genet.* **26**:211-215.

182. Delettre,C., Lenaers,G., Griffoin,J.M., Gigarel,N., Lorenzo,C., Belenguer,P., Pelloquin,L., Grosgeorge,J., Turc-Carel,C., Perret,E., starie-Dequeker,C., Lasquellec,L., Arnaud,B., Ducommun,B., Kaplan,J., and Hamel,C.P. 2000. Nuclear gene OPA1, encoding a mitochondrial dynamin-related protein, is mutated in dominant optic atrophy. *Nat. Genet.* **26**:207-210.

183. Mai,S., Klinkenberg,M., Auburger,G., Bereiter-Hahn,J., and Jendrach,M. 2010. Decreased expression of Drp1 and Fis1 mediates mitochondrial elongation in senescent cells and enhances resistance to oxidative stress through PINK1. *J. Cell Sci.* **123**:917-926.

184. Wang,X., Su,B., Fujioka,H., and Zhu,X. 2008. Dynamin-like protein 1 reduction underlies mitochondrial morphology and distribution abnormalities in fibroblasts from sporadic Alzheimer's disease patients. *Am J Pathol* **173**:470-482.

185. Waterham,H.R., Koster,J., van Roermund,C.W., Mooyer,P.A., Wanders,R.J., and Leonard,J.V. 2007. A lethal defect of mitochondrial and peroxisomal fission. *N. Engl. J. Med.* **356**:1736-1741.

186. Higgins,G.C., Beart,P.M., and Nagley,P. 2009. Oxidative stress triggers neuronal caspase-independent death: endonuclease G involvement in programmed cell death-type III. *Cell Mol. Life Sci.* **66**:2773-2787.

187. Hattori,Y., Hattori,S., and Kasai,K. 2001. 4-hydroxynonenal prevents NO production in vascular smooth muscle cells by inhibiting nuclear factor-kappaB-dependent transcriptional activation of inducible NO synthase. *Arterioscler. Thromb. Vasc. Biol.* **21**:1179-1183.

188. Brown,G.C. 2010. Nitric oxide and neuronal death. *Nitric. Oxide.* **23**:153-165.

189. Knott,A.B., and Bossy-Wetzel,E. 2008. Impairing the mitochondrial fission and fusion balance: a new mechanism of neurodegeneration. *Ann N Y Acad Sci* **1147**:283-292.

190. Knott,A.B., and Bossy-Wetzel,E. 2008. Nitric Oxide in Health and Disease of the Nervous System. *Antioxid Redox Signal*.

191. Knott,A.B., and Bossy-Wetzel,E. 2010. Impact of nitric oxide on metabolism in health and age-related disease. *Diabetes Obes. Metab* **12 Suppl 2**:126-133.

192. Bossy,B., Petrilli,A., Klinglmayr,E., Chen,J., Lutz-Meindl,U., Knott,A.B., Masliah,E., Schwarzenbacher,R., and Bossy-Wetzel,E. 2010. S-Nitrosylation of DRP1 does not affect enzymatic activity and is not specific to Alzheimer's disease. *J. Alzheimers. Dis.* **20 Suppl 2**:S513-S526.

193. Fass,U., Panickar,K., Williams,K., Nevels,K., Personett,D., and McKinney,M. 2004. The role of glutathione in nitric oxide donor toxicity to SN56 cholinergic neuron-like cells. *Brain Res.* **1005**:90-100.

194. Mitra,K., Wunder,C., Roysam,B., Lin,G., and Lippincott-Schwartz,J. 2009. A hyperfused mitochondrial state achieved at G1-S regulates cyclin E buildup and entry into S phase. *Proc. Natl. Acad. Sci. U. S. A* **106**:11960-11965.

195. Lutz,A.K., Exner,N., Fett,M.E., Schlehe,J.S., Kloos,K., Lammermann,K., Brunner,B., Kurz-Drexler,A., Vogel,F., Reichert,A.S., Bouman,L., Vogt-Weisenhorn,D., Wurst,W., Tatzelt,J., Haass,C., and Winklhofer,K.F. 2009. Loss of parkin or PINK1 function increases Drp1-dependent mitochondrial fragmentation. *J. Biol. Chem.* **284**:22938-22951.

196. Wang,X., Su,B., Lee,H.G., Li,X., Perry,G., Smith,M.A., and Zhu,X. 2009. Impaired balance of mitochondrial fission and fusion in Alzheimer's disease. *J. Neurosci.* **29**:9090-9103.

197. Chen,H., Chomyn,A., and Chan,D.C. 2005. Disruption of fusion results in mitochondrial heterogeneity and dysfunction. *J. Biol. Chem.* **280**:26185-26192.

198. Chen,H., Vermulst,M., Wang,Y.E., Chomyn,A., Prolla,T.A., McCaffery,J.M., and Chan,D.C. 2010. Mitochondrial fusion is required for mtDNA stability in skeletal muscle and tolerance of mtDNA mutations. *Cell* **141**:280-289.

199. Ishihara,N., Nomura,M., Jofuku,A., Kato,H., Suzuki,S.O., Masuda,K., Otera,H., Nakanishi,Y., Nonaka,I., Goto,Y., Taguchi,N., Morinaga,H., Maeda,M., Takayanagi,R., Yokota,S., and Mihara,K. 2009. Mitochondrial fission factor Drp1 is essential for embryonic development and synapse formation in mice. *Nat. Cell Biol.* **11**:958-966.

200. Wakabayashi,J., Zhang,Z., Wakabayashi,N., Tamura,Y., Fukaya,M., Kensler,T.W., Iijima,M., and Sesaki,H. 2009. The dynamin-related GTPase Drp1 is required for embryonic and brain development in mice. *J. Cell Biol.* **186**:805-816.

9 Publications

9.1 Original papers

J Grohm, S-W Kim, U Mamrak, S Tobaben, A Cassidy-Stone, J Nunnari, N Plesnila, C Culmsee**,** Inhibition of Dynamin-realted protein 1 (Drp1) prevents mitochondrial fission and provides neuroprotection *in vitro* and in a mouse model of cerebral ischemia Submitted for publication

J Grohm, N Plesnila and C Culmsee, Bid mediates fragmentation, membrane permeabilization and perinuclear accumulation of mitochondria as a prerequisite for oxidative neuronal death, Brain, Behavior, and Immunity, 24: 831-838, 2010

S Tobaben, **J Grohm**, A Seiler, M Conrad, N Plesnila, C Culmsee, Bid-mediated mitochondrial damage accelerates glutamate-induced oxidative stress and AIF-dependent death in neurons, Cell Death and Differentiation, 18: 282-292, 2011

S Diemert, **J Grohm**, S Tobaben, A Dolga, C Culmsee, Real-Time Detection of neuronal Cell Death by Impedance-Based Analysis using the xCELLigence System, Application Note, Issue 06, Roche Diagnostics GmbH, Roche Applied Science, Penzberg, Germany, 2010

JE Slemmer, C Zhu, S Landshamer, R Trabold, **J Grohm**, A Ardeshiri, E Wagner, MI Sweeney, K Blomgren, C Culmsee, JT Weber, N Plesnila, Causal Role of Apoptosis-Inducing Factor for Neuronal Cell Death Following Traumatic Brain Injury, Am. J. Pathol., 173: 1795-1805, 2008

9.2 Poster presentations

2010

AM Dolga, **J Grohm**, S Pfeifer, S Tobaben, N Plesnila, C Culmsee, Small conductance KCa2.2 channels are essential for preventing delayed calcium deregulation in models of glutamate toxicity, N.: 341.13/F56, Society for Neuroscience Annual Meeting, Neuroscience 2010, San Diego, USA, 13.11.2010-17.11.2010

J Grohm, SW Kim, U Mamrak, A Cassidy-Stone, J Nunnari, N Plesnila, C Culmsee, Dynamin-related protein 1 (Drp1) as therapeutic target to prevent mitochondrial pathways of neuronal cell death *in vitro* and *in vivo*, Restorative Neurology and Neuroscience; Special Issue: Abstracts of the 6th international Symposium on Neuroprotection and Neurorepair RNNEEL 28 (5) 605- 716, IOS Press, Nr.: PP IV-2; 6th international Symposium on Neuroprotection and Neurorepair, Rostock, Germany 01.10.2010-04.10.2010

S Diemert, S Tobaben, **J Grohm**, R Hartmannsgruber, N Plesnila, C Culmsee, Inhibition of p53 preserves mitochondrial morphology and function protects against glutamate-induced cell death, Restorative Neurology and Neuroscience; Special Issue: Abstracts of the 6th international Symposium on Neuroprotection and Neurorepair RNNEEL 28 (5) 605-716, IOS Press, Nr.: PP IV-1; 6th international Symposium on Neuroprotection and Neurorepair, Rostock, Germany 01.10.2010-04.10.2010

S Tobaben, A Dolga, **J Grohm**, U Mamrak, M Conrad, N Plesnila, C Culmsee, 12/15 Lipoxygenases play a key role in AIF mediated neuronal cell death induced by oxidative stress, Restorative Neurology and Neuroscience; Special Issue: Abstracts of the 6th international Symposium on Neuroprotection and Neurorepair RNNEEL 28 (5) 605-716, IOS Press, Nr.: PP III-27; 6th international Symposium on Neuroprotection and Neurorepair, Rostock, Germany 01.10.2010-04.10.2010

S Diemert, S Pfeifer, **J Grohm**, S Tobaben, A Dolga, C Culmsee, Real-time detection of neuronal cell death by the xCelligence system, Naunyn-Schmiedeberg`s Arch Pharmacology (2010) 381 (Suppl 1):1-92 Nr.: 404; 51. Jahrestagung der Deutschen Gesellschaft für Experimentelle und Klinische Pharmakologie und Toxikologie Mainz, Germany 23.03.2010- 25.03.2010

S Tobaben, **J Grohm**, A Seiler, M Conrad, N Plesnila, C Culmsee, Bid-induced damage of mitochondrial integrity play a key role in neuronal oxytosis, Naunyn-Schmiedeberg`s Arch Pharmacology (2010) 381 (Suppl 1):1-92 Nr.: 69; 51. Jahrestagung der Deutschen Germany 23.03.2010-25.03.2010

2009

J Grohm, A Cassidy-Stone, J Nunnari, C Culmsee, A small molecule inhibitor of Bid prevents mitochondrial fission and cell death signaling in neurons exposed to oxidative stress, 50. Jahrestagung der Deutschen Gesellschaft für Experimentelle und Klinische Pharmakologie und Toxikologie Mainz, Deutschland 10.03.2009-12.03.2009

S Diemert, **J Grohm**, R Hartmannsgruber, C Culmsee, Inhibition of p53 preserves mitochondrial morphology and function, and prevents glutamate-induced cell death in neurons, 50. Jahrestagung der Deutschen Gesellschaft für Experimentelle und Klinische Pharmakologie und Toxikologie Mainz, Deutschland 10.03.2009-12.03.2009

J Grohm, A Cassidy-Stone, J Nunnari, C Culmsee, The Bid inhibitor BI-6c9 prevents mitochondrial fission and cell death in neurons exposed to oxidative stress, 9th International Conference AD/PD 2009, Prag, Tschechische Republik, 11.03-15.03.2009

J Grohm, SW Kim, A Cassidy-Stone, J Nunnari, N Plesnila, C Culmsee, Pharmacological inhibitors of dynamin-related protein (Drp1) prevent mitochondrial fission and neuronal cell death *in vitro* and *in vivo* / p106, 17th ECDO Euroconference. Destruction, Degradation and Death, Cell Death Control in Cancer and Neurodegeneration. Institut Pasteur, Paris, Frankreich, 22.09-26.09.2009

S Tobaben, **J Grohm**, A Dolga, N Plesnila, C Culmsee, 12/15-lipoxygenases are key regulators of mitochondria damage and sustained disturbances of calcium homeostasis in glutamate-induced neurotoxicity / p141, 17th ECDO Euroconference. Destruction, Degradation and Death, Cell Death Control in Cancer and Neurodegeneration. Institut Pasteur, Paris, Frankreich, 22.09-26.09.2009

J Grohm, S Tobaben, S Diemert, C Culmsee, Pharmacological inhibition of mitochondria fission exerts neuroprotective effects in neurons exposed to oxidative stress, Nr.: D08, Jahrestagung der Deutschen Pharmazeutischen Gesellschaft, DPhG, Jena, Deutschland, 28.9.2009-01.10.2009

S Tobaben, **J Grohm**, M Hoehn, N Plesnila, C Culmsee, 12/15-Lipoxygenases mediate mitochondrial AIF release and mitochondrial fission upstream of Bid in oxidative stressinduced neuronal cell death, Nr.: D09, Jahrestagung der Deutschen Pharmazeutischen Gesellschaft, DPhG, Jena, Deutschland, 28.9.2009-01.10.2009

S Diemert, **J Grohm**, S Tobaben, A Dolga, C Culmsee, Real time detection of neuronal cell death by the xCELLigence system Inhibition of p53 preserves mitochondrial morphology and function and prevents glutamate-induced cell death in neurons, Nr.: D15, Jahrestagung der Deutschen Pharmazeutischen Gesellschaft, DPhG, Jena, Deutschland, 28.9.2009-01.10.2009

J Grohm, SW Kim, A Cassidy-Stone, J Nunnari, N Plesnila, C Culmsee, Inhibition of dynamin-related protein (Drp1) prevents mitochondrial fission and neuroprotection *in vitro* and *in vivo*, N.: 440.13/O14, Society for Neuroscience Annual Meeting, Neuroscience 2009, Chicago, USA, 17.10.2009-21.10.2009

S Tobaben, A Dolga, **J Grohm**, M Conrad, N Plesnila, C Culmsee, Activation of 12/15-lipoxygenases plays a key role in neuronal cell death induced by oxidative stress, Nr.: 56.3/K27, Society for Neuroscience Annual Meeting, Neuroscience 2009, Chicago, USA, 17.10.2009-21.10.2009

9.3 Oral presentations

J Grohm, A Cassidy-Stone, J Nunnari, N Plesnila, C Culmsee, Bid and Drp1 are key regulators of mitochondrial dynamics in cell death in neurons, Naunyn-Schmiedeberg`s Arch Pharmacology (2010) 381 (Suppl 1):1-92 Nr.: 198, 51. Jahrestagung der Deutschen Gesellschaft für Experimentelle und Klinische Pharmakologie und Toxikologie Mainz, Germany, 23.03.2010-25.03.2010

J Grohm, Bid and Drp1 regulate mitochondrial dynamics in neuronal cell death, Invited talk at the Department of Molecular & Cellular Biology, J. Nunnari, UC Davis, Davis, California, USA, 19.11.2010

10 Acknowledgements

First of all I would like to say thank you very much to my supervisor Prof. Dr. Carsten Culmsee who gave me this great, amazing and exciting theme and all his superb support and motivation. He always had time for discussions not only on problems and gave me a lot of free space to flourish and guided me in the right direction just in the right time. Additionally, I greatly appreciate the chance he gave me to attend several national and international meetings, which were always pleasant and unforgettable events.

I would like to thank all my colleagues of the Institute of Pharmacology and Clinical Pharmacy. Without their support, my research would not have been as successful and of course as much fun as it turned out to be, and writing this thesis would have been impossible. Thank you all for your help, your motivation, constructive discussions and also for our evenings together with a lot of international food and drink. I would especially like to mention the very good and friendly atmosphere in the institute, where there was also time to laugh during the whole period of my PhD.

I would like to thank Sebastian Diemert and Svenja Tobaben for the great time from the beginning of our lab and our funny events with representatives of companies in the beginning and our talks about the “world and no lab staff”. Both of you thank you for the introduction into the pharmaceutical knowledge and also private events with cinema, dancing, and cooking. Thanks to Svenja for our “sport-evenings” and spinning, were we had a lot of fun with our crazy coaches and also with our Christmas baking. Thanks to Sebastian, as he always brought the right wine to the parties.

Thank you very much to Amalia Dolga for your great support, constructive discussions and talks about the world. Special thanks for your critical revision of my thesis. I will never forget our day in the San Diego Zoo and the summer days in November 2010.

I would also like to mention Prof. Dr. Nikolaus Plesnila, who supported all my projects and always had good ideas on how to go on with the studies and helped critical with the finishing of the papers. Thank you for the amusing times during the conferences.

I would like to say a special thank-you to Renate Hartmansgruber and Sandra Engel. They taught me many methodical secrets and the preparation of primary cultures. Sandra, thank you very much for the diverting time and kind talks about “everything” during the early Friday morning preparation and that you believed in Svenja and me, as we started out learning the preparation and said “Oh no, we will never be able to do this like you do, not even in ten years time!”. Thank you, Renate, for your help with cell

culture experiments and for our talks about life, hiking routes and other important things.

Thank you very much Emma Esser, you were every time reachable and helpful when I had problems with the bureaucratic affairs and the excellent barbecue in your families garden.

Great thanks go to my parents, my brother Philipp, my grandparents and the whole family, who always believed in me and made every weekend at home for me to a small holiday which gave me new strength. Without my family`s support I would never have been able to complete this thesis.

It is very hard to put into words my thanks to you Torsten. Thank you very much for all your great support every day, your belief in me and your appreciations for my work. Thank you for living experiencing the intensive and nice weekends together with me in Marburg with sightseeing, hiking and biking in the near area. The weekends with you are always the highlight of the week. You built me up and always found the right words and your relaxing style brought me back down to earth. Without your support I would never have been able to complete this thesis. Special thanks for your critical revision of my thesis and your help with all my computer problems.

Finally I would like to thank all my dear friends, who didn’t forget me, visiting me in Marburg and spending great evenings with me here and in the various nightlife of the big city Stuttgart. Thank you, Monika, for our telephone talks and nice weekends in Marburg, where we were always successful in shopping despite the constant rainy weather. Thank you “Fantastic 3” for all our fun on our evenings, concerts and perfect dinners in Marburg, Steinheim, Tübingen and Maad. Thank you, Wencke, for your enthusiastic and supportive words. Thank you all for the time spending together.

Thank you all for reminding me that there is a life outside of the lab.

11 Curriculum vitae

Personal data

Date of birth: 24.06.1982

Place of birth: Stuttgart, Germany

Marital status: unmarried

Education

02/2008 to present	PhD thesis at the Department of Pharmacology and Clinical Pharmacy, Philipps-University of Marburg, Germany; supervisors: Prof. Dr. Carsten Culmsee
01/2008	Diplom Biologist (technical-orientated)
10/2005-11/2005	Internship Selecta Klemm GmbH & Co. KG, Stuttgart, Germany
08/2005-09/2005	Internship Dr. Margarete Fischer-Bosch-Institut für Klinische Pharmakologie am Robert-Bosch-Krankenhaus, Stuttgart, Germany
010/2001-01/2008	Studies of Technical Biology, University of Stuttgart, Stuttgart, Germany
09/1998-07/2001	Secondary school, Berufliches Gymnasium, Hedwig-Dohm-Schule, Stuttgart, Germany
09/1992-07/1998	Secondary school, Ostertag-Realschule, Leonberg
09/1988-07/1992	Primary school, Grundschule Leonberg-Warmbronn, Leonberg, Germany